The effects of landscape changes on the Brazilian spotted fever incidence in the Atlantic Forest over the last two decades.

Auteur : Conserva, Nicolas
Promoteur(s) : Vanderpoorten, Alain; 20941
Faculté : Faculté des Sciences
Diplôme : Master en biologie des organismes et écologie, à finalité approfondie
Année académique : 2023-2024
URI/URL : http://hdl.handle.net/2268.2/19401

University of Liège - Faculty of sciences - Biology of Evolution and Ecology department
University Federal of ABC - Environmental and Urban Systems Integration Laboratory

The effects of landscape changes on the Brazilian spotted fever incidence in the Atlantic Forest over the last two decades.

Master thesis presented by **Nicolas Conserva**, with a view to obtaining the degree of Master in Biology of Organisms and Ecology, with research focus purpose.

Supervisors: Dr. Leandro Riverberi Tambosi, Dr. Gabriela Farias Asmus, Dr. Paula Ribeiro Prist, Dr. Alain Vanderpoorten

Academic year
2023 – 2024

January 2024

Acknowledgements

I would like to thank my advisors:

I am very grateful to Mrs Paula Prist without whom this thesis and my travel in Brazil would not have been possible and for her supervision. It is crazy how two years ago I did not imagine receiving a positive respond the next day to my request to do my mater thesis with you.

Thank you Mr. Leandro Tambosi and Mrs. Gabriela Asmus for welcoming me in your laboratory at the UFABC and for your guidance.

Many thanks Mr. Alain Vanderpoorten for you tourough reviewing, good advice and disponibility for helping me.

To thank my friends:

Adèle and Robin for mental supports, Marie where are you? Besides, can you complet our friends quest on Duolingo, Gauth for your presence, sometimes.

Lucas, thanks four your support, I was glad having you by my side at the beginning, I wish you were still there to see the end of this work.

Obrigado para meus amigos brasileiros (ou não), Jaime, Maria, Nicolas, Lucas, André, Caio, e cada pessoa que eu encontrei là ao Brasil. Amo vocês e não vou esquecer, estamos sempre juntos. Obrigado a Universidade Federal do ABC, a melhor das federais.

Thanks to my parents that always conforted and supported me in the choice of my studies and for my projects.

The effects of landscape changes on the Brazilian spotted fever incidence in the Atlantic Forest over the last two decades.

Nicolas Conserva **|** Supervisors: Dr. Leandro Riverberi Tambosi, Dr. Gabriela Farias Asmus, Dr. Paula Ribeiro Prist, Dr. Alain Vanderpoorten **|** Environmental and Urban Systems Integration Laboratory **|** January 2024

Abstract

Zoonoses have become an increasing area of concern since the last decades. Landscape changes increase the spatial overlap between reservoir hosts and human habitats, thereby raising the risk of effective spillover. It is crucial to monitor the emergence patterns of zoonoses to reduce their incidence, which can be done in light of environmental epidemiology. The Brazilian spotted fever (BSF) is a vector-born disease transmitted by ticks of the *Amblyomma* genus and whose etiological agents are *Rickettsia* bacteria. Despite low incidence of the disease, it has a high annual lethality rate. Moreover, the BSF sylvatic cycle involves amplifier hosts that can raise up pathogen prevalence in the environment. The Atlantic Forest is a tropical biome that has undergone several landscape changes, especially deforestation for pasture and agriculture expansion, and is known to contain most of the BSF incidence. Hence, this thesis aims at characterizing the effects of landscape changes on the BSF incidence, and in particular, at assessing which landscape features promote high incidence levels. Several hypotheses based on the host ecology were tested using different variables of landscape structure and configuration. Epidemiologic data of BSF by municipality were downloaded. Data on land use and land cover were retrieved from the MapBiomas initiative. Additional data on municipalities, hydrography, elevation, and climate were gathered. For each municipality, landscape structure and additional data were processed using geographic information systems. Landscape configuration metrics were calculated using the FRAGSTATS software. Subsequently, the relationships between BSF incidence and landscape features were assessed using generalized linear mixed models in RStudio. First, general explanatory model using environmental principal component analysis was carried out. Second, competing hypotheses regarding the role of specific environmental features were tested using multiple Akaike information criterion model selection. The results shows that BSF cases have increased over the last two decades and most of them were located in the Atlantic Forest. There was a significant correlation between BSF incidence and forest cover, especially riparian forests cover immersed in pasture and agriculture landscape matrices. The results are interpreted by the ecological requirements of BSF tick vectors and their hosts in the context of landscape changes in the Atlantic Forest over the period studied. Finally, applications for an enhanced preventive framework of the disease are discussed.

The effects of landscape changes on the Brazilian spotted fever incidence in the Atlantic Forest over the last two decades.

Nicolas Conserva | Supervisors: Dr. Leandro Riverberi Tambosi, Dr. Gabriela Farias Asmus, Dr. Paula Ribeiro Prist, Dr. Alain Vanderpoorten | Environmental and Urban Systems Integration Laboratory | January 2024

Résumé

Les zoonoses sont devenues un problème majeur de ces dernières décennies. Les modifications des paysages augmentent le contact entre les espèces réservoirs et les humains, augmentant ainsi le risque de zoonoses. Il est crucial d'étudier leur émergence afin de réduire leur incidence, ce qui peut être réalisé à la lumière de l'épidémiologie environnementale. La fièvre pourprée des montagnes rocheuses (FPMR) est une maladie à transmission vectorielle transmise et maintenue par les tiques appartenant au genre *Amblyomma* et dont les agents pathogènes sont des bactéries Rickettsiales. Malgré la faible incidence de la maladie, elle a un taux élevé de mortalité annuel. De plus, la FPMR a un cycle sylvatique impliquant également des hôtes amplificateurs de la prévalence des pathogènes dans l'environnement. La Forêt Atlantique est un biome tropical qui a subi de nombreuses modifications de ses paysages, principalement dues à la déforestation pour étendre le pâturage et l'agriculture. Elle est aussi connue pour héberger la FPMR. Delà, ce mémoire a pour but de caractériser les effets des modifications du paysage sur l'incidence de la FPMR, et en particulier, évaluer quelles caractéristiques favorisent une haute incidence. Plusieurs hypothèses basées sur l'écologie des hôtes ont été testées en utilisant différentes variables de structure et de configuration du paysage. Les données épidémiologiques de la FPMR par municipalité ont été téléchargées. Les données de couverture et d'utilisation des terres ont été récupérées de l'initiative MapBiomas. Des données additionnelles sur les municipalités, l'hydrographie, le reliefs et le climat ont été rassemblées. Pour chaque municipalité, la structure du paysage et les données additionnelles ont été traitées via des systèmes d'information géographique, les mesures de configuration du paysage, quant à elles, ont été calculées via FRAGSTATS. Par après, les relations entre l'incidence de la FPMR et les caractéristiques du paysage ont été évaluées en utilisant des modèles linéaires généralisés mixtes dans RStudio. Premièrement, un modèle général exploratoire utilisant des composantes principales environnementales a été réalisé. Deuxièmement, des hypothèses investiguant le rôle spécifique de caractéristiques environnementales ont été testées les unes contre les autres en utilisant de multiples sélections de modèles basées sur le critère d'information d'Akaike. Les résultats montrent que les cas de FPMR ont augmenté durant les deux dernières décennies et la majorité d'entre eux se localisaient dans la Forêt Atlantique. Il y a corrélation significative entre l'incidence de la FPMR et la couverture forestière, en particulier la couverture de forêts ripariennes immergées dans une matrice paysagère de pâturage et d'agriculture. Les résultats sont interprétés par les besoins écologiques des tiques vecteurs de la FPMR et de leurs hôtes dans le contexte des modifications du paysage de la Forêt Atlantique durant la période étudiée. Pour finir, des applications pour améliorer le cadre de prévention de la maladie sont discutées.

Table of Contents

Table of Figures and Tables

Lexicon

Epidemiological terms

Zoonosis	An animal origin disease that can be transmitted to humans (Biology Online, 2021a).
Incidence	The new cases rate of a disease occurring in a specific population over specified period.
Emerging disease	A disease, previously known or not, whose incidence is rapidly increasing in a population (NIH, 2018).
Etiological/aetiological agent	A pathogenic microorganism responsible of a given disease (Biology Online, 2021b).
Host	An organism that can potentially get infected or fed upon by a parasite or a pathogen (Biology Online, 2022a).
Reservoir host	An organism that can be infected by a pathogen without presenting any symptom of illness. A reservoir host is therefore a source of a disease (Biology Online, 2022b).
Vector	An organism that ensures the transmission of an etiological agent from the reservoir to the host (WHO team, 2020).
Vector-borne disease	A human disease caused by a pathogen agent transmitted by vectors (WHO team, 2020).
Amplifier host	In vector-borne diseases, a host that presents a high multiplication rate of the infectious agent, providing the vectors an important source of infection (Biology Online, 2021c). The amplifier host is susceptible to infection but remains asymptomatic (Souza et al., 2009).
Transovarial transmission	A vertical transmission of an infectious agent from female to offspring (Harris et al., 2017).
Transstadial transmission	A transmission of an infectious agent through different developmental stages of a host (Harris et al., 2017).
Sylvatic/enzootic cycle	The cycle of an infectious agent that involves non-human animals and vectors (Domingo, 2016).
Cross-species transmission	The transmission of a disease/pathogen agent between different host species (Keesing and Ostfeld, 2021).
Zoonotic spillover	A cross-species transmission to a potential new host population. Frequent spillover events and suitable conditions or adaptations for the pathogen can lead a disease to become endemic in the new infected host population (Ellwanger and Chies, 2021).
Dilution effect (of biodiversity)	Epidemiological concept for zoonoses stating that higher diversity (and abundance) of other species reduces the abundance of the host species considered, thus the prevalence of the pathogen in the environment and the risk of effective zoonotic spillovers (Civitello et al., 2015; Keesing and Ostfeld, 2021).

Quantitative parasitology terms

Prevalence	The proportion of infected hosts that were examined for a given parasite (Reiczigel and Rozsa, 2010).
Mean intensity	The average number of parasite organisms found in infected hosts. The uninfected hosts are not included (Reiczigel and Rozsa, 2010).
Mean abundance	The average number of parasite organisms found in all hosts. The uninfected hosts are thus included. This measure merges the two

	previous ones, prevalence and mean intensity (Reiczigel and Rozsa, 2010).

Landscape analysis terms

(Several definitions can be given depending on the study context, the following definitions were constructed or chosen for this study based on McGarigal and Marks (1995))

Patch	A patch is a continuous spatial domain of relatively homogenous environmental conditions regarding the biotope and the biocenose.
Landscape	A land with mosaic of patches, or cluster of ecosystems interacting.
Matrix	The most extensive and continuous patch within a landscape.
Landscape context	Landscapes are defined with a specific scale and are often arbitrarily delimited. Therefore, a landscape is always nested within a larger landscape which represents its landscape context.
Landscape structure	Also called landscape composition, the analysis of the patches diversity (presence and amount) regardless of their spatial distribution within a landscape.
Landscape configuration	The physical distribution and spatial pattern of patches within a landscape.

Abbreviations

SF	Spotted fever.
BSF	Brazilian spotted fever.
RMSF	Rocky mountain spotted fever.
SFG	Spotted fever group of the *Rickettsia* genus.
AF	The Brazilian Atlantic Forest.
LULC	Land use and land cover.
CRS	Coordinate Reference Systems (QGIS)

1 Introduction

1.1 Environmental epidemiology

Today (February 2023), most parts of the world recovered from the COVID-19 pandemic (WHO team, 2023a) that cost the lives of almost 7 million of people (WHO team, 2023b) and brought significant economic losses. The last 3 years informed lots of people on the risks of epidemic and pandemic from zoonotic diseases. Although still uncertain, the most likely candidate for the original SARS-COV-2 (the etiological agent of the COVID-19) reservoir species is the Horseshoe bat, presumably from the Chinese street markets (mostly wet markets) (Wu et al., 2020). Nevertheless, the zoonotic status of the COVID-19 is undiscussed (Boni et al., 2020; Lytras et al., 2021). This pandemic provided a strong example of the zoonoses exposure risk from the close contact between wild animals and humans. As a more recent example, the monkey pox disease has been declared emerging in non-endemic countries (WHO team, 2022). This re-emerging outbreak is also likely to be associated with wild-life and human contact (Reynolds et al., 2019). However, as the erosion of the natural habitats of wild animals is still ongoing, an increasing overlapping between humans and wild animal habitats is to be expected in the future, thus allowing more zoonoses to emerge (Gibb et al., 2020). Indeed, deforestation has been associated with multiple outbreaks of zoonotic and vector-borne diseases, mostly in intertropical regions whereas opposite patterns occur in temperate countries, with a reforestation associated with zoonoses emergence (Morand and Lajaunie, 2021a). For instance, the Ebola epidemics in Africa (Olivero et al., 2017; Rulli et al., 2017), as well as the recent resurgence of malaria in Brazil (MacDonald and Mordecai, 2019), took place in a context of deforestation. Land use changes, and in particular, oil palm plantation in tropical countries (Morand and Lajaunie, 2021b), which is commonly associated with vector-borne disease outbreaks (Loh et al., 2015), the agriculture industry, international travel, and trading, are the top drivers of zoonotic disease occurrences (Loh et al., 2015). This is a serious area of concern as land use changes are likely to increase in the future (Patz et al., 2004). Furthermore, deforestation and biodiversity loss favour reservoir and vector populations, increasing their contact with humans (Morand and Lajaunie, 2021b). Climate changes, which can be exacerbated by forest loss and land use changes, also enhance vector-borne diseases transmission by shifting the geographic range of vectors, increasing their reproduction, their biting rate, and shortening their incubation period (Patz et al., 2005; Vezzulli et al., 2013).

Therefore, it is important to ensure monitoring of these diseases, which can be achieved in the light of environmental epidemiology. Environmental epidemiology studies the distribution and environmental factors of diseases. More precisely, environmental epidemiology focuses on the physical, chemical, and biological agents that can affect the disease occurrences (Bloom, 2019). In the last two decades, new opportunities in this framework have been paving the way to a better understanding of epidemiological situations, such as analyses at the ecosystem level. This level includes climate changes, underlying land use changes (Dale, 1997), and their impacts on the ecology of pathogens, vectors and hosts, and human societies (Pekkanen and Pearce, 2001).

The present thesis is embedded in the ecosystem level of environmental epidemiology, as it characterizes landscape changes as factors of the Brazilian spotted fever risk. Therefore, the thesis contributes to improve our knowledge on the environmental zoonoses risk at a new-born level of the last decades.

1.2 Febre maculosa: The Brazilian spotted fever

1.2.1 Spotted fever epidemiology and features

The spotted fevers (SF) are zoonotic vector-bone diseases distributed in several continents: America, Africa, Europe, and Asia. The vectors are hematophagous arthropods such as lice, fleas, but mostly tick species (Blanton, 2019; Parola et al., 2013). The *Rickettsia* bacteria genus is the etiological agent of these diseases. Four groups compose the genus and three of them display pathogenic species of *Rickettsia*: the spotted fever group (SFG), the typhus group, and the transitional group, which includes organisms with features that are intermediate between the two others (Gillespie et al., 2008). Nevertheless, spotted fevers refer to the SFG, despite the typhus group and transitional bacteria being sometimes also involved in SF studies (Blanton, 2019; Moerbeck et al., 2016; Ogrzewalska et al., 2012). The bacteria are gram-negative bacilli, and they are intracellular obligated, as confirmed by their important genome reduction. Located in the endothelial host cell cytosol, they transport actively amino acids, phosphorylated sugars and adenosine triphosphate from the cell (Blanton, 2019).

The transmission of SFG bacteria occurs through the skin when an infected tick is feeding. Dendritic cells phagocytize the pathogens, which are then transported in the lymph to local lymph nodes. After replications in the lymph nodes, they enter the bloodstream and spread in the microcirculation where they infect endothelial cells. As the infection progresses, damage results, thereby increasing vascular permeability (Mansueto et al., 2011). Finally, rashes, eschars (Spolidorio et al., 2010), sometimes lymphadenopathy (Silva et al., 2011), and in severe cases, interstitial pneumonia, meningoencephalitis, several organ failures and death, can occur (Mansueto et al., 2011). The pathogenicity ranges from seroconversions with no symptom to high lethality rate (Figure 1). Most SFG members also induce febrile illnesses manifestations such as fever, headache, and myalgia, that are undifferentiable from other endemic diseases, especially in tropical regions (Blanton, 2019).

Although no vaccine exists, treatments are available. For example, the efficiency of bacteriostatic tetracyclines (Biggs et al., 2016), doxycycline (Todd et al., 2015), and the new macrolides (Azithromycin)(Anton et al., 2016) has been demonstrated. As soon as a SF is suspected, preventive administration of antibiotics should be carried out. Yet, physicians sometimes fail to diagnose SF diseases in the early stage because their symptoms are similar to those of other more prevalent illnesses (Blanton, 2019; Regan et al., 2015). Moreover, some serological identification techniques, such as PCR targeting *Rickettsia* DNA, are ineffective, as the bacteria infect endothelial cells, thereby presenting very low level of abundance in the host bloodstream (Paris and Dumler, 2016; Souza et al., 2009). PCR can only confirm the SF diagnosis at the late stage of infection, when performed on biopsies from the eschars (Morand et al., 2018). The early stage diagnosis should be performed by immunofluorescence assay (IFA)(Biggs et al., 2016). This technique is effective despite the fact that a large species diversity of *Rickettsia* exists because the group-specific antigens are cross reactive (Delisle et al., 2016). Additionally, investigating historical details of the patient should suggest a potential SF infection, for instance, recent travels, recreational activities, and main occupation, in relationship to the endemic areas of the SF (Blanton, 2019; Ogrzewalska et al., 2012).

The main vectors of SFG *Rickettsia* are ticks. The ubiquitous feature of the SFG is due to their ability to infect various tick species worldwide (Parola et al., 2013). For most of the SFG rickettsioses, ticks are considered as vectors but also reservoir hosts, as the bacteria can be transmitted transovarially and transstadially. However, sustained vertical transmission is not common and does not seem to depend on tick species. Hence, the prevalence of *Rickettsia* among ticks is variable (Harris et al., 2017). Moreover, the peaks of SFG rickettsioses are intimately linked to the ecology of the main vector tick species, so that most of the peak occur during the warm seasons when the ticks are the most active. Nonetheless, few examples show rickettsiose peaks during the cold seasons, during which peculiar tick species with different ecological features are present (Blanton, 2019).

The Brazilian spotted fever (BSF), or febre maculosa, is known in the American continent as the rocky mountain spotted fever (RMSF)(Souza et al., 2009) because the disease was originally described in the Idaho state of the USA (Labruna et al., 2014). The BSF is mainly transmitted by *Amblyomma* tick species. It is known in Brazil since the 1920s (Labruna, 2009). Until the 2000s, this rickettsiose was thought to be caused by a sole bacterium, but today, several *Rickettsia* etiological agents are known to be involved in the BSF (Labruna and V, 2011), and more recently, an Atlantic rainforest strain was discovered (M. P. J. Szabó et al., 2013). Over the years, the number of reported and confirmed BSF cases increased (Figure 1) as this disease has to be notified in the disease information system since 2007 (Oliveira et al., 2016) and efficient techniques to diagnose it have become increasingly available. However, the number of cases is underestimated since the disease is still neglected or sometimes hardly distinctive from other tropical febrile illnesses (Biggs et al., 2016). The average BSF case-fatality rate in Brazil between 2007 and 2015 was 33% (Figure 1).

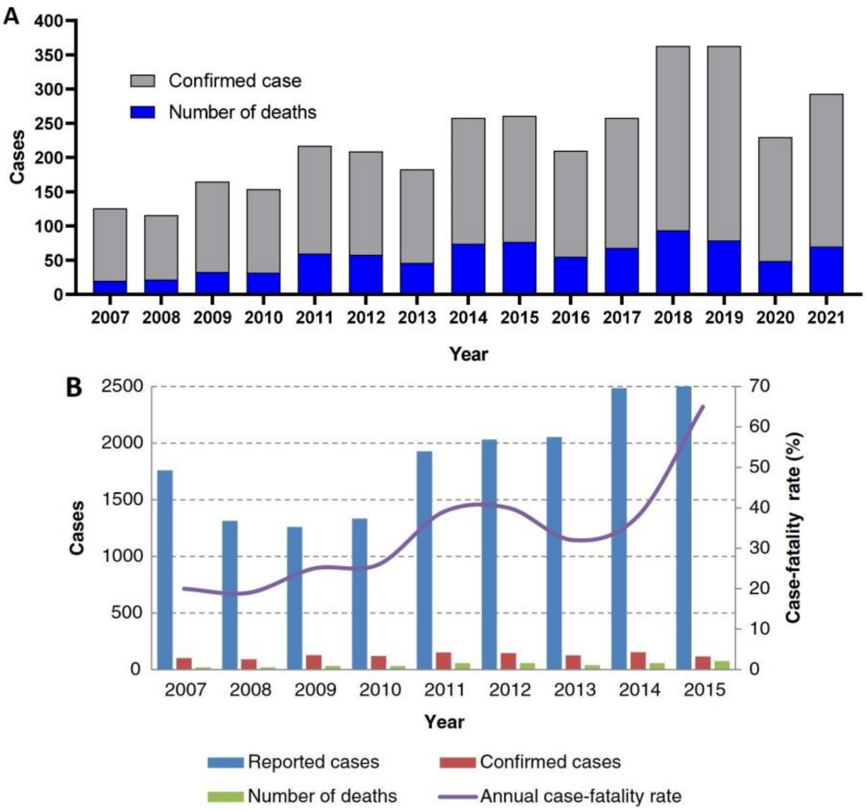

Figure 1 : **A.** Number of Brazilian spotted fever confirmed cases and death cases per year, 2007 to 2021 (Alcon-Chino and De-Simone, 2022). **B.** Annual number of reported, confirmed, and death cases of BSF, with their case-fatality rate, 2007 to 2015 (Oliveira et al., 2016).

This severe disease presents the common symptoms of a SF listed previously. More rarely, eschars formations, but additional vomiting, nausea, and abdominal pains, were reported (Blanton, 2019). The most concerning and lethal SF pathogen in Brazil is *Rickettsia rickettsii* (Walker et al., 2008), with a lethality of 40%, involving pulmonary deficiency, acute kidney tubular necrosis, and neurologic troubles (Blanton, 2019). In comparison, the RMSF can have lower lethality rate in other countries of the American continent, between <1% in USA and 30% in Mexico (Blanton, 2019; Dahlgren et al., 2012; Openshaw et al., 2010), and the Mediterranean spotted fever (MSF) has a lethal rate of 2.5%, which is the second most severe SF disease (Herrador et al., 2017).

1.2.2 BSF eco-epidemiology

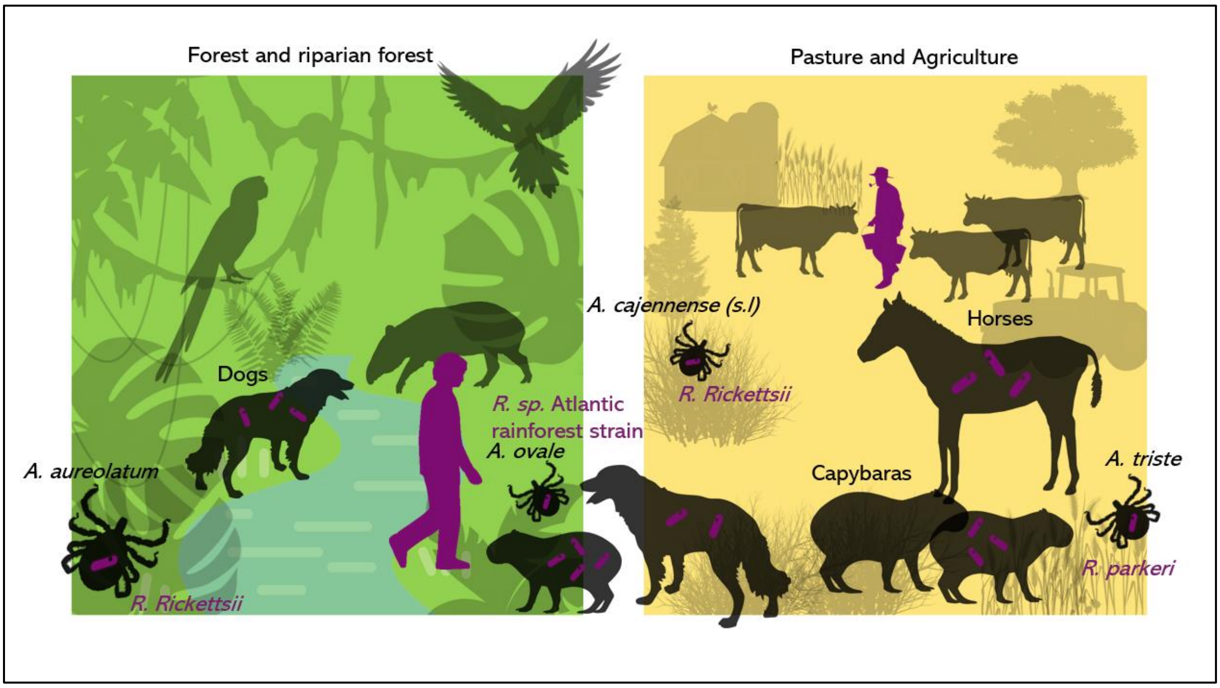

Figure 2 : Overview of the main features of the Brazilian spotted fever eco-epidemiology found in the literature. Left side represents dense vegetation environments, with riparian features. Right side represents open landscapes, mainly pasture and agriculture in the Atlantic Forest. The four main *Amblyomma* vector species are represented in the habitat that is the most associated with them in the literature. The main *Rickettsia* bacterium associated with a tick species is written in purple. The main three BSF amplifier hosts are also represented in their main environment. Non amplifier hosts are also represented and can also contribute to the BSF cycle by maintaining tick populations or translocating them.

Today, the main BSF agents known are *Rickettsia rickettsii*, *Rickettsia parkeri* (Labruna, 2009), and the newly discovered *Rickettsia sp.* Atlantic rainforest strain, which is a *R. parkeri*-like bacterium (Spolidorio et al., 2010; M. P. J. Szabó et al., 2013). In Brazil, some patients (Ministério da Saúde do Brazil, 1991) suspected of BSF were sometimes found infected with *Rickettsia bellii (basal group)*, *R. prowazekii* and *R. typhi* (typhus group), and *R. felis* (transitional group), but the pathogenicity of this last one is still discussed and these bacteria are not part of the SFG (Blanton, 2019; Labruna, 2009). Each of these bacteria species have specific vectors species that, in the case of vector-borne disease, are also their main reservoir hosts (Labruna, 2009). Except for *R. felis* and *R. thypi* whose vector species are fleas of the *Ctenocephalides* genus and *Xenopsylla cheops* respectively, and *R. prowazekii*, which is associated with the human body lice, *Pediculus humanus corporis*, others *Rickettsia* (SFG) spread by tick species, especially the *Amblyomma* genus in Brazil. The main vectors of *R. rickettsii* are the common tick species *Amblyomma cajennense* (*s.l.*) in southern Brazil and *A. aureolatum*, especially in the São Paulo metropolitan area (Labruna, 2009; Ogrzewalska et al., 2012). *Rhipicephalus sanguineus* was also observed (Ogrzewalska et al., 2012) and proven in laboratory (Piranda et al., 2011) to be a competent vector of this agent. For *R. parkeri*, the main vector is the tick species *A. triste* (Silveira et al., 2007). Although the fact that *A. dubitatum* is a vector of human diseases is not established, this tick species is frequently associated with *R. bellii* (Sakai et al., 2014). Ultimately, the Atlantic rainforest *Rickettsia* strain is found strongly associated with *A. ovale* (M. Szabó et al., 2013) (Figure 2).

Most etiological agents of BSF also spread by vertical (from female to offspring) and horizontal transmissions (between individuals of the same generation) among vector species. However, the highly lethal *Rickettsia rickettsii* is pathogenic and partially deleterious for its *Amblyomma* vector species; therefore, the pathogen remains in the environment mostly by horizontal transmissions rather than vertical transmissions. It is also worth noting that although the bacterium is not deleterious for its *R. sanguineus* vector, this tick species is not as aggressive to humans as the *A. cajennense* vector (M. Szabó et al., 2013). To allow these horizontal transmissions to occur and the subsistence of *R. rickettsii*, amplifier hosts (Lexicon) are thus required (Ogrzewalska et al., 2012; Walker et al., 2008). On the other hand, less pathogenic *Rickettsia* (also for humans), such as *R. felis* and *R. parkeri* (Labruna, 2009), have effective transovarial transmissions. Additionally, one bacterium species infecting a vector host can interfere with the transovarial transmission of another *Rickettsia* species in that same host (Sakai et al., 2014).

Despite vertical transmissions do not always occur, depending on the pathogenicity of the *Rickettsia* species, horizontal transmissions allow the persistence of pathogens in the environment as soon as the vectors are able to parasite amplifier hosts (Blanton, 2019). In Brazil, and more precisely the Atlantic Forest, the biome studied in the present thesis, several candidates were identified as amplifier hosts for the spotted fever. For instance, domestic dogs (Moerbeck et al., 2016; Ogrzewalska et al., 2012), horses (Souza et al., 2016), capybaras (*Hydrochoerus hydrocaeris*) (Souza et al., 2009; M. Szabó et al., 2013) have been identified as amplifier hosts, and potentially some small rodents (Lopes et al., 2018; M. P. J. Szabó et al., 2013). The amplifier role of passerine birds is also suspected but there is still no consistent data to support this hypothesis (Ogrzewalska and Pinter, 2016). There is also little but not strong evidences of coatis (*Nasua nasua*) implication in the *Rickettsiales* cycle in the Atlantic Forest (Magalhães-Matos et al., 2022). Domestic dogs were found competent amplifier host, in association with *Amblyomma aureolatum* (prevalence of 19.3%, mean intensity of 3.8) and *Rhipicephalus sanguineus* (prevalence of 10.6%, mean intensity of 19.3) tick species, in the Atlantic Forest (Ogrzewalska et al., 2012). The amplifier host and epidemiological features of a given BSF *Rickettsia* are a function of the vector species ecology (M. Szabó et al., 2013). For example, *Amblyomma cajennense* (*A. sculptum*)(Martins et al., 2016), one of the main tick vector species of BSF, was shown to be a three-host species (M. Szabó et al., 2013) and to present differential vector competence, depending on the tick developmental stages. The nymphs of this tick species are also more active and aggressive to humans (Soares et al., 2011) during the winter and spring, where BSF is the most prevalent (Pinter et al., 2011). It is also now accepted that capybaras play a major role in the BSF infection of *R. rickettsii* lethal agent, with the three stages of *A. cajennense* tick species by infecting up to 35% of individuals feeding on them (Souza et al., 2009) (Figure 2).

Most of the studies previously cited investigate the BSF occurrence in the south of Brazil, especially across the Atlantic Forest municipalities. These highlighted some environmental and ecological variables that might trigger BSF outbreaks. Szabó et al. (2009) suggest that dense rainforest environments, with a high humidity and darkness, could decrease the abundance of *A. cajennense* (*A. sculptum*) and *A. dubitatum* in bushes, since these species thrive on degraded and open areas with no primary forest. However, in this study such open environments were near an artificial water body where capybaras were found abundantly, which may have confused the relationship with the landscape. In opposition, for *A. aureolatum* and *A. ovale*, dense vegetation seems to be the areas the most at risk (Szabó et al., 2009). Another study shows that temperature seems to drive *A. cajennense* distribution more than humidity. High altitude temperatures may be also deleterious environment for this tick species (Estrada-Peña et al., 2004).

Another important factor accounting for the BSF incidence is the dynamic of amplifier host populations. Although their natural habitat are environments close to waterbodies such as riparian forest fragments (M. Szabó et al., 2013) or seasonally flooded savanna (Verdade and Ferraz, 2006), capybaras are semi-aquatic rodents that can also be adapted to anthropogenic ecosystem, where they are found even more abundantly, such as rivers crossing cities like São Paulo, agroecosystems like crops not far from water (Verdade and Ferraz, 2006) or artificial waterbodies create by dams (M. Szabó et al., 2013; Szabó et al., 2009). Excepted for riparian forests, forests are usually habitats avoided by them, they show higher preference for open areas of grasses or shrubs, especially in human-modified landscapes (Dias et al., 2020). Moreover, the landscape changes of the Atlantic Forest also tends to promote forest regeneration in high altitudes or steep slopes (Lira et al., 2021). We assume that steep slopes may be an additional factor influencing their frequentation, but also by humans and domestic dogs. Nonetheless, the recent and important land conversion dynamic of pasture lands to crops (such as sugar cane) in the Atlantic forest (Ferraz et al., 2014; Lira et al., 2021) increases formation of grazing environments for capybaras as well, particularly near water streams (Felix et al., 2014; Verdade and Ferraz, 2006). In the last decades, increasing capybara populations is suspected to be partially responsible of the increasing BSF cases, as they are involved in the sylvatic cycle of *R. rickettsii* (Souza et al., 2009; M. Szabó et al., 2013). However, controlling the capybara populations raises some ethical and political issues in Brazil. Dogs are amplifier hosts as well, and sensibilizing the population about the risk of unrestrained or wild ownerless dogs that travel through dwellings and wildlife areas, or about the ticks themselves (the use of repellent), should be used as preventive measures. Furthermore, the BSF risk is multifactorial and complex as it involves several host species with different ecological requirements, thus such a risk cannot be attributed only to capybaras (Labruna, 2013). Nonetheless, hot-spots of BSF infection frequently correspond to areas shared by the tick vectors and capybaras (M. Szabó et al., 2013) and potentially by domestic animals that can act as amplifier hosts of this pathogen. Additionally, other non-amplifier host animals (birds, felines, cattle, etc.) can host secondarily the ticks and thus translocate them between areas (de Paula et al., 2022) (Figure 2).

Finally, the landscape accounted as a variable of the BSF risk is worthy to study as it implies the ecological niches of both vector and host species. A study carried out in the São Paulo metropolitan areas (Ogrzewalska et al., 2012) showed that endemic areas of BSF harbour smaller forest patches with less connectivity between them (higher nearest neighbour distance), and additionally, lower species richness of birds and small mammals than non-endemic areas. These endemic areas of BSF have also prevalent young secondary forests whereas non-endemic ones are covered by late and intermediate secondary forests. Then, the landscape matrix should be considered. For instance, crops (corn, rice, soybeans or sugar cane) and grazing pastures are preferred environment of capybaras according to their feeding behaviour (Felix et al., 2014). Moreover, in areas of pasture, implantation of small bushes and shrubs provides the questing spots required for ambushed tick species involve in rickettsioses cycle (Labruna et al., 2001). For example, *A. cajennense* (*s.l.*), one of the main vector species of the highly lethal *R. rickettsii* (Szabó et al., 2009), is favoured by degraded areas or landscapes with large amounts of forest edge (M. Szabó et al., 2013). On the other hand, *A. ovale*, the Atlantic rainforest *Rickettsia* reservoir, is more abundant near trails in dense canopy (Szabó et al., 2009). However, the impact of this species on BSF incidence could be less significant as the major amplifier host known are not found in abundance under dense canopy.

The BSF risk is thereby directly correlated with suitable environmental conditions associated to the landscape for vector species, but also amplifier host. Unfortunately, these landscapes tend to be more present as degradations of the Brazilian Atlantic Forest are still ongoing.

1.3 The Brazilian Atlantic Forest

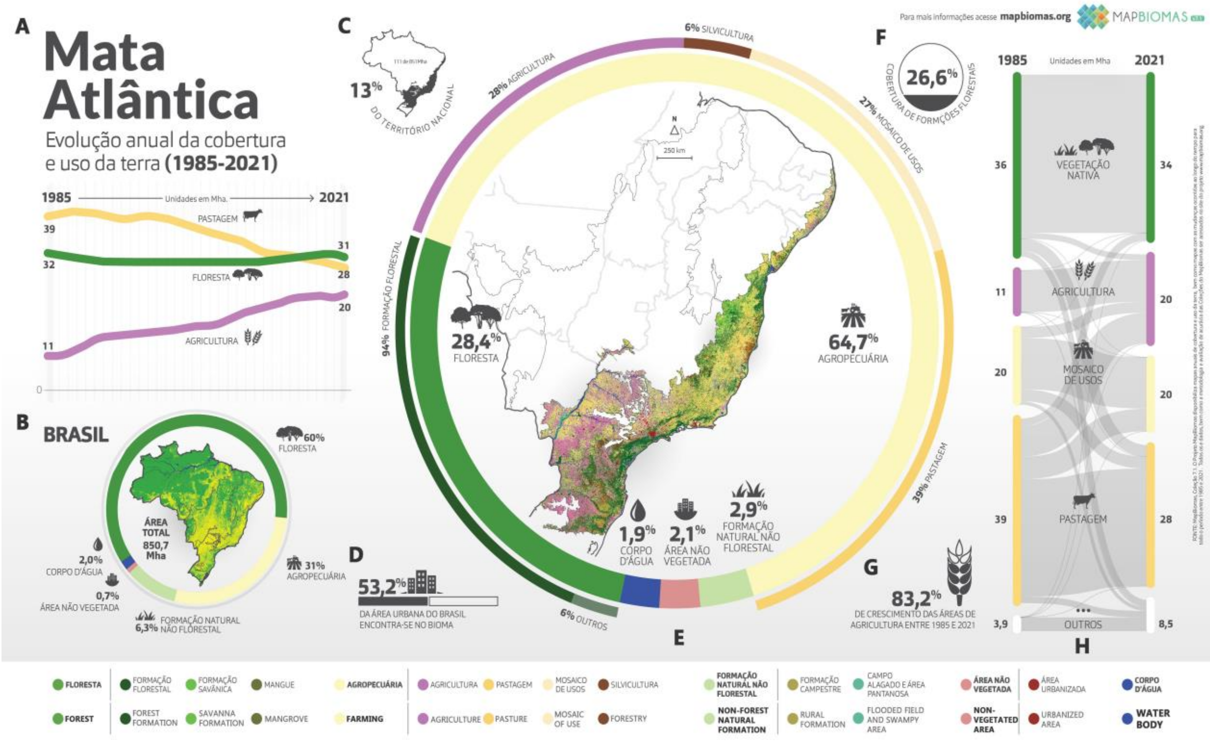

Figure 3 : Overall land use and land cover state of the Brazilian Atlantic Forest (Mata Atlântica) for the year 2021 (MapBiomas Brasil, 2021). **A.** Annual evolution of the major land cover and land use of the biome between 1985 and 2021. **B.** Perspective of the land use categories for the whole Brazil. **C.** Percentage of Brazilian land cover of the biome. **D.** Proportion of urban area encountered in the biome. **E.** Land use and land cover of the biome. **F.** Native vegetation cover. **G.** Increase in agricultural cover between 1985 and 2021. **H.** Land use and Land cover transition between 1985 and 2021 in millions of hectares.

Most of the prior studies on Febre maculosa evaluated the risk of infection in specific states of Brazil. This study takes place in the Brazilian Atlantic Forest (AF) municipalities. The Atlantic Forest (Mata Atlântica) is a tropical hotspot of biodiversity that crosses south-eastern municipalities of Brazil and their coasts within multiple states. The biome is composed of several ecosystems which raise important levels of endemism and species richness (Ribeiro et al., 2011). The AF is a relevant biome to study the emergence of tropical zoonotic diseases as it underwent several land use and land cover conversion during the last decades (Box 1).

Forest fragmentation Indeed, forest degradation is the major threat of the AF. Pastures were the main land use 30 years ago, followed by native forest land cover. While the agriculture has increased, pasture has decreased, partially because of pastures conversion to agriculture lands, and especially with the expansion of sugarcane and *Eucalyptus* plantations (Lira et al., 2021; Ribeiro et al., 2011). Pasture and agriculture are now the principal occupation of the territory (Figure 3A and 3H). However, with the agricultural mechanisation some areas were let to regenerate, such as in steep slopes and riparian zones (Ferraz et al., 2014; Teixeira et al., 2009). This passive regeneration, or sometimes active, has increased the last decades (Crouzeilles et al., 2019). Over the last decade, the AF was at 28% of its original native forest cover extent (Figure 3E, see also appendix Figure A1). Yet, as the deforestation still occurs concurrently with the forest regeneration, the old primary native forests are thus replaced by young secondary forests (Ferraz et al., 2014; Teixeira et al., 2009). As a consequence, the mitigation services of zoonotic diseases among several others ecosystem services provided by the AF are weakened, as secondary forests were shown to provide services of lesser quality (Ferraz et al., 2014)(Box 1). This diseases mitigation service was also suggested to occur with the BSF in the AF (Claudia Araujo Scinachi, 2022; M. Szabó et al., 2013). The importance of primary forest conservation has been many times highlighted as well (Calaboni et al., 2018; Ferraz et al., 2014).

Today, the AF are fragmented landscapes with mainly agricultural and pasture matrix (Figure 3A, 3E, 3H). Most of the forest fragments are smaller than 5 hectares (Lira et al., 2021). This landscape configuration threatens the biodiversity. Then, high biodiversity ecosystems when threatened are directly correlated with the risk of new emerging zoonoses (Allen et al., 2017; Keesing and Ostfeld, 2021). The zoonoses mitigation service of biodiversity through a dilution effect is now quite accepted in the scientific community. This dilution effect implies that biodiversity loss gives opportunities to reservoir species to increase in abundance, thus increasing the risk of an effective zoonotic spillover in human populations (Keesing and Ostfeld, 2021). Investing more efforts on the restoration and conservation of functional landscapes (for example, with bigger forest patches) can provide efficient mitigation of zoonoses (Ferraz et al., 2014).

Box 1 : Summary of historical land use and land cover changes and current stage of the Brazilian Atlantic Forest (AF).

As the Portuguese arrived in south America in 1500, the exploitation of the Brazilwood tree (*Paubrasilia echinate*) started for dyes then instruments manufacturing (Lira et al., 2021) and its overexploitation led the species to be threaten today (Martinelli and Moraes, 2013). Between the 18th and the middle of the 20th century, the AF went through important cycles of degradation caused by sugarcane agriculture, pasture, gold mining, coffee plantation, araucaria trees (*Araucaria angustifolia*) logging, that after being gone, were replaced by forestry of *Eucalyptus* and *Pinus spp.* In 1985, pastures were the main land use in the AF biome but in the following 3 decades they were progressively replaced by agriculture areas. This land use conversion has resulted in a reduction of 25% of pastures and a double increase in agriculture areas from 1985 to 2021 (Figure 3A and 3H). During the last 50 years, sugarcane plantation has expanded especially for ethanol production (Lira et al., 2021). Additionally, the construction of multiple hydroelectric dams (Lira et al., 2021) and the expansion of urban areas (especially country houses for leisure) have also contributed to the forest cover lost (Teixeira et al., 2009). Forestry with short rotation cycles has also increased by 200% (Ribeiro et al., 2011; Teixeira et al., 2009). Over the last decade, this biome counted 28% of remaining native forest (Figure 3E, see also appendix Figure A1) including 9% in strictly protected areas (IUCN categories I-IV) (Rezende et al., 2018). Forest degradation is the current major threat of these ecosystems in Brazil, especially due to agricultural expansion, mostly sugarcane crops and *Eucalyptus* plantations (Ribeiro et al., 2011).

However, there are passive and active ongoing processes of restoration that have increased over the last decades (Crouzeilles et al., 2019). As agriculture and forestry expansion also rely on heavy mechanisation (Calaboni et al., 2018) and the international market demand, some areas with low productivity such as those in steep slopes and riparian zones were allowed to regenerate passively, and in some cases, underwent active restoration (Ferraz et al., 2014; Teixeira et al., 2009). The guidance of the active regeneration can be carried out by organisation such the Atlantic Forest restoration pact. It is a national organism that gather private institutions, governments, and scientific actors, among others, interested in restoring the forest. The main purpose of this pact is to restore 15 million hectares by the year 2050 (Pact for the Restoration of the Atlantic Forest, 2023) to comply with the Brazilian environmental legislation (Ribeiro et al., 2011). In Brazil, there is a native vegetation proctection low (NVPL) which was instored in 2012 (TJDFT, 2015). This NVPL includes the legislation of areas in permanent preservation (APP). These legislation implies areas bodering any river streams, natural water bodies and artificial ones when these are created by dams, and also some areas under specific conditions of topography. In such areas, the land owners must preserve the vegetation regardless of the presence of native vegetation or not. The alteration or degradation of the native vegetation is restricted to cases of public utility, social interest or low environmental impact. Since 2008, landowners must favorised the regeneration in case of unauthorized degradations. The APP not only preserve the landsacapes of riparian environments, but also insure geological and soil stability, and biodiversity conservation by acting as ecological corridors (TJDFT, 2015). Although APP can be opportunities for the native vegetation to regrowth, most remaining vegetation of the Atlantic Forest is located in non protected rural properties (Rezende et al., 2018). Thereof, the current vegetation proctection laws may present a lack in conservation of the native primary forests, promoting younger secondary forest formations (Teixeira et al., 2009). Additionnaly, a study by Molin et al. (2018) shows that in the AF a scenario of forest regeneration solely focusing on riparian areas may not be the most cost-effective strategy. The most cost-effective scenario would take into account the main drivers of natural regeneration opportunities to save efforts invested in active regeneration. Distance to water streams and distance to forest remnants are the main keys of this natural passive regeneration, steep slopes also but depending of the main land use type in the landscape (Molin et al., 2018). Therefore, areas with important cover of forest remnants are more suitable for regeneration as they are a direct source of seeds, hence the importance of their conservation (Calaboni et al., 2018).

Restoring this threatened forest is crucial since it provides several support, regulation, and cultural ecosystem services. For example, the AF biome provides 50% of the freshwater for the coastal populations, mostly in the Rio de Janeiro and São Paulo cities, and a significant contribution to the global carbon balance (Ribeiro et al., 2011). Furthermore, prior studies pointed out the mitigation service on the transmission risk of zoonotic diseases such as those caused by hantaviruses (Prist et al., 2021), and others suggested the same effect of tropical forests on the BSF (Claudia Araujo Scinachi, 2022; M. Szabó et al., 2013). Nevertheless, the fast anthropogenic landscape changes can provide new opportunities of tick-host relationships by offering suitable habitats for vectors and hosts or disturb existing relationships, thus facilitating the emergence of this tick-borne diseases (M. Szabó et al., 2013). Besides restoration, conservation of the primary forests is also important for the provisioning of ecosystems services with higher quality (Ferraz et al., 2014).

Today the forest cover of the Atlantic Forest has been increasing. However, the biome faces an important turnover of its old native pristine vegetation by young secondary forests as deforestation still occurs simultaneously with restoration (Ferraz et al., 2014; Teixeira et al., 2009). Moreover, studies pointed out that these regenerated forests tend not to persist in tropical regions (Piffer et al., 2022a, 2022b; Reid et al., 2018). Therefore, despite the forest cover has increased, its quality has decreased (Ferraz et al., 2014). Some studies highligthed this phenomenon as an hidden destruction of the old native forests (Rosa et al., 2021). The forest covers of the AF are fragmented landscapes whose main matrix types are now pasture and agriculture (Figure 3A, 3E, 3H). The forest fragments larger than 10.000 ha represent 0.03% of the total, when more than 80% are smaller than 5 ha. The distance edge-to-edge between forest fragments is less than 250 m in 73% of the cases and the mean distance between forest fragments is 1440 m but the role of small ones (<50 ha) is important in increasing the connectivity (Lira et al., 2021). This landscapes configuration is a threat for the biodiversity. Indeed, only 5% of the extent of the Atlantic forest reach the minimum amount of forest to preserve high levels of biodiversity (Tambosi et al., 2014) when most of the biome is below that threshold (Banks-Leite et al., 2014). Additionally, as a consequence of forest fragmentation, a consequent part of the forest is under an edge effect process which provokes changes in abiotic conditions (Laurance et al., 2002), providing unsuitable habitats for many forest-dependent species (Oliveira et al., 2004; Pfeifer et al., 2017). The matrix type also plays a significant role in the forest fragment connectivity and thereby in the biodiversity integrity by mitigating or increasing the edge effect. For instance, when small forest fragments are surrounded by a more permeable matrix type (with forest-like vegetation structure), it decreases the intensity of the edge effect and it allows more biological flow (Boesing et al., 2018a, 2018b). Moreover, the small forest fragments of the Atlantic Forest are more likely to undergo a "secondarization" process. This is a retrogressive succession where shade-tolerant species of old growth forests are replaced by sets of pioneer fast-growing species (Oliveira et al., 2004). Secondarization processes were also shown to be driver of defaunation (Canale et al., 2012). Overall, all these processes disturb the functionality of the AF ecosystems.

1.4 Objectives and hypotheses

This master thesis aims to understand the effects of the landscape dynamics over the number of humans cases of the Brazilian spotted fever in the Atlantic Forest municipalities, over the last 2 decades. Underlying more specific objectives such as (1) creating a temporal database of forest cover and configuration in the studied areas based on land use and land cover data available from the MapBiomas initiative, (2) assessing land use changes in the Atlantic Forest by conducting analyses in geographic information system environment, (3) collecting and organizing data on BSF occurrence in each municipality, and finally (4) analysing the relationship between landscape changes and BSF occurrences using generalized linear mixed models.

Several hypotheses can already be stated about the epidemiological risk of BSF across the Atlantic Forest based on the current literature:

(1) Forest amount and regeneration hypothesis: We hypothesise that high amount of forest cover could reduce the transmission risk of spotted fever. However, some ticks species are also favoured by forest cover and municipalities with high level of secondary regenerated forests can also increase the risk of BSF.

(2) Landscapes configuration hypothesis: Higher number of BSF cases are expected to be found in landscapes with an increased number of forest fragment, and thus forest edge effect, with low connectivity between them and immersed in a human modified landscape matrix especially pasture and agriculture. This landscape scenario would be the most at risk because open degraded areas gather the ecological features of some tick species but, above all, the major amplifier hosts.

(3) Riparian forest hypothesis: Municipalities with low forest cover but large amount of riparian forests, and consequently of forest edge, within agricultural matrices would increase the transmission risk.

(4) Land conversion hypothesis: Municipalities where a high rate of land conversion occurred in the past could present higher BSF incidence.

(5) Topography hypothesis: Presence of steep slopes and high-altitude mounts in municipalities may reduce the BSF incidence.

This study will contribute to the outcomes of the scientific community engaged in the restoration pact (Box 1) and will provide knowledges to help the management of the Atlantic Forest. It will also inform on the landscapes presenting higher risk of BSF infection within the AF, thereby helping physician diagnoses to suspect this disease and propose the suitable treatment. Finally, It will help suggest improvement of the overall one-health (FAO, OIE, WHO, UNEP, 2021) of the Brazilian people and the environment.

2 Material and methods

2.1 Data collection

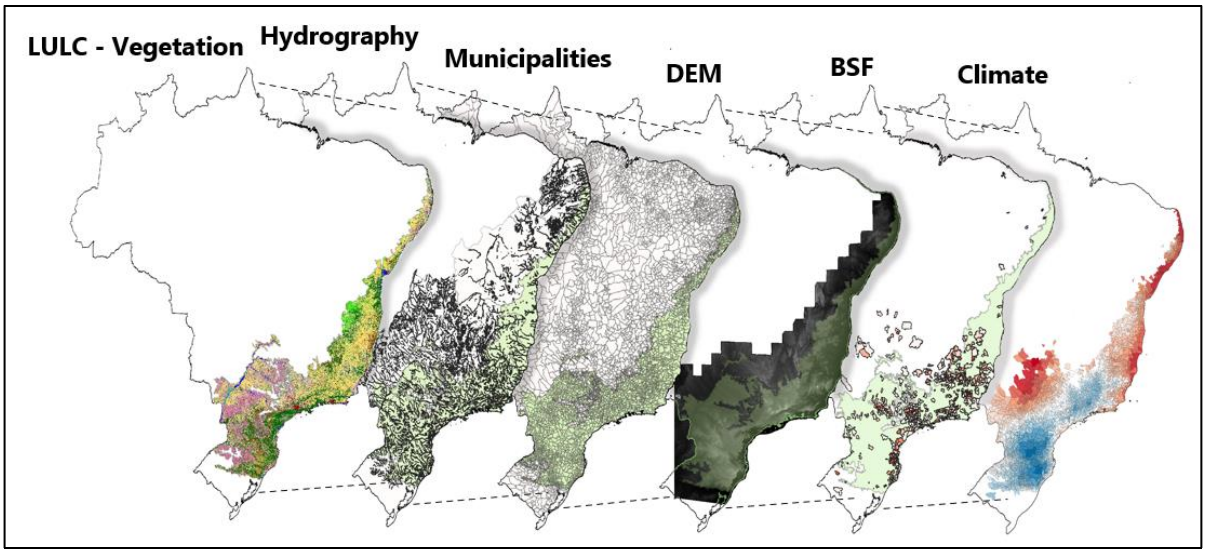

Figure 4 : Summary of the data used for the present thesis and the period covered by each. Raster: Land use and Land cover (LULC) (2001 to 2021), Primary and secondary vegetations data (2001 to 2019), and digital elevation model (DEM) (2000). Shapefiles: Hydrography of Brazilian states within the Atlantic Forest biome (2015), municipalities of Brazil (2022). Dataset: climatic data of temperature and precipitation (2000 to 2021), BSF cases per year (2001 to 2022), table of LULC transitions (2001 to 2021).

2.1.1 Brazilian spotted fever data

Brazilian spotted fever data were collected on the mandatory notifiable diseases information system (SINAN) from the Brazilian health ministry web site (Ministério da Saúde do Brazil, 1991). Data on BSF confirmed cases per year of notification and per municipality of residence were retrieved within tabNet. Reported cases were extracted from the TabWin database. Confirmed cases were defined as mentioned by the ministry of health (Ministério da Saúde, 2021). Cases concerning patients not residing in Brazil were excluded from the dataset available. Because any case of BSF has to be notified since 2007 (Oliveira et al., 2016) and a few confirmed cases were notified before this year, BSF data covering the period from 2001 to 2022 were available and thus collected for these years. The numbers of autochthon cases, for which probable place of infection is the residence municipality, among confirmed cases per year were collected on the same platform. Besides, data were gathered on the probable place of infection between the following categories: workplace, leisure, home, others, and unknown. The probable place of infection, reported, autochthon, and death cases, were not available before 2007, and 2022 data are still preliminary. The estimate numbers of inhabitants per municipalities were also collected (2000 to 2021 - Preliminary estimates by the Ministry of Health (Brazil)/SVSA/DAENT/CGIAE). Then, BSF incidence per municipalities per 100.000 inhabitants were calculated (BSF incidence = (BSF confirmed cases/number of inhabitants) * 100.000) as carried out in a similar study (Vassari-Pereira et al., 2022). The period available for studying BSF incidences is thus reduced to the years from 2001 to 2021 because of the demographic data availability. BSF cumulative incidences per municipalities for this period were also calculated. Tabulation and calculation were performed using R software (version 4.1.2)(R Core Team, 2021).

2.1.2 Land use and land cover data

Annual raster data on the land use and land cover (LULC) of the whole Brazil from the MapBiomas initiative (collection 7)(MapBiomas Project, 2022a) were downloaded on the MapBiomas Brazil website, for the 1985 to 2021 period. See the appendices for the LULC classes details (Table A1, Table A3). From the same collection, raster data on the deforestation and secondary vegetation were retrieved. These rasters contain information on the persistence or deforestation through time of the primary and secondary vegetation classes (MapBiomas Project, 2022b). Only data until 2019 were available, thus these rasters were collected from 2001 to 2019 as no BSF data were available before 2001. Landsat satellite images are used by MapBiomas to develop the LULC rasters for each biome of Brazil with a 30 m resolution (MapBiomas Project, 2015). Moreover, the table of transitions over the years between the different LULC categories of the collection 7.1 was acquired (number of hectares for each municipality). The Atlantic Forest biome delimitation was downloaded from MapBiomas. A vector layer of the Brazilian municipalities (2022) was also downloaded from the Brazilian institute of geography and statistic website (Instituto Brasileiro de Geografia e Estatística - IBGE, 2022), this shapefile includes municipality names and their identification code, superficies, and the abbreviation letters of their respective federal unit (states of Brazil).

2.1.3 Others abiotic data

The hydrography shapefiles per Brazilian states of the AF were downloaded from the project of high-resolution biome mapping of the Brazilian foundation for sustainable development (FBDS, 2015). The detailed hydrography includes rivers less than 10 m wide, river more than 10 m wide, and waterbodies (>10 m). Per these previous categories, each hydrography shapefiles of the AF states were merged.

Furthermore, climatic data on the monthly mean temperature and total precipitation were gathered for each municipality (average value across the extent) of the studied zone (See section 2.2.2) and for the period considered. The gridded land surface temperature data are provided by the National Centers for Environmental Prediction (NOAA NCEP). These data are combined data from GHCN and CAMS stations at a 0.5° spatial resolution (Fan and van den Dool, 2008, 2004). The precipitation data are supplied by the University of California Santa Barbara, using the Climate Hazards Group Infrared Precipitation with Stations (CHIRPS) dataset of the 10-day averages precipitation, with a 0.05° resolution (Funk et al., 2014). Both climate datasets were retrieved using the Data Library (IRI, 2023, 2020) of the International Research Institute for Climate and Society (IRI).

Digital elevation model scenes for a broader region of the AF were retrieved from the NASA SRTM 1-Arc Second Global mission (2000)(approximately 30 m resolution)(Farr et al., 2007; NASA JPL, 2013), using Google Earth Engine (Earth Engine, 2013). Then, all the scenes were merged. All shapefile and raster manipulations were carried out in the QGIS software.

2.2 Analysis

2.2.1 Exploratory analyses of BSF data

Number of spotted fever cases, death cases, and case-fatality rate per year were plotted. The number of suspected cases from the reported cases were established according to the definitions provided by the ministry of health of Brazil (Ministério da Saúde, 2021) and inspired by Oliveira et al. (2016). The annual case-fatality rate was calculated with the absolute number of deaths caused by SF and the confirmed SF cases. The average case-fatality rate was calculated for the period of data availability. Moreover, the global proportion per year of BSF cases that are autochthon of the municipality of residence were assessed. Because this feature of the cases was not notified before the year 2007, the proportion of autochthon cases per municipalities per year were not evaluated for the further analyses. Solely the percentage of autochthon BSF cases per year was plotted and the estimated average percentage for the whole period was calculated (assuming a Student distribution) to provide an overview on the proportion of cases incidence that can be related to the municipality landscape. Additionally, the total percentages of probable place of infection were rendered. These results were plotted using Microsoft Excel.

2.2.2 Zone studied

The BSF incidence data for each year and the cumulative cases incidence were thereafter merged with their respective municipalities according to their code, and then mapped. Considering the distribution of the municipalities with BSF incidences in Brazil, see results section (Figure 8), we decided that the zone studied would comprise all the municipalities that intercept the AF biome and the municipalities with BSF incidences that intercept a 100 km buffer around the AF (see the extent of the studied zone in the appendices, Figure A2). From this selection, the 2 municipalities included in the AF (Fernando de Noronha and Vitória) but composed solely of islands further than 100 km from the continent were excluded because no LULC data are available for them. In total, 3121 municipalities are thus considered in the present study. All the operations were conducted within the QGIS software (version 3.26.3)(QGIS Development Team, 2022).

2.2.3 Land use and Land cover processing

First, considering the hypotheses stated above, a reclassification of the 27 classes of LULC (Table A1) from the 7th collection of MapBiomas rasters were carried out in QGIS. Indeed, the present study only used 9 classes which are: native forest, non-forest native formation (wetland, grassland, others), pasture, agriculture, mosaic of uses (pasture and agriculture), silviculture, non-vegetated area (sand spot, mining, others), urban area, and water, for more details see the appendices (Table A2). A special attention was taken for the savanna formation: this class gathers savannas from the wooded savannas at the borders and within the AF biome to the grassy savannas of the Cerrado. Because of their lower and variable canopy cover, savannas are not expected to have the deleterious effect of the rainforest on the tick species that thrive in open areas such as *A. cajennense (s.l)* (Matias Pablo Juan Szabó et al., 2007; Veronez et al., 2010). Moreover, savannas are found in important proportion of the landscape in a few municipalities with incidence of BSF. Thereof, savanna formation was reclassified in the non-forest native formation class because of its features are closer to open areas than dense rainforests. Landscapes metrics and variables for each hypothesis (Table 1) were selected based on literature research about landscape studies and species involved in the BSF epidemiology. See lexicon at the beginning for terms used here relating to landscape analysis.

Landscapes structure and configuration metrics were chosen in the FRAGSTATS manual, a spatial pattern analysis and quantifying landscape structure software (McGarigal and Marks, 1995), in the "class metrics" section as our interest is focused solely on forest patches configuration. Class area (CA), percentage of landscape cover (%LAND), patch density (PD), mean nearest neighbour distance (MNN), nearest neighbour standard deviation (NNSD), nearest neighbour coefficient of variation (NNCV), mean proximity index (MPI), total edge (TE), edge density (ED), and main matrix type, were the landscape metrics calculated per municipalities as described in the Table 1, using FRAGSTATS. Connectivity between forest patches were assessed with the MNN, which accounts for the mean nearest edge-to-edge distance between forest patches thus their aggregation level, and the NNSD, which stands for characterizing the distribution of the patches. The NNSD assumes a normal distribution of the nearest neighbour distance. These two measures are complementary and cannot be considered separately to overview the spatial distribution pattern presented by the patches, and thereby their connectivity. NNCV is also an interesting landscape metric to compare spatial pattern variability among landscapes. However, its interpretation must be taken with caution when the patch density is not known. Two landscapes may present the same NNCV, but one with a smaller PD than the other, and therefore with a lesser connectivity between the patches. Additionally, to these connectivity metrics, the mean proximity index (MPI) was also considered. MPI evaluates the global size of neighbouring patches within a specified radius around a focal patch of the same type and their relative proximity of it. The MPI radius was set at 800 meters (McGarigal and Marks, 1995). To compute every metrics for each municipality on FRAGSTATS in batch process, the vector layer of the municipalities restrained and the LULC rasters were reprojected in a meter unit CRS (South America Albers Equal Area Conic - ESRI:102033). Then, the municipalities were split into several vector files and the LULC rasters were cut by each municipality extent, forcing the pixels size to 30 meters.

Next, the relevance of use for this study of the secondary forest age data from the collection 7.1 were briefly investigated. This was performed based on a distribution of the canopy height through time evaluated in secondary forests in the AF (Becknell et al., 2018). It is expected that only after 25-35 years the mean height of the canopy of secondary regenerated forests can overcome the approximate 15 meters observed in the secondary forests that prevailed in the non-endemic BSF areas of São Paulo (forests in intermediate and late stage)(Ogrzewalska et al., 2012). Secondary forest age rasters were downloaded for 3 different years within the period studied. By subtracting the corresponding raster of secondary forests with the raster of secondary vegetation ages and applying a raster layer unique values report (QGIS), it was calculated that: in 2001, approximately 11% of the secondary forest in the entire AF biome were older than 16 years; In 2005, approximately 4% of the secondary were older than 20 years; and in 2019, approximately 7% of the secondary forest were older than 34 years. These data are consistent with Piffer et al. (2022b) which showed that in the AF approximately 15% of secondary forests lasted more than 25 years between 1985 and 2019. Therefore, a lesser proportion of the secondary forests are in intermediate and late stage, evaluating the BSF incidence as a function of forest ages would probably not bring significant explanation at this scale of the AF biome. Proportion of secondary forests can thus be used as a proxy of young forest in the context of this study. The proportion of primary forest was also calculated.

History of land conversion of pasture to agriculture in municipalities was investigated with the total area (ha) and the proportion of superficies (%) that became agriculture each year compared to the previous one in the entire period studied. Moreover, riparian forest pixel status was assessed using a 500 m buffer from water streams and permanent water bodies. This distance from the water is where 95% of the capybaras observed by radiotelemetry were found in some studies reviewed (Campos Krauer et al., 2014), beyond this range the probability to encounter a capybara became low (Dias et al., 2020). Percentage of riparian forests (<500m) were calculated per municipalities, once considering the whole hydrography (small and major rivers, with waterbodies) and then considering only the main streams hydrography (major rivers and waterbodies only). Secondarily, the proportion of riparian non-forest vegetation, pasture, Agriculture, and mosaic of uses were retained to include in the further model selection process.

The hydrographical data were not covering 11 municipalities present in the studied zone. For these, the water streams were extracted from the DEM in the r.watershed function of the QGIS GRASS package using a 250 and 100.000 watershed size parameter for the comprehensive hydrography and the main streams hydrography respectively. Then, the 500 meters buffer were also performed for those streams.

2.2.4 Other abiotic data processing

The DEM raster of the AF was reclassified within 5 categories (Table 1). The altitude categories were instituted as: anthropic land use is expected to occur mainly in the 2 first categories, most of the remaining forest in the AF is located between the category 2 and 4, and most tick-vectors do not support cold mountain temperatures probably in the last category which is above the trees line in the AF (Ribeiro et al., 2011). Slopes were calculated in ArcGIS (ESRI, 2017)(version 10.6.1)(planar method with an appropriate CRS, ESRI:102033) with the DEM raster, then the resulting raster of slopes was binary reclassified regarding their steep feature or not. Steep slopes were defined as slope steeper than 20°. This value is a rounded mean of maximum declivity for the agricultural/forestry mechanisation found or used in some studies: 1) considering crops or pastures that mainly dominate some landscapes of the Cerrado do not exceed 30° of inclination (Carvalho et al., 2009), 2) a study on a forestry site in the AF found a maximum operational slope of 24° for the machinery (Pereira et al., 2011), 3) a study on the agricultural expansion in the state of Bahia considered 17° as a maximum slope for agriculture activities. Proportion of altitude categories and proportion of steep slopes per municipalities were calculated. The main altitude category per municipality was also spotted.

Furthermore, the average of the monthly precipitation was calculated per year and per municipality from the climatic data. The mean temperature of the coldest and hottest month of each year for each municipality was also selected, as cold weather may limit the growth of tick populations (Estrada-Peña et al., 2004) and to use as a proxy of the mean temperature of the dry and wet season. The average temperature of each year was also calculated.

Table 1 : Summarize of the main data of interest and their respective landscape metrics/variables involved in each hypothesis.

Hypothesis	**Data of interest**	**Landscape metrics/variables (per municipalities)**
Forest amount and regeneration	Forest amount	Class area (ha): $CA = \frac{\sum_{j=1}^{n} a_{ij}}{10.000}$
		Percentage of landscape (%): $\%Land = \frac{\sum_{j=1}^{n} a_{ij}}{A} \cdot 100$ a_{ij}: area of the j^{th} patch of the considered class i (m^2) A: total landscape/municipality superficies (m^2)
	Young secondary forest	Proportion of secondary forests as a proxy of early-stage forests
Landscapes configuration	Number of forest fragments	Patch density per 100 hectares: $PD = \frac{n_i}{A} \cdot (10.000)(100)$ n_i: number of patches of the same type A: total landscape/municipality superficies (m^2)
	Connectivity	Mean proximity index: $MPI = \frac{\sum_{j=1}^{n} \sum_{s=1}^{n} \frac{a_{ijs}}{{h_{ijs}}^2}}{n_i}$ a_{ijs}: area of the s^{th} patch that intercept a defined distance radius around the focal j^{th} patch of the same class type (m^2) h_{ijs}: nearest edge-to-edge distance between the s^{th} patch that intercept the radius and the focal patch (m)
		Mean nearest neighbour distance (m): $MNN = \frac{\sum_{j=1}^{n'} h_{ij}}{n'_i}$
		Nearest neighbour standard deviation (m): $NNSD = \sqrt{\frac{\sum_{j=1}^{n'} \left[h_{ij} - \left(\frac{\sum_{j=1}^{n'} h_{ij}}{n'_i} \right) \right]^2}{n'_i}}$

		h_{ij}: nearest edge-to-edge distance from the j[th] patch to the nearest neighbouring patch of the same type (m) n'_i: number of patches of the same type
		Nearest neighbour coefficient of variation: $$NNCV = \frac{NNSD}{MNN} \cdot 100$$
	Forest edge	Total Edge (m): $$TE = \sum_{k=1}^{m'} e_{ik}$$
		Edge density (m/ha): $$ED = \frac{\sum_{k=1}^{m'} e_{ik}}{A} \cdot (10.000)$$ e_{ik}: the lengths of all edge segments within the considered landscape of the k[th] patch (m) m': number of patches of the same type A: total landscape/municipality superficies (m^2)
	Matrix type	Main matrix type: considered as the dominant class in the landscape
Riparian forest	Forest near river/water bodies	Percentage of forests near rivers or water bodies (<500 m): $$rFC = \frac{rF}{A} \cdot 100$$ rF: superficies of all forest pixels within the 500 m buffer (m^2) A: total landscape/municipality superficies (m^2)
	Agricultural matrix	Main matrix type
Land conversion	Pastoral areas convert in agricultural areas	Percentage of conversion of pastoral areas in agricultural areas trough time: $$c_{p \to a} = \frac{S_{p \to a}}{A}$$ $S_{p \to a}$: pastoral superficies convert into agriculture (m^2) since the previous year. A: total landscape/municipality superficies (m^2)
Topography	Slope	Percentage of steep slope areas (>20°)
	Altitude	Percentage cover of each categorial altitude: alt 1: ≤ 200 m alt 2:]200 – 400] m alt 3:]400 – 800] m alt 4:]800 – 1200] m alt 5: > 1200 m

2.2.5 Models

Because BSF cases have a zero inflated distribution, generalized linear mixed models were carried out using a negative binomial family with a log link function (Brooks et al., 2017). For each model, BSF cases was the respond variable, numeric predictor variables were scaled, municipality and year were set as random effects, and the population (number of inhabitants per municipality) was set as an offset variable to consider BSF incidence when fitting the model (Eq.1).

Eq. 1:

$$Log(Y_{ij}) = (\beta_0 + u_{0j}) + \beta_1 X_{1ij} + \beta_2 X_{2ij} + \cdots + \beta_n X_{nij} + \varepsilon_{ij} + Log(P_i)$$

Y : response variable (BSF cases).
β_0 : intercept.
$\beta_{1\to n}$: coefficients of predictor variables.
$X_{1\to n}$: predictor variables.
u_0 : random intercept (Year and Municipality).
ε : residuals.
P : offset variable (Population).
i : i^{th} observation.
j : j^{th} group.

Non-assigned (NA) values were handled by removing them from the dataset, thus reducing also the period studied to 2001-2019 (missing data on primary and secondary forest cover for the years 2020 and 2021). Some NA were also generated due to the lack of forest cover within municipalities when the calculation of landscapes metrics was performed.

Collinearity issues were assessed and avoided for each model: before the model construction, by checking the spearman correlation between candidate variables and enabling their gathering in a same model at a 0.7 maximum correlation threshold (absolute value), then, by discarding models that could contain variables with a Variance Inflation Factor (VIF) greater than 5 (Lüdecke et al., 2021).

The study of the BSF incidence as a function of landscape features in the Atlantic Forest was performed using two approaches: 1) one general approach involving principal component analysis (PCA) carried out on a subset of the dataset, then fitting all possible models from selected PCA axes with the additional two factorial variables. Subsequently, an AICc model selection was implemented to the all set of PCA models and the results was interpreted to assess the global effects of combined variables on the disease incidence. 2) Multiple AICc selections of different model sets, one for each hypothesis stated in the section 1.4 : Objectives and hypotheses. Each set of models involving variables supporting the hypothesis tested. Then, a second AICc selection on an array of models mixing up all the hypotheses. This second approach was fulfilled to investigate the more relevant land use and land cover variables to explain the BSF incidence.

2.2.6 Modelling with PCA components

As a first approach to investigate the landscapes changes impact in the AF on the BSF incidences, principal component analysis (PCA) was performed on a subset of the data (Kassambara and Mundt, 2020; Lê et al., 2008). To select interesting variables, each variable was fit in an individual model than compared by likelihood ratio test (LRT) to the null model. Every variable that leads to a significant LRT p-value (error α=0.05) was included in the later mentioned subset. The 7 first dimensions of the PCA were retained, together they explained almost 75% of the total variance (see the appendix for the scree plot, Figure A3). The PCA axes (dimensions) were selected to explained sufficient variance, but also to have at least each variable correlated to one axis at a minimum arbitrary correlation level of 0.4 (Figure 10). Percentages of contribution to the total variance of each variable were assessed. This was calculated by multiplying the r^2 of a variable (square of the correlation to the axis) by the percentage of explained variance of that same axis (Figure 10).

The selected axes of the PCA were fitted in a model additionally with the two qualitative variables : the main land cover type (Matrix) and the main altitude class (Main alt) by municipality (appendices, Table A5). This latter model, labelled the full model (complete model), was thereafter dredged when keeping the random effects structure and the offset variable in each sub-model generated (Bartoń, 2023). The sub-models were classified according to their corrected Akaike Information Criterion (AICc). Calculation of the relative importance of variables among the set of PCA axes models that were dredged from the full model was performed. It is calculated as the sum of the models AICc weights that contain the variable, the interpretation is the probability of the variable to be in the best model if the data were resampled. As a rule of thumb, when the relative importance is smaller than the presence frequency of the variable among the all set of sub-models, this variable is more likely not to be significant in the best models (appendices, Table A6). From this method, the dimension 2 was expected not to be retained in the best models. Subsequently, the best models, equally supported by the data (with ΔAICc < 2), were averaged using the shrinkage coefficients averaging method (Bartoń, 2023; Symonds and Moussalli, 2011).

The resulting averaged coefficients were reported, with the correlation and proportion of total variance explained by the variables in PCA axes, to investigate the relative effects of the variables to the BSF incidence (Figure 9, Figure 10).

2.2.7 Hypothesis testing

For each hypothesis, a set of models were fitted using the variables related to it (appendices, Table A5) and a first AICc selection was performed to highlight the best competitor models for each one. In the case where no other model competed within the ΔAICc < 2 range with the lowest AICc model, this model was considered as the best model of the hypothesis tested. When several models were retained in the best models set, these were averaged using a natural averaging method (Symonds and Moussalli, 2011). Each model was fitted with and without the mean annual temperature (temp) in the formula to control for the effect of climate with the land use and land cover variables. The mean annual temperature was considered as the best variable to account for the climate through an AICc selection of models containing only climate variables. Then, coefficients of the best models for each hypothesis were plotted to investigate the relative effects of variables on the BSF incidence. The coefficients were displayed when being significant at a 85% confidence level (~0.157 p-value) to be consistent with the AICc selection method of best models as advised by Sutherland et al. (2023)(Arnold, 2010; Sutherland et al., 2023).

Moreover, a second AICc selection was carried out among all the models fitted for the hypotheses testing, in order to evaluate which hypothesis of landscape structure or configuration is the most relevant to explain BSF incidence within the Atlantic Forest. Therefore, AICc rankings of models that did not contain any land use or land cover variables were not considered. Then, the random effects ('municipality' and 'year') significance was tested on the best model retrieved from the previous selection, by contrasting the AICc of competing nested models with only fixed factors, a random intercept for 'municipality', a random intercept for 'year', and a random intercept for both 'municipality' and 'year'.

Finally, on the model selected as the best to explain BSF incidence as a function of landscapes, spatial autocorrelation was tested with two Moran's I tests: one using distances between the centroids of municipalities, and another using the contiguity matrix based on queen neighbourhood relation (Cliff and Ord, 1970; Suryowati et al., 2018)(appendices, Table A8). Then, several spatial models using different methods were fitted to account for the spatial autocorrelation (Appendices, Table A5) and went through an AICc selection (Table A7).

3 Results

3.1 Exploratory analyses of BSF data

The number of BSF confirmed cases has been increasing since 2007. Considering the 2007 to 2022 period, the mean case-fatality rate is 33%. The maximum value was reached in 2015 with 42% (Figure 5).

Figure 5 : **A.** Number of spotted fever cases, death cases, and case-fatality rate per year in Brazil, 2007 to 2022. **B.** Closer view on the confirmed cases and number of deaths. Dashed 2022 data are preliminary.

The BSF proportion of autochthon cases per year ranged from 69% to 84% with an estimate average proportion of 74.49 ± 0.02% inferred for the entire period (Figure 6). The main probable place of infection among all cases over the 2007 to 2022 period was the place where people live followed by their leisure activities and their workplace (Figure 7).

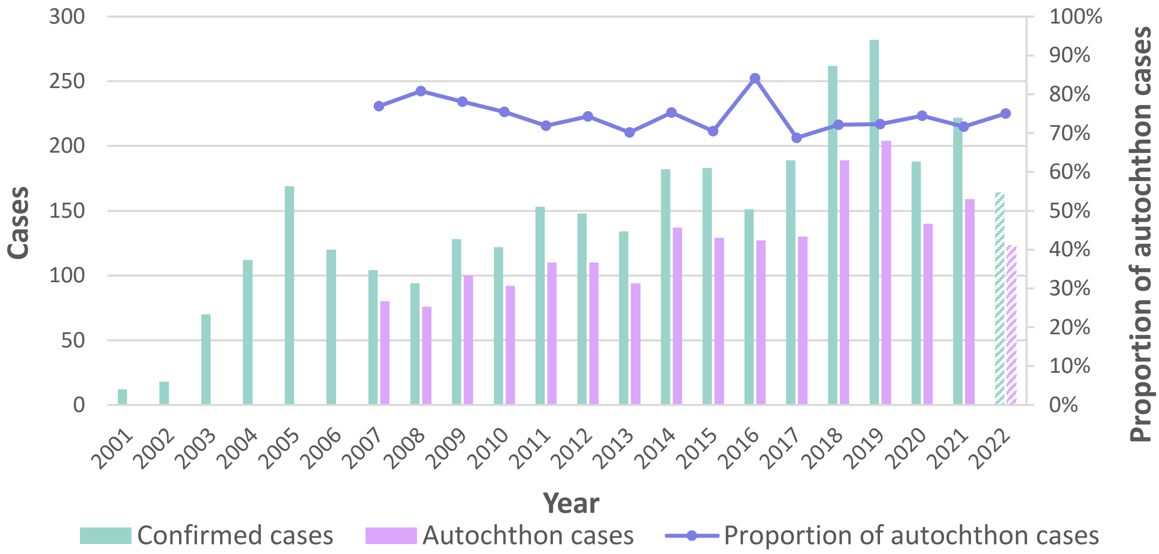

Figure 6 : Overall number and proportion of autochthon cases among the BSF confirmed cases per year, 2007 to 2022. Dashed 2022 data are preliminary.

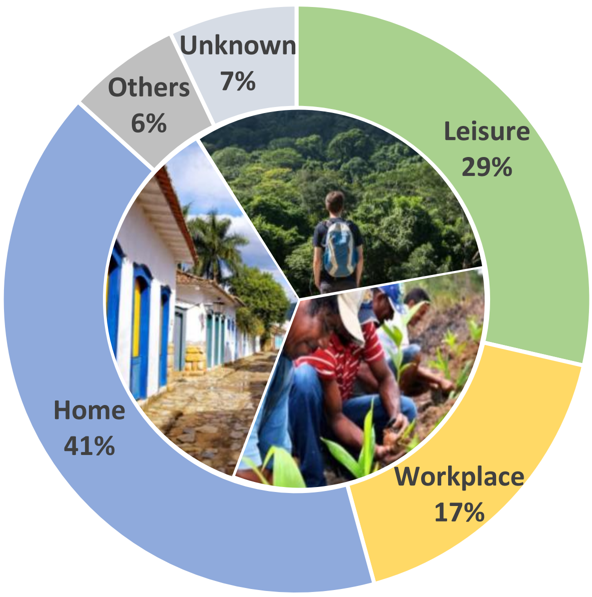

Figure 7 : Proportion of probable place of infection among the BSF confirmed cases for the period 2007 to 2022.

The mapping of the BSF cases over the studied period shows 589 municipalities with cumulative incidences ranging from less than 1 case per 100.000 inhabitants to 226 cases for the last 20 years. 562 of these municipalities (95%) was located within the Atlantic Forest or less than 100 km away from the biome. The cases remained mainly in the southern regions (states of Santa Catarina, Paraná, São Paulo, Rio de Janeiro, Espírito Santo, and Minas Gerais), while the northern regions of the biome are more spared (Figure 8).

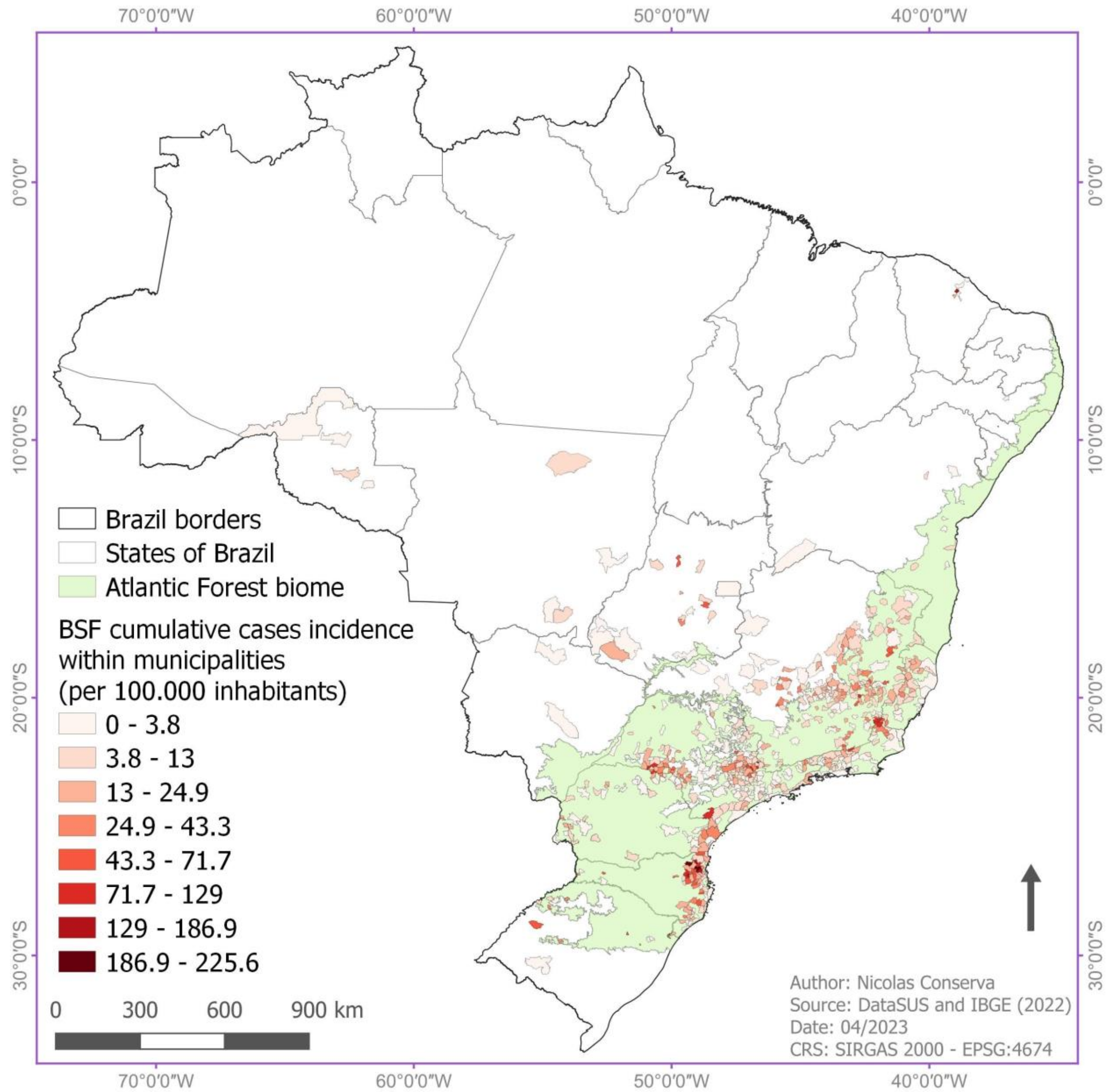

Figure 8 : BSF cumulative cases incidence per 100.000 inhabitants for each municipality of Brazil, during the period considered: from 2001 to 2021. Only the municipalities with confirmed BSF cases are represented.

3.2 BSF incidence Modelling

3.2.1 General approach involving principal component analysis (PCA)

The general modelling approach considered all potential predictors summarized through a PCA of their variation and utilizing PCA axes as predictors of the BSF incidence. The model averaging result of the 3 best-fit models (appendices, Table A5) pinpoints the main effect of groups of variables on the BSF incidence (Figure 9, Figure 10). The first principal component (PCA1) alone explains 26% of the variance of the data. The variables most contributing to this axis are variables of forest cover (e.g., CA, PLAND, Riparian Forest) and temperature, which are positively and negatively correlated with the axis, respectively (Figure 10). The positive averaged coefficient of PCA1 in the model thus indicates that BSF incidence increases with forest cover and decreases with temperature. The temperature effect is in agreement with the mapping of BSF incidence showing concentration of impacted municipalities in the south region of the Atlantic Forest biome. This region is where temperatures are known to be colder than in the northeastern part of Brazil (Figure 8, appendices Figure A5). Moreover, the section of the Figure 10 on the relative importance of variables highlights that forest cover is mostly represented by the percentage of forest cover (PLAND), the edge density (ED), the riparian forests, and the primary forests followed by the secondary forests. The savanna in the AF seems not to have a significant effect on BSF incidence, considering that PLAND Savanna do not have much importance even in the PCA axis 6 and that PLAND Savanna combined with the percentage of forest cover (PLAND Savanna Forest) have less importance than the percentage of forest cover alone.

Landscape metrics such as the mean proximity index (PROX MN), the nearest neighbour standard deviation (ENN SD), and the nearest neighbour coefficient of variation (ENN CV) have effects on the BSF incidence but the edge density (ED) is the landscape metric that should explain it the best (Figure 10). The PCA1 having a positive coefficient in the models and the mean proximity index being positively correlated to this axis, high value of this landscape metric is associated with higher BSF incidence. Therefore, less fragmented and bigger forest patches in landscapes are correlated with an increasing BSF incidence. This is also corroborated by the nearest neighbour standard deviation and the neighbour coefficient of variation which appear to be negatively correlated with the axis 1 and thus associated with lower BSF incidence. However, increasing mean nearest neighbour distance (ENN MN) and neighbour coefficient of variation (ENN CV) have also a positive correlation to the 7th axis, this latter having a positive coefficient. These two variables represent landscapes with distant and unevenly distributed forest patches that are thus also associated with high BSF incidence. Still, the PCA7 is the most significant after the PCA1, and is exclusively explained by these two metrics (at a minimum 0.4 level of correlation) unlike the PCA1 which is inflated by several other variables (Figure 10). Thus, ENN SD and ENN CV could also be irrelevant in the first component.

Following the models averaging, the dimensions 2 and 4 turn out not to be significant at a 85% level (Figure 9). These dimensions contain mainly agriculture variables and some altitude classes, with additional variables of pasture, mosaic of uses and agriculture near main water streams (Main str Agriculture, Main str Pasture, Main str Mosaic of Uses) (Figure 10). The factorial main altitude variable (Main alt), that represents the main altitude class present in the municipality, is significant at 85% for the first (alt1, ≤ 200 m) and third (alt3, 400 – 800 m) elevation range, the last elevation range (alt5, > 1200 m) is included in the intercept. Nonetheless, their effect is difficult to compare as their confidence intervals are wide (Figure 9). The main altitude class might thus not be an appropriate variable to qualify the topography regarding the BSF incidence. On the other hand, the main matrix type occupied in the landscape have positive coefficient at a 85% significant level for the agriculture and mosaic of uses types. Native non forest natural formation as a positive coefficient but a wider confidence interval, making difficult comparison with the two others matrix type. Nevertheless, agriculture, mosaic of uses, and native non forest formation matrix, tend to increase BSF incidence compared to forest matrix (included in the intercept) (Figure 9).

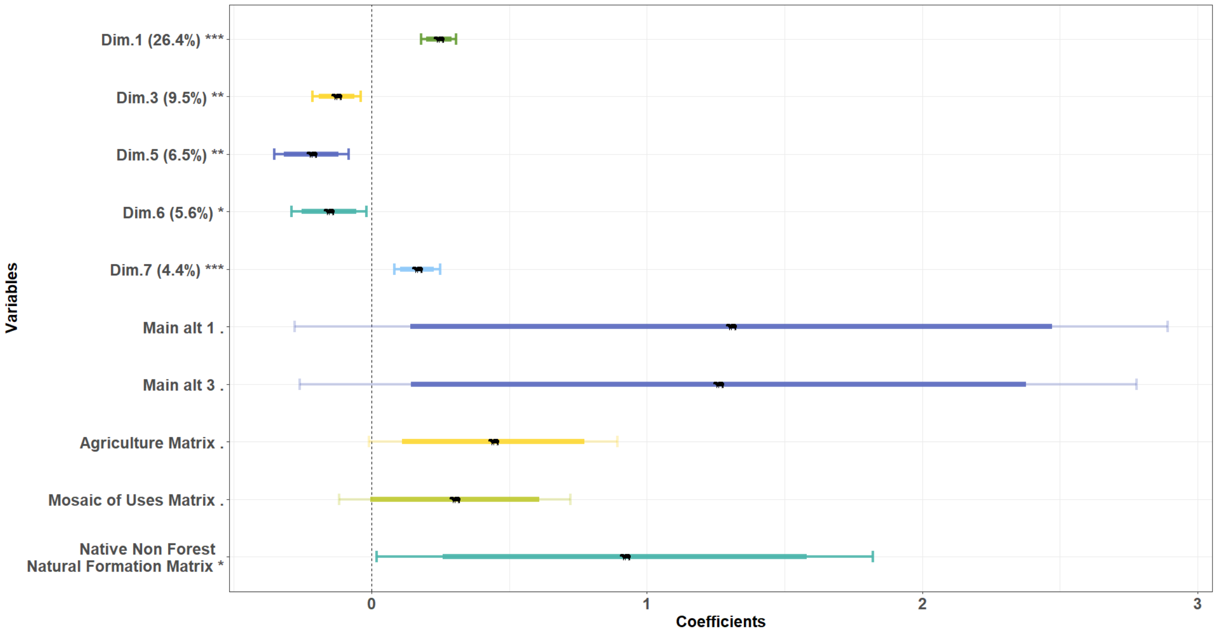

Figure 9 : Coefficients averaging results based on the best models from the AICc selection (ΔAICc < 2) considering dredged sub-models combination of the PCA axes full model. Percentage of axes explained variance in parentheses. Only coefficients with a 85% significance level are plotted (p-value < 0.157). Range of p-values of each variable in the model are represented: 0.157 (.) 0.05 (*) 0.01 (**) 0.001 (***) 0.000. Confidence Intervals (IC) are represented by a thin line (95% IC) and a bold line (85% IC), uninformative variables within a 95% IC (crossing the 0 dotted line) have a pellucid IC. The colours of the ICs highlight the approximated similar “thematic” of the variables in the Figure 10. Main alt: main elevation range, Matrix : main land cover type present in the landscape. Forest matrix and alt5 are included in the intercept of the models.

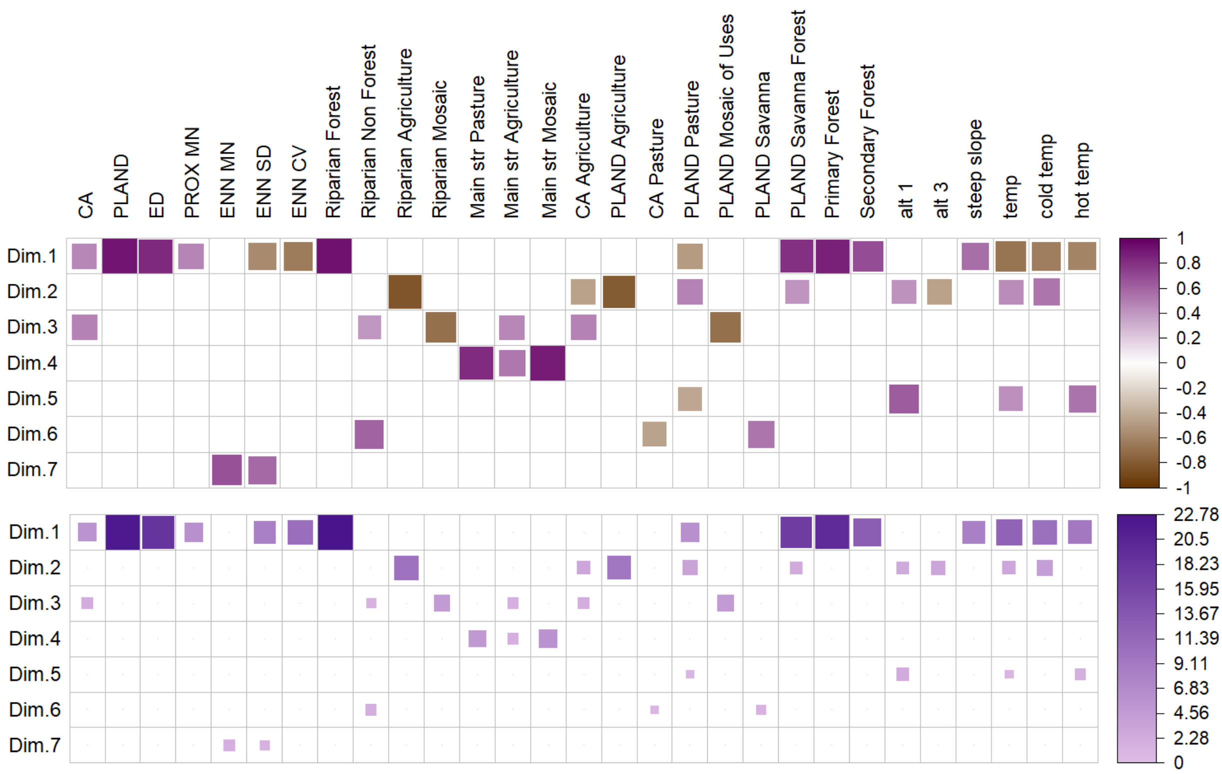

Figure 10 : Above section: Correlation coefficient between the axes of a PCA (Dim.) of the landscape features used as predictors of BSF incidence and each of these predictors individually. Correlation coefficients under 0.4 are not shown. Under section : Percentage of contribution to the total variance of each variable, calculated by

multiplying the r^2 of a variable (based on the correlation above) by the percentage of explained variance of the axis. Abbreviations, by municipality : CA: forest class area (ha), PLAND: percentage of forest cover, ED: forest edge density (m/ha), PROX MN: Mean proximity index, ENN MN: Mean nearest neighbour distance between forest patches (m), ENN SD: nearest neighbour distance standard deviation (m), ENN CV: nearest neighbour coefficient of variation, Riparian [class]: percentage of the specified class near rivers, Main str [class]: percentage of the specified class near main streams (> 30 m wide), CA [class] : class area (ha), PLAND [class]: percentage cover of the class specified, Primary/Secondary Forest: percentage of primary/secondary forests, alt1/alt3: percentage of area in the first/third elevation range, steep slope: percentage of steep slope, temp: mean annual temperature, cold/hot temp: mean annual minimum/maximum temperature.

PCA axes 3, 5 and 6 have negative coefficients in the models (Figure 9). On these axes, riparian non forest natural formation, agriculture near main stream, agriculture cover (in ha) are related to low BSF incidence considering their positive correlation with their respective PCA axis. While pasture, mosaic of uses cover and riparian mosaic of uses are associated with higher BSF incidence because they are negatively correlated to the axes. High percentages cover of the altitude class 1 (alt1, ≤ 200 m), being positively correlated to PCA5, is also linked to lower disease incidence (Figure 10).

3.2.2 Hypotheses testing and best landscape features to explain BSF risk

Results of the best models by hypothesis tested are presented in Figure 11. In each model, municipalities with higher mean annual temperature (temp) are associated with lower BSF incidence as described by the PCA analysis (Figure 9, Figure 10).

In contrast to the forest amount and regeneration hypothesis that BSF incidence decreases with forest cover and increases with secondary forests, the results (Figure 11, H1) indicate that BSF incidence increases with the percentage of forest cover (PLAND) and primary forests within the municipalities of the Atlantic Forest. Secondary forests might be involved too, yet with a smaller effect than primary forests, considering that the percentage of forest cover sums the percentage of primary and secondary forests. Additionally, when investigating the distribution of the forest cover variable, it appears that most of the municipalities present a low forest cover (Appendices, Figure A4).

According to the landscape configuration hypothesis, more fragmented landscapes, with high forest edge effects, low connectivity between patches, and immersed in rural land use matrices would be more at risk. As the results of the PCA analysis suggest too, mean nearest neighbour distance, nearest neighbour standard deviation, and neighbour coefficient of variation, were less significative to explain the disease incidence as the models containing these variables did not stand out from the AICc selection. Instead, the forest patch density (PD) and total edge amount (TE) are the main landscape configuration variables explaining the BSF incidence (Figure 11, H2). The TE effect is mitigated as its significance level rest on the 85% IC. However, the forest edge density (ED) is included in another model that support the third hypothesis (Figure 11, H3) at a more significant level, thereby it bears out the that forest edge effects is associated with lower BSF incidence. The patch density (PD) has also a negative coefficient. Hence, in opposition to the hypothesis, more fragmented landscapes are correlated with lower BSF occurrence. The percentage of forest, pasture and mosaic of uses have positive coefficients (Figure 11, H2). Regarding that with the previous considerations, it seems that huge patches of continuous forest with low edge amount and immersed in pasture areas, and in a lesser proportion, agricultural areas contained in the mosaic of uses, increase the spotted fever risk.

The results support the third hypothesis stating that low forest cover but large amount of riparian forests, and consequently of forest edge, within agricultural matrices would be associated with high BSF risk. Indeed, the positive coefficient of the best model (Figure 11, H3) corroborates the effect of forests cover (PLAND) described above, especially when those are riparian (Riparian Forest). However, the edge density (ED) displays a negative coefficient despite increasing with the riparian forest (Spearman correlation of 0.87, not shown). Agriculture, pasture, and mosaic of uses matrices increase the BSF risk with a lesser significant effect of the agriculture matrix (informative at a 85% significant level). It is important to keep in mind that matrix type coefficients are to be interpreted in comparison with the intercept, which contains the forest matrix. Hence, riparian forests immersed in rural matrices raise the BSF incidence. As stated before, most of these landscapes present a low forest cover (Appendices, Figure A4), which is in agreement with the prior hypothesis settled.

Furthermore, the results of the fourth set of models (Figure 11, H4) are provided to highlight that the amount of pastoral lands converted into agriculture are not correlated with the BSF incidence significantly. These land conversions were evaluated by municipality and between a year and the one before. The land conversion hypothesis expected to have higher BSF incidence in municipalities that underwent more conversion of pasture area into agricultural ones. However, the results do not underlie that correlation. Those transition rate variables were not significant after the model averaging of the best models (ΔAICc < 2)(Appendices, Table A7). They were also not selected in the subset of the data for the PCA analysis because they failed the LRT test comparing them in an individual model with the null model. Moreover, the effects of pasture and the mosaic of uses were less significant following this model averaging than observed in the two previous hypothesis results (Figure 11, H2 and H3), pasture displaying a negative coefficient in this case. While, the effect of agriculture is more significant than in the others hypothesis and appears to be associated with lower disease incidence.

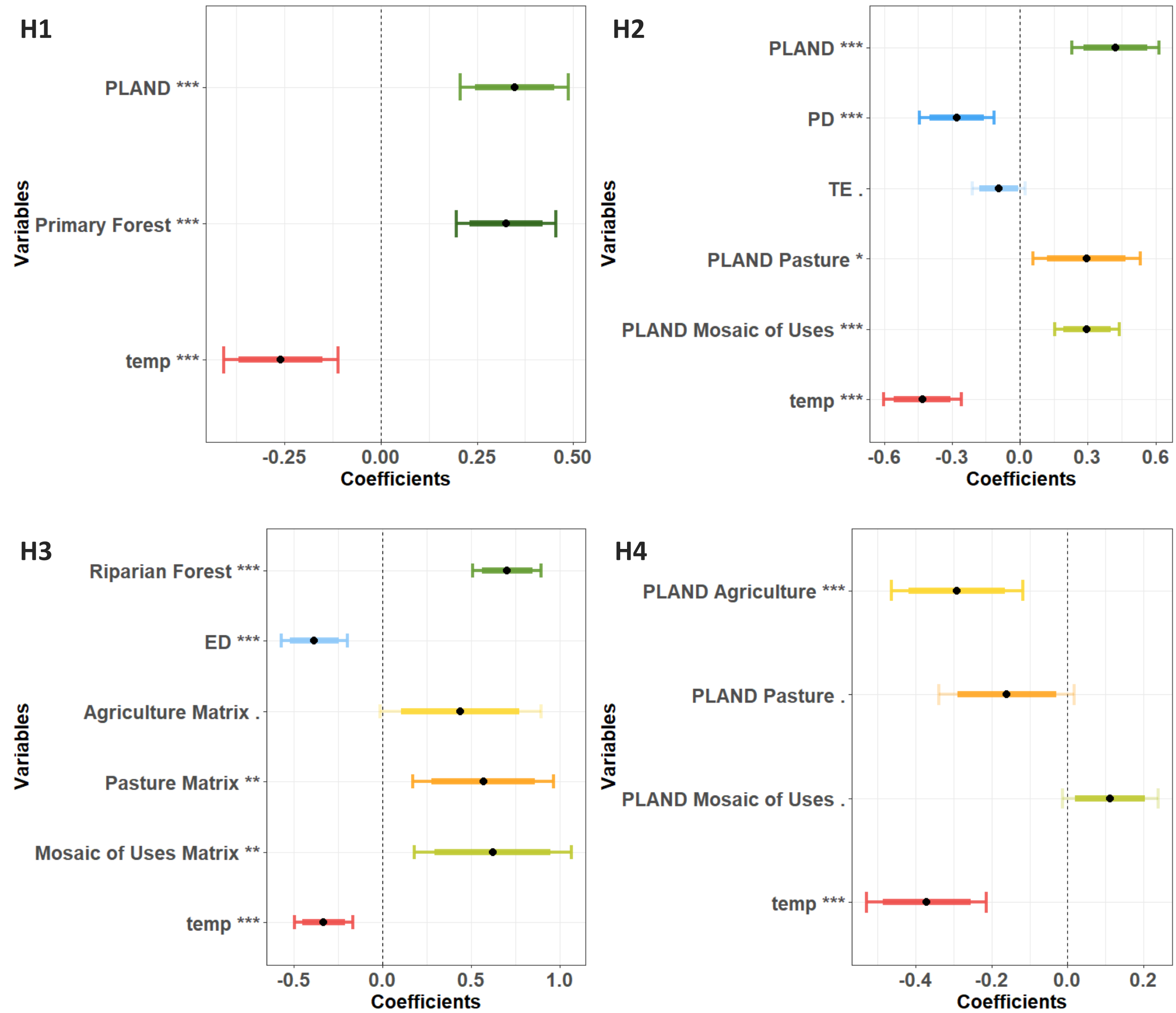

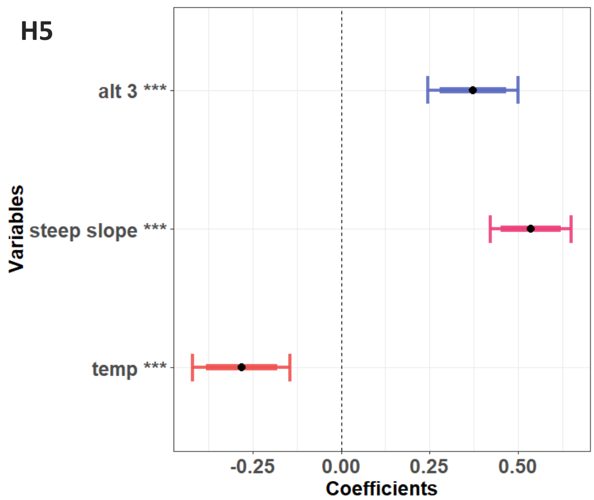

Variable header	Meaning
Matrix	Dominant Land Use or Land cover type
PLAND	Percentage of Forest cover
PD	Patch density (patches/100 ha)
TE	Total Edge (m)
ED	Edge Density (m/ha)
Riparian Forest	Percentage of riparian Forest
PLAND Agriculture	Percentage of Agriculture cover
PLAND Pasture	Percentage of Pasture cover
PLAND Mosaic of Uses	Percentage of Mosaic of Uses cover
Primary Forest	Percentage of Primary Forest
Alt 3	Percentage of pixels within the category 3 of altitude classes:]400 – 800] m
Steep slope	Percentage of steep slope
temp	Mean annual temperature (°C)

Figure 11 : Coefficients of the best model by hypothesis (log scale). **H1** : Forest amount and regeneration hypothesis. **H2** : Landscapes configuration hypothesis. **H3** : Riparian Forests hypothesis. **H4** : Land Conversion hypothesis. **H5** : Topography hypothesis. Only coefficients with a 85% significance level are plotted (p-value < 0.157). Range of p-values of each variable in the model are represented: 0.157 (.) 0.05 (*) 0.01 (**) 0.001 (***) 0.000. Confidence Intervals (IC) are represented by a thin line (95% IC) and a bold line (85% IC), uninformative variables within a 95% IC (crossing the 0 dotted line) have a pellucid IC. The colours of the ICs highlight the approximated similar theme of the variables. Forest matrix and alt5 are included in the intercept of the models.

The last hypothesis assessed the effect of landscape topography on the BSF incidence. Presence of steep slope (>20%) and high-altitude mounts would reduce the incidence. The results underline the positive effect of steep slope on the BSF risk (Figure 11, H5). The third altitude class (alt3: 400 to 800 m) has also a positive correlation with the BSF cases. Steep slopes in the landscape present thereby opposite patterns as expected by the hypothesis by increasing the BSF incidence, whereas municipalities in high altitude seem more spared as it was assumed.

Finally, after the overall AICc selection to evaluate the best model to explain BSF incidence between the hypotheses tested, the topographic model (Figure 11, H5) was the first model followed by the riparian forest model (Figure 11, H3). Yet, the topographic model did not account explicit land use and land cover variables. Therefore, the riparian forest model was used to answer the main investigation: how land use and land cover changes of the Atlantic forest can affect the BSF incidence. The model was thereafter used to assess the significance of the random intercepts. The riparian forest model including the two random intercepts was ranked higher than the same models containing only the fixed effects or with one of the intercepts, evidencing the spatiotemporal variability of the data and the necessity to control for it in the analyses. Spatial autocorrelation of the riparian forest model was assessed with two different methods (Table A8). The results indicate significant autocorrelation for the majority of the years, irrespectively of the method used. The results of the best spatial model accounting for the autocorrelation are shown in Figure 12. Edge density and mean annual temperature are no longer significant when a spatial exponential covariate term (Kristensen and McGillycuddy, 2023) is added to the riparian forest model. It also appears that riparian forests have a smaller coefficient in this spatial model. However, its significance is still higher than that of the other variables.

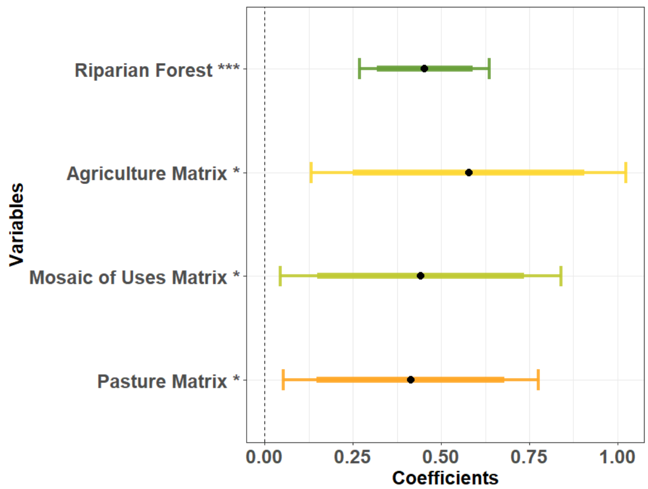

Figure 12 : Coefficients of the best spatial model of the riparian forest hypothesis (log scale). Only coefficients with a 85% significance level are plotted (p-value < 0.157). Range of p-values of each variable in the model are represented: 0.157 (.) 0.05 (*) 0.01 (**) 0.001 (***) 0.000. Confidence Intervals (IC) are represented by a thin line (95% IC) and a bold line (85% IC). Forest matrix is included in the intercept of the models.

4 Discussion

4.1 Spatiotemporal variation of the BSF incidence

Over the years, the number of confirmed cases has increased as stated before by Alcon-Chino and De-Simone (2022) (Figure 5, B). Yet, the increasing number of cases could also reflects the increasing number of reported cases, as the awareness of physicians regarding the BSF would have raised since the disease was mandatory to report in 2007 (Oliveira et al., 2016). The mean case-fatality rate of 33% for the 2007-2022 period is the same as Oliveira et al. (2016) previously found. Finally, the years 2020 and 2021, discarded from the dataset due to the lack of information on primary and secondary forests cover, show a drop in the case-fatality rate that could be explained by the covid-19 pandemic (Figure 5). Indeed, practicians would have been more likely to disregard others diseases such as spotted fever during the pandemic, especially when those have quite similar first stage symptoms (Blanton, 2019; Regan et al., 2015).

The mapping of the BSF cases shows that 95% of the Brazilian municipalities with confirmed cases of spotted fever are within the Atlantic Forest biome. The municipalities affected are mostly located in the southeastern part of the biome (Figure 8). It is more likely that when BSF cases are notified, these cases correspond to people infected by the most pathogenic *Rickettsia* bacteria of Brazil: *R. rickettsii* (Ministério da Saúde do Brazil, 1991) followed by *R. parkeri* and the Atlantic rainforest *Rickettsia* strain (Labruna, 2009; Spolidorio et al., 2010; M. P. J. Szabó et al., 2013). Therefore, the tick species (mainly *A. cajannense (s.l.)*, *A. aureolatum* (Ogrzewalska et al., 2012), *A. triste* (Silveira et al., 2007), and *A. ovale*) associated with these bacteria (M. Szabó et al., 2013), and their ecology, would be the main drivers of the BSF and its distribution in the environment.

4.2 Environmental drivers of the BSF

4.2.1 Forest cover

From the PCA analysis (Figure 9, Figure 10) and the best-fit models (Figure 11, H1) including forest cover variables, municipalities with high forest cover, especially primary forests, are the most likely to exhibit high BSF incidence levels. Because spotted fever is a vector-born disease propagated by ticks (Parola et al., 2013), this correlation likely stems from the preference of tick species for forest environments. In the Brazilian Atlantic Forest (AF), *A. aureolatum* and *A. ovale*, thrive in dense vegetations (Szabó et al., 2009). Such dense vegetation conditions mostly correspond to primary forests, which could explain that the primary forest cover is also positively correlated with BSF incidence. In contrast to this, it was expected that primary forests would strongly mitigate zoonoses (Claudia Araujo Scinachi, 2022; M. Szabó et al., 2013) by the dilution effect principle (Civitello et al., 2015; Keesing and Ostfeld, 2021), while secondary forests would supply weaker ecosystems services (Ferraz et al., 2014). However, the classification from the MapBiomas initiative of primary forest can be misleading. Primary vegetation status was attributed to every forest mapped at the beginning of the data availability, namely in 1985, whether or not these forests had already been used before. This status was only lost when a land cover change was observed after this year (MapBiomas Project, 2022b). Therefore, the primary forests considered in this study for the period of 2001 until 2019 may in fact correspond to young forest stands. Such forests would probably not contribute as much as pristine forests in the mitigation services of zoonoses, which could explain the association between primary forest cover and BSF incidence. In general, ecosystem services in the Atlantic Forest will be mostly effective when forest are at least 25 years old. Nonetheless, the current forest cover is mainly composed of heterogenous forests of different age in a same patch, compromising the ecosystem services provisioning (Ferraz et al., 2014).

Additionally, considering the results (Figure 11, H1), it is unclear whether secondary forests have a greater effect on the global BSF incidence than primary forests. Indeed, despite that the percentage of forest cover (PLAND) is also correlated to secondary forests, when taking a closer look at the mean forest cover by municipality and by year (Figure 13), we can see that the proportion of primary forests outweighs the proportion of secondary forests. Consequently, it can justify why secondary forests are not as significant as primary forests to explain BSF incidence. It is also worthy to mention that 75% of the municipalities in the Atlantic Forest and during the period studied presented less than 30% of forest cover (Appendices, Figure A4). Thus, the positive correlation established between the spotted fever incidence and the forest cover mainly involves a deforested landscapes context.

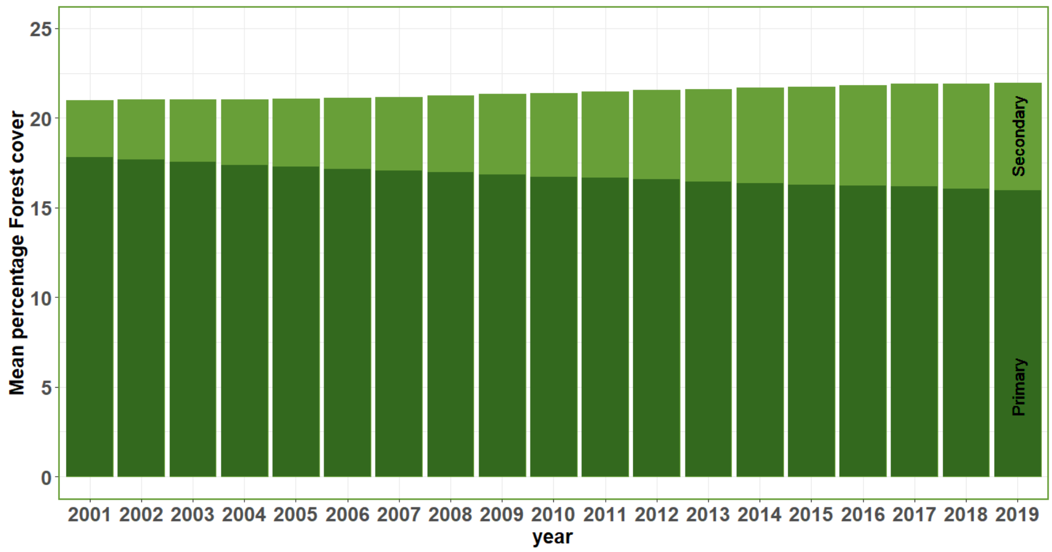

Figure 13 : Mean percentage of forest cover by municipality and by year in the Atlantic Forest. Proportion of primary forest and secondary forest are shown in dark green and light green respectively.

4.2.2 Landscape metrics

Concerning the landscape metrics, it appears that municipalities with large continuous forest patches (with small patch density, low forest edge effects (Figure 11, H2 and H3), and a high proximity index (Figure 10)) are more at risk of BSF. Forest fragmentation, in synergy with secondarization processes, is responsible for the biodiversity loss of forests (Oliveira et al., 2004; Pfeifer et al., 2017). Those effects are also drivers of defaunation, especially mammalian defaunation (Canale et al., 2012). Ticks being hematophagous parasite, low animal diversity and abundance might decrease tick abundance too for populations affiliated with forest environments. This could explain why continuous and more biodiverse forests are more suitable habitats for these ticks, thereby putting forward an argument against the dilution effect of biodiversity on the BSF (Civitello et al., 2015; Keesing and Ostfeld, 2021). However, it could also rely on the fact that more fragmented landscapes exhibit a less structured and dense vegetation adapted for the tick species, or as previously stated, that the environment of the "pseudo primary forests" considered in this study could actually be considered as secondary forests.

Landscape metrics, such as mean nearest neighbour distance and the proximity index between forest patches, were not the most relevant variables to explain the BSF incidence. Such metrics seem to have more utilities in observational studies at a smaller scale than over an entire biome (Ogrzewalska et al., 2012). Indeed, unlike Ogrzewalska et al. (2012), who have found that endemic areas of BSF in the metropolitan region of São Paulo contain smaller forest patches with high nearest neighbour distance, in this present thesis the opposite pattern was observed at the scale of the whole biome. This is most likely due to the difference of scale and design of these studies, which make their results difficult to compare. What can be true for a smaller region, may not necessarily be extensible to broader geographic scales.

4.2.3 Riparian forest immersed in rural matrices

Concerning the different land use types, it is less obvious to draw conclusions using the PCA analysis, especially because it seems to depend on the proximity to water. However, agriculture seems to have less effect in increasing the BSF risk than pastures and mosaics of uses as these last two variables have more relative importance than agriculture in the PCA axes (Figure 10). However, the results from the best-fit model of all the hypotheses involving land use and land cover variables (Figure 11, H3) suggest that landscapes with increasing amount of continuous and riparian forests immersed in pasture and agriculture matrices (Pasture, Agriculture and Mosaic of Uses) increase the BSF risk. While the tick vectors previously cited have a preference for dense canopies, *A. cajannense (s.l.)* and *A. triste*, can be found in more open landscapes (Matias P. J. Szabó et al., 2007; Szabó et al., 2009). Such open areas, including pasture and agriculture, are, more than any other land cover types, shaped by human activities (Lira et al., 2021). *A. cajannense (s.l.)* and *A. triste* might increase the BSF risk in such environments. This is also supported by the cluster of BSF incidence in Santa Catarina that matches with the distribution of *A. ovale* in the state (Figure 14). In this cluster, native forest cover more than 60% of the territory in most municipalities. By contrast, the other states such as São Paulo and the Minas Gerais are dominated by municipalities with agriculture and pasture as main landscape (Figure 3). These others states correspond to the large geographic distribution of *A. cajannense (s.l.)* (M. Szabó et al., 2013) and probably also *A. triste* as its ecological requirements are similar (Szabó et al., 2009)(Figure 14).

Furthermore, although spotted fever is a vector born disease, tick vertical transmissions of the pathogens do not allow alone the persistence of the zoonosis in the environment (Blanton, 2019), as some highly pathogenic *Rickettsia* can be partially deleterious for its tick vector (M. Szabó et al., 2013). Consequently, amplifier hosts are required in the enzootic cycle. The species known in the Atlantic Forest to intensify pathogen prevalence in vector populations are capybaras (Souza et al., 2009; M. Szabó et al., 2013), horses (Souza et al., 2016), and domestic dogs (Moerbeck et al., 2016; Ogrzewalska et al., 2012). The ecology and habits of these species are thus directly related to the BSF risk in municipalities. Riparian forests are favoured environments by some tick species (Osava et al., 2016; M. Szabó et al., 2013) but also by capybaras (Brites-Neto et al., 2015; M. Szabó et al., 2013), which underscores the implication of riparian forests in the BSF risk. Capybaras are also well adapted to human-modified landscapes with agricultural and pastoral environments (Dias et al., 2020; Verdade and Ferraz, 2006). Moreover, after the proximal environment where people live, leisure areas are the second most probable place of infection that was reported among the spotted fever cases (Figure 7). Forests and riparian environments are both well appreciated by humans for leisure (Appendices, Figure A6). Specifically, if people hike with dogs in these environments, vectors, amplifier hosts and final hosts (human), are concentrated at the same place, thereby increasing the transmission risk. Since domestic dogs are known to be the most associated amplifier hosts with *A. aureolatum*, some epidemiologic issues might thus be expected with wild ownerless dogs that are also frequent in Brazil (Claudia Araujo Scinachi, 2022; Labruna, 2013).

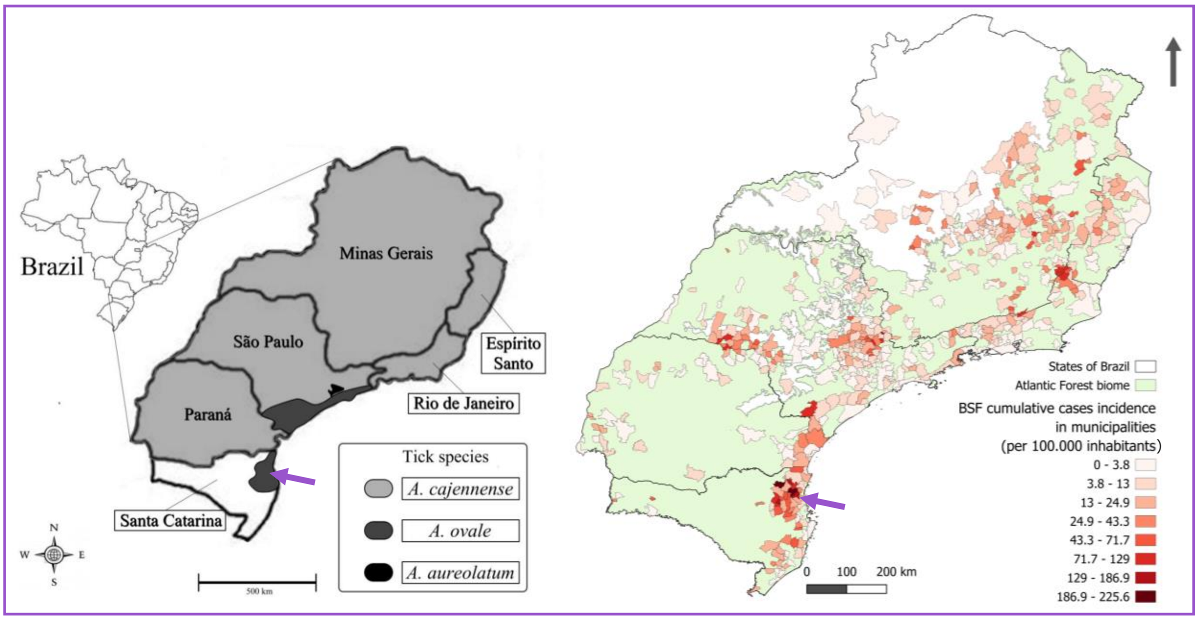

Figure 14 : Left side: distribution of host tick species in the main states of Brazil touched by the spotted fever, from M. Szabó et al. (2013). Right side: BSF cumulative cases incidence per 100.000 inhabitants, from 2001 to 2021, for each municipality (Figure 8) restricted to the main infected states of Brazil. Only the municipalities with confirmed cases are represented. Purple arrows highlight the coincidence between the *A. ovale* distribution and the main BSF cluster of the Santa Catarina state.

The best-fit model (Figure 11, H3) points out that pasture, mosaic of uses or agriculture matrices in a municipality increase the BSF risk. Variables representing the pasture land use conversion in agriculture were not selected in the best model testing their potential correlation with BSF incidence (Figure 11, H4). The major land use change in the Atlantic forest during the last decades was the expansion of agriculture, with additional land conversions of pasture areas to agricultural ones (Lira et al., 2021; Ribeiro et al., 2011). The increasing agriculture cover provides new grazing areas for capybaras (Felix et al., 2014; Verdade and Ferraz, 2006) and their increasing population is suspected to be involved in the raise of BSF cases (Souza et al., 2009; M. Szabó et al., 2013). The pasture to agriculture conversion between two consecutive years do not explain the BSF incidence. Nonetheless, there might be some delays between the BSF occurrence and the land transition that could take more than one year. It could still be interesting to test this effect in further studies accounting this lagged response, for example, by modelling BSF cases upon the entire period as a function of total land conversions that occurred in that same period and investigate for potential correlations.

Additionally, it is worthy to remember that amplifier hosts are not the only hosts that drive tick species distribution. Although horses are amplifier hosts (Souza et al., 2016) and can be found in pasture, the latter also includes other animals among the cattle that can host BSF tick species without amplifying the pathogen prevalence. Those non-amplifier hosts sustain the tick populations and can therefore contribute to raise the BSF risk in landscape with pasture matrix. The same features are known in other animal species, among felines and birds for instance, present in more dense vegetation and that can help translocate ticks and spotted fever into new areas (de Paula et al., 2022).

4.2.4 Topography relationship with land use and land cover

Two altitude ranges considered in this study and the percentage of steep slopes were further shown to correlate with BSF incidence. Low elevations (alt1, ≤ 200 m), are characterized by high levels of pasture and agriculture, and thus, high level of potential tick infection by farmers. At medium elevation (alt3, 400 – 800 m), wherein high BSF risks were also identified (Figure 11, H5), forest cover distribution reaches its maximum (30%), notably due to environmental law enforcement on steep slopes. However, only 10% are remanent forests (from the original distribution), which is the lowest level of remnant forests observed among the others altitude classes (Ribeiro et al., 2011). In this aforementioned elevation range, mitigation services of zoonoses are thus expected to be weakened. This information also corroborates the previous statement claiming that primary forests as classified by the MapBiomas initiative do not reflect pristine forests with highly valuable mitigation ecosystem services.

4.2.5 Temperature effect

Moreover, the analyses strongly highlighted that high mean annual temperatures are associated with low incidence, but its relevance varied among analyses. The Moran's I statistic was low for most of the years (<0.1), which is expected knowing that spotted fever transmissions do not occur between humans (IDPH, 2023), by contrast with others diseases like COVID-19 that present higher spatial autocorrelation (Castro et al., 2021), but was nonetheless significant. When spatial autocorrelation was controlled for in the riparian model, temperature (and edge density) was not selected in the best model. Temperature variation in fact exhibits a strong spatial structure, so that its effects cannot be decoupled from simple spatial effects, but likely plays a role in the BSP incidence. Temperature was in fact shown to drive *A. cajennense* distribution in south America (Estrada-Peña et al., 2004). Likewise, it is likely that mean annual temperature is a driver of the distribution of others tick species involved in the BSF cycle (Oliveira et al., 2017; M. Szabó et al., 2013), thus explaining that BSF risk are lower in municipalities with high mean annual temperature (Appendices, Figure A5). The spatial model also bears out the assertions made before on the effect of riparian forests immersed in pasture or agriculture matrices on the BSF incidence.

4.2.6 Spatiotemporal validity of the results

The riparian forest model containing 'municipality' and 'year' in the random structure was the best ranked by AICc compared to the same models without random effects or only one of them. The results thus evidence the spatiotemporal variation of the BSF incidence and its relationships with landscape features.

4.3 Potential limitations of the study

It is important when interpreting these results to keep in mind that because data on BSF have begun to be mandatory to report only since the last 20 years (Oliveira et al., 2016), the increasing cases might thus reflect the increasing number of reports rather than the real increasing of BSF cases. Consequently, the increase of the correlation with recent landscape changes in the Atlantic Forest (Box 1, Figure 3) may be over-inflated. Also, some variability is added knowing that on average, 75% of the reported cases are autochthon to the municipality, thus 25% could be wrongly associated with the municipality (Figure 6).

Furthermore, the results show the effects of land cover and land uses on the BSF in the entire Atlantic Forest biome during the period covering 2001 until 2019. However, BSF is a multi-vector born disease involving several etiological agents, tick species with different ecological requirements, and different tick hosts, amplifier or not. The complexity of the sylvatic cycle produces pattern of landscape effects on the BSF that can differ depending on the location. The global trend observed in the Atlantic Forest might not reflect what is observed at a smaller scale.

Finally, the present study was not able to corroborate strong evidences of dilution effect of the rainforest biodiversity, most likely for the reasons mentioned earlier related to the data. Some studies have however suggested that the dilution, which apply to most of the zoonoses known, would also be effective for the BSF (Claudia Araujo Scinachi, 2022; Ogrzewalska et al., 2012). This thesis investigation is mainly about the environmental epidemiology of the BSF and did focus on the relationship between the eco-epidemiology of the hosts and the risk of transmission. Therefore, the results should be taken with caution when attempting to draw conclusions on potential dilution effect.

4.4 Applications

Under the current environmental law in the Atlantic Forest (Brancalion et al., 2016), riparian remanent forests are semi-protected areas and are needed to be restored. These environments are thus expected to increase (Molin et al., 2018; Teixeira et al., 2009). However, this study shows that riparian forests tend to increase the BSF risk as features of these areas allow to gather tick vectors and their hosts, sometimes some *Rickettsia* amplifier hosts (M. Szabó et al., 2013). This effect of riparian forests is also incremented in pasture or agriculture matrices. However, the tropical rainforests supply several others important ecosystem services (Ribeiro et al., 2011) and their important biodiversity is needed to be conserved. Molin et al. (2018) suggested that the regeneration of the Atlantic Forest prioritizing the riparian environments as the current law compelled was not the most effective strategy. Indeed, regeneration processes can be active or passive (Crouzeilles et al., 2019). Molin et al. (2018) proposed an alternative relying more on effective passive regenerations, by selecting areas near large and ancient forest fragments with higher natural regeneration potential. Hence, the authors provide evidences that this strategy would be more cost-effective than focusing regeneration processes on riparian environments where active restauration sometimes are required. This thesis puts forward another argument relative to the BSF that riparian forests might not be the most appropriate strategy in a context of zoonotic mitigation services, thereby supporting the cost-effective strategy evoked by Molin et al. (2018). Indeed, riparian forest cover was more relevant to, explain BSF incidence than the simple forest cover.

The spotted fever can be lethal for the most pathogenic *Rickettsia* agents, however, antibiotic are available to help people to recover and prevent death (Blanton, 2019; Regan et al., 2015). Effective prevention and education should be the first measure settled to limit spotted fever casualties. For instance, sensibilizing the public to environment at risk for the disease, spreading the use of tick repellents and preventive antibiotic administration in case of suspicious symptoms following activities in BSF risky areas. Besides, education of owners about the risk of unrestrained domestic dogs and dogs abandoning consequences. Finally, capybaras are either well appreciated by the public or depreciated because these rodents are also considered as major crops destroyer (Dias et al., 2020). In both of these cases, people can be led to approach closely the animal to pet or chase it, which represent a risk of transmission that they should be informed. As the increasing population of capybaras in Brazil is suspected to be involved in the BSF incidence (Souza et al., 2009; M. Szabó et al., 2013), controlling capybara populations may seem to be a solution to reduce the zoonotic risk. However, regardless of the ethical and environmental policies issues this would raise, the BSF enzootic cycle is too complex to designate capybaras as a major cause of the disease transmission (Labruna, 2013).

Although dense forests are associated with BSF risk, deforestation and expansion of pasture and agriculture increase further more the risk. Indeed, deforestation seems to have a double cost regarding the spotted fever: one for the resulting rural land use matrices of the landscape, and another for the following regeneration process (probable weaker mitigation services) that also increases BSF incidence, especially when occurring in riparian areas. Reinforcing conservation of pristine primary forests and the integrity of their ecosystem services in synergy with slowing down deforestation caused by the agricultural expansion, rather than controlling amplifier host populations, would probably have much higher mitigation impact on the BSF incidence. Moreover, knowing that 30% of the forest cover is within private properties. Sensibilizing the landowners of the issues associated with deforestation is urging (Rezende et al., 2018).

Besides, a useful application of environmental epidemiology studies is the prediction of diseases incidence as a function of landscape changes. Knowing which landscape parameters are the most correlated with the BSF incidence, these variables can be included in various inference analysis types to assess risk of future landscape scenarios. In this study, the spatial model (Figure 12) is an example of model that could be used for prediction of the BSF incidence (see Box 2 for instance).

Box 2 : Example of a model inference to assess the effect from an increase in additional 10% of riparian forest cover in a municipality immersed in a pasture matrix.

This example is given with the following prior assumptions: the increase of riparian forest cover occur in the same municipality and in the same year (no random intercepts), the population is assumed to be constant (BSF cases = BSF incidence). A coefficient represents the increase in BSF cases on a logarithm scale for each standard deviation unit of the variable associated (scaled variables), when the other variables of the model are kept constant. The riparian forest cover standard deviation (σ) is 17.73, therefore, 10% increase of riparian forest cover represents an increase of (1/17.73)x10 which is equal to 0.56 x σ. Hence, the model equation (Eq.1) becomes:

$$Log(BSF\ cases) = -16.37 + 0.45 \text{ x } 0.56 + 0.41$$

with intercept (β_0) = -16.37, $\beta_{\text{pasture matrix}}$ = 0.41 (factor), $\beta_{\text{Riparian Forest}}$ = 0.45, which is equal to:

$$BSF\ cases = exp(-16.37) \text{ x } exp(0.45 \text{ x } 0.56) \text{ x } exp(0.41)$$

Therefore, in this fictive example, BSF incidence increases by 2.79 cases per 100.000 inhabitants (confidence interval 95% : 2.21 – 3.61) in response to an additional 10% increase in riparian forest cover.

5 Conclusion and perspectives

In the context of constant landscape changes, zoonoses became an actual area of concern. Studying and monitoring the emergence of zoonotic diseases is crucial to adapt ourselves to face epidemics and prevent a maximum of casualties. Environmental epidemiology studies can provide a good assessment of environments that are the more at risk of a given zoonosis. This thesis is embedded in such a background as it aims at appraising how landscape changes of the last two decades in the Atlantic Forest have affected the Brazilian spotted fever incidence. To do so, the more specific objectives were collecting spotted fever data in each municipality of the biome, creating a temporal database of land use and land cover and the assessment of their changes, and finally, investigating the relationship between landscape changes and the BSF incidence.

In conclusion, the main results point out that forest cover, especially riparian forest cover, are associated with spotted fever risks. However, that risk is increased when such riparian forests are immersed within pastoral and agricultural landscape matrices. Unlike landscape structure, landscape metrics were not as much useful to clarify the BSF incidence at the scale of the biome. The results are explained by the tick species ecology and their hosts, as they can colonize both densely vegetated and open environments. Therefore, knowing the structure and the configuration of landscapes with BSF risk, adequate prevention measures can be undertaken. Now, physicians should also take the recent activity history of patients (for instance, rural fields work, riparian leisure activities) with suspect symptoms of fever and potential recent tick bites into account. Education of the public about behavioural risks is also important. For example, informing people on the risk of unrestrained or ownerless dogs, or the close contact with capybaras and cattle. Moreover, sensibilization to the use of repellents when visiting such environments and the preventive antibiotics administration in case of BSF suspicion, would be the most effective measures to avoid lethality.

The results also highlight the importance of pristine forests conservation, as they suggest that the majority of forest cover of the Atlantic Forest do not provide efficient mitigation services for the spotted fever incidence, probably because of their young age. Furthermore, the study supplies another argument that the current environmental law, promoting restoration of riparian environments, would be more cost-effective if it would focus on areas with higher potential of natural forest regeneration.

Finally, the method of the present study has generated a vast temporal database on the Atlantic Forest biome containing landscape structure and configuration data that could be used in further studies, thereby sparing considerable time of data generation. It will be also interesting in further studies to break down the analysis and compare the trends observed in the different regions of the biome that include different tick species involved in the BSF cycle. For example, comparing the effects of landscape between the states of Santa Catarina mostly colonized by *A. aureolatum* and the others states colonized by *A. cajannense (s.l.)*. Further studies are also needed to confirm a dilution effect of the rainforest biodiversity on spotted fever. This could be achieved by assessing the effect of biodiversity on the hosts eco-epidemiology and the transmission risk.

6 References

Alcon-Chino, M.E.T., De-Simone, S.G., 2022. Recent Advances in the Immunologic Method Applied to Tick-Borne Diseases in Brazil. Pathogens 11, 870. https://doi.org/10.3390/pathogens11080870

Allen, T., Murray, K.A., Zambrana-Torrelio, C., Morse, S.S., Rondinini, C., Di Marco, M., Breit, N., Olival, K.J., Daszak, P., 2017. Global hotspots and correlates of emerging zoonotic diseases. Nat Commun 8, 1124. https://doi.org/10.1038/s41467-017-00923-8

Anton, E., Muñoz, T., Travería, F.J., Navarro, G., Font, B., Sanfeliu, I., Segura, F., 2016. Randomized Trial of Clarithromycin for Mediterranean Spotted Fever. Antimicrobial Agents and Chemotherapy 60, 1642–1645. https://doi.org/10.1128/AAC.01814-15

Arnold, T.W., 2010. Uninformative Parameters and Model Selection Using Akaike's Information Criterion. The Journal of Wildlife Management 74, 1175–1178. https://doi.org/10.1111/j.1937-2817.2010.tb01236.x

Bartoń, K., 2023. MuMIn: Multi-Model Inference.

Becknell, J.M., Keller, M., Piotto, D., Longo, M., Nara dos-Santos, M., Scaranello, M.A., Bruno de Oliveira Cavalcante, R., Porder, S., 2018. Landscape-scale lidar analysis of aboveground biomass distribution in secondary Brazilian Atlantic Forest. Biotropica 50, 520–530. https://doi.org/10.1111/btp.12538

Biggs, H.M., Behravesh, C.B., Bradley, K.K., Dahlgren, F.S., Drexler, N.A., Dumler, J.S., Folk, S.M., Kato, C.Y., Lash, R.R., Levin, M.L., Massung, R.F., Nadelman, R.B., Nicholson, W.L., Paddock, C.D., Pritt, B.S., Traeger, M.S., 2016. Diagnosis and Management of Tickborne Rickettsial Diseases: Rocky Mountain Spotted Fever and Other Spotted Fever Group Rickettsioses, Ehrlichioses, and Anaplasmosis — United States: A Practical Guide for Health Care and Public Health Professionals. MMWR Recomm. Rep. 65, 1–44. https://doi.org/10.15585/mmwr.rr6502a1

Biology Online, 2022a. Host [WWW Document]. Biology Articles, Tutorials & Dictionary Online. URL https://www.biologyonline.com/dictionary/host (accessed 2.25.23).

Biology Online, 2022b. Reservoir host [WWW Document]. Biology Articles, Tutorials & Dictionary Online. URL https://www.biologyonline.com/dictionary/reservoir-host (accessed 2.25.23).

Biology Online, 2021a. Zoonosis [WWW Document]. Biology Articles, Tutorials & Dictionary Online. URL https://www.biologyonline.com/dictionary/zoonosis (accessed 2.26.23).

Biology Online, 2021b. Aetiology [WWW Document]. Biology Articles, Tutorials & Dictionary Online. URL https://www.biologyonline.com/dictionary/aetiology (accessed 2.25.23).

Biology Online, 2021c. Amplifier host [WWW Document]. Biology Articles, Tutorials & Dictionary Online. URL https://www.biologyonline.com/dictionary/amplifier-host (accessed 2.25.23).

Bivand, R., 2022. R Packages for Analyzing Spatial Data: A Comparative Case Study with Areal Data. Geographical Analysis 54, 488–518. https://doi.org/10.1111/gean.12319

Blanton, L.S., 2019. The Rickettsioses: A Practical Update. Infect Dis Clin North Am 33, 213–229. https://doi.org/10.1016/j.idc.2018.10.010

Bloom, M.S., 2019. Environmental Epidemiology, in: Nriagu, J. (Ed.), Encyclopedia of Environmental Health (Second Edition). Elsevier, Oxford, pp. 419–427. https://doi.org/10.1016/B978-0-12-409548-9.10635-9

Boni, M.F., Lemey, P., Jiang, X., Lam, T.T.-Y., Perry, B.W., Castoe, T.A., Rambaut, A., Robertson, D.L., 2020. Evolutionary origins of the SARS-CoV-2 sarbecovirus lineage responsible for the COVID-19 pandemic. Nat Microbiol 5, 1408–1417. https://doi.org/10.1038/s41564-020-0771-4

Brancalion, P.H.S., Garcia, L.C., Loyola, R., Rodrigues, R.R., Pillar, V.D., Lewinsohn, T.M., 2016. A critical analysis of the Native Vegetation Protection Law of Brazil (2012): updates and ongoing initiatives. Natureza & Conservação 14, 1–15. https://doi.org/10.1016/j.ncon.2016.03.003

Brites-Neto, J., Brasil, J., Roncato Duarte, K.M., 2015. Epidemiological surveillance of capybaras and ticks on warning area for Brazilian spotted fever. Vet World 8, 1143–1149. https://doi.org/10.14202/vetworld.2015.1143-1149

Brooks, M., Bolker, B., Kristensen, K., Maechler, M., Magnusson, A., McGillycuddy, M., Skaug, H., Nielsen, A., Berg, C., Bentham, K. van, Sadat, N., Lüdecke, D., Lenth, R., O'Brien, J., Geyer, C.J., Jagan, M., Wiernik, B., Stouffer, D.B., 2023. glmmTMB: Generalized Linear Mixed Models using Template Model Builder.

Brooks, M.E., Kristensen, K., Benthem, K.J. van, Magnusson, A., Berg, C.W., Nielsen, A., Skaug, H.J., Mächler, M., Bolker, B.M., 2017. glmmTMB Balances Speed and Flexibility Among Packages for Zero-inflated Generalized Linear Mixed Modeling. The R Journal 9, 378–400.

Calaboni, A., Tambosi, L., Igari, A., Farinaci, J., Metzger, J.P., Uriarte, M., 2018. The forest transition in São Paulo, Brazil: historical patterns and potential drivers. Ecology and Society 23. https://doi.org/10.5751/ES-10270-230407

Campos Krauer, J., Wisely, S., Benitez, I., Robles, V., Golightly, R., 2014. Rango de Hogar y uso de Hábitat de Carpinchos en Pastizales recién invadido en el Chaco Seco de Paraguay. Therya Vol.5, 61–79. https://doi.org/10.12933/therya-14-177

Canale, G.R., Peres, C.A., Guidorizzi, C.E., Gatto, C.A.F., Kierulff, M.C.M., 2012. Pervasive Defaunation of Forest Remnants in a Tropical Biodiversity Hotspot. PLOS ONE 7, e41671. https://doi.org/10.1371/journal.pone.0041671

Carvalho, F.M.V., De Marco, P., Ferreira, L.G., 2009. The Cerrado into-pieces: Habitat fragmentation as a function of landscape use in the savannas of central Brazil. Biological Conservation 142, 1392–1403. https://doi.org/10.1016/j.biocon.2009.01.031

Castro, R.R., Santos, R.S.C., Sousa, G.J.B., Pinheiro, Y.T., Martins, R.R.I.M., Pereira, M.L.D., Silva, R. a. R., 2021. Spatial dynamics of the COVID-19 pandemic in Brazil. Epidemiology & Infection 149, e60. https://doi.org/10.1017/S0950268821000479

Civitello, D.J., Cohen, J., Fatima, H., Halstead, N.T., Liriano, J., McMahon, T.A., Ortega, C.N., Sauer, E.L., Sehgal, T., Young, S., Rohr, J.R., 2015. Biodiversity inhibits parasites: Broad evidence for the dilution effect. Proceedings of the National Academy of Sciences 112, 8667–8671. https://doi.org/10.1073/pnas.1506279112

Claudia Araujo Scinachi, 2022. Evaluation of domestic dogs as competent amplifier hosts of the bacterium Rickettsia rickettsii for Amblyomma aureolatum ticks and predictive spatial ecological modeling for the occurrence of Brazilian Spotted Fever in the State of São Paulo. (Doctoral thesis). Universidade de São Paulo - Faculdade de Saúde Pública, São Paulo.

Cliff, A.D., Ord, K., 1970. Spatial Autocorrelation: A Review of Existing and New Measures with Applications. Economic Geography 46, 269–292. https://doi.org/10.2307/143144

Crouzeilles, R., Santiami, E., Rosa, M., Pugliese, L., Brancalion, P.H.S., Rodrigues, R.R., Metzger, J.P., Calmon, M., Scaramuzza, C.A. de M., Matsumoto, M.H., Padovezi, A., Benini, R. de M., Chaves, R.B., Metzker, T., Fernandes, R.B., Scarano, F.R., Schmitt, J., Lui, G., Christ, P., Vieira, R.M., Senta, M.M.D., Malaguti, G.A., Strassburg, B.B.N., Pinto, S., 2019. There is hope for achieving ambitious Atlantic Forest restoration commitments. Perspectives in Ecology and Conservation 17, 80–83. https://doi.org/10.1016/j.pecon.2019.04.003

Dahlgren, F.S., Holman, R.C., Paddock, C.D., Callinan, L.S., McQuiston, J.H., 2012. Fatal Rocky Mountain Spotted Fever in the United States, 1999–2007. Am J Trop Med Hyg 86, 713–719. https://doi.org/10.4269/ajtmh.2012.11-0453

Dale, V.H., 1997. The Relationship Between Land-Use Change and Climate Change. Ecological Applications 7, 753–769. https://doi.org/10.1890/1051-0761(1997)007[0753:TRBLUC]2.0.CO;2

de Paula, L.G.F., do Nascimento, R.M., Franco, A. de O., Szabó, M.P.J., Labruna, M.B., Monteiro, C., Krawczak, F. da S., 2022. Seasonal dynamics of Amblyomma sculptum: a review. Parasites & Vectors 15, 193. https://doi.org/10.1186/s13071-022-05311-w

Delisle, J., Mendell, N.L., Stull-Lane, A., Bloch, K.C., Bouyer, D.H., Moncayo, A.C., 2016. Human Infections by Multiple Spotted Fever Group Rickettsiae in Tennessee. Am J Trop Med Hyg 94, 1212–1217. https://doi.org/10.4269/ajtmh.15-0372

Dias, T.C., Stabach, J.A., Huang, Q., Labruna, M.B., Leimgruber, P., Ferraz, K.M.P.M.B., Lopes, B., Luz, H.R., Costa, F.B., Benatti, H.R., Correa, L.R., Nievas, A.M., Monticelli, P.F., Piovezan, U., Szabó, M.P.J., Aguiar, D.M., Brites-Neto, J., Port-Carvalho, M., Rocha, V.J., 2020. Habitat selection in natural and human-modified landscapes by capybaras (Hydrochoerus hydrochaeris), an important host for Amblyomma sculptum ticks 15, e0229277. https://doi.org/10.1371/journal.pone.0229277

Domingo, E., 2016. Chapter 4 - Interaction of Virus Populations with Their Hosts, in: Domingo, E. (Ed.), Virus as Populations. Academic Press, Boston, pp. 123–168. https://doi.org/10.1016/B978-0-12-800837-9.00004-6

Earth Engine, 2013. NASA SRTM Digital Elevation 30m [WWW Document]. Earth Engine Data Catalog. URL https://developers.google.com/earth-engine/datasets/catalog/USGS_SRTMGL1_003 (accessed 7.11.23).

Ellwanger, J.H., Chies, J.A.B., 2021. Zoonotic spillover: Understanding basic aspects for better prevention. Genet Mol Biol 44, e20200355. https://doi.org/10.1590/1678-4685-GMB-2020-0355

ESRI, 2017. ArcGIS.

Estrada-Peña, A., Guglielmone, A.A., Mangold, A.J., 2004. The distribution and ecological “preferences” of the tick Amblyomma cajennense (Acari: Ixodidae), an ectoparasite of humans and other mammals in the Americas. Annals of Tropical Medicine & Parasitology 98, 283–292. https://doi.org/10.1179/000349804225003316

Fan, Y., van den Dool, H., 2008. A global monthly land surface air temperature analysis for 1948–present. Journal of Geophysical Research: Atmospheres 113. https://doi.org/10.1029/2007JD008470

Fan, Y., van den Dool, H., 2004. Climate Prediction Center global monthly soil moisture data set at 0.5° resolution for 1948 to present. Journal of Geophysical Research: Atmospheres 109. https://doi.org/10.1029/2003JD004345

FAO, OIE, WHO, UNEP, 2021. Tripartite and UNEP support OHHLEP's definition of "One Health" [WWW Document]. World Health Organization. URL https://www.who.int/news/item/01-12-2021-tripartite-and-unep-support-ohhlep-s-definition-of-one-health (accessed 3.10.23).

Farr, T.G., Rosen, P.A., Caro, E., Crippen, R., Duren, R., Hensley, S., Kobrick, M., Paller, M., Rodriguez, E., Roth, L., Seal, D., Shaffer, S., Shimada, J., Umland, J., Werner, M., Oskin, M., Burbank, D., Alsdorf, D., 2007. The Shuttle Radar Topography Mission. Reviews of Geophysics 45. https://doi.org/10.1029/2005RG000183

FBDS, 2015. Desenvolvimento Rural Sustentável - Repositório público de mapas e shapefiles para download - Projeto de Mapeamento em Alta Resolução dos Biomas Brasileiros [WWW Document]. FBDS - Fundação Brasileira para o Desenvolvimento Sustentável. URL https://www.fbds.org.br/article.php3?id_article=594 (accessed 4.18.23).

Felix, G.A., Almeida Paz, I.C.L., Piovezan, U., Garcia, R.G., Lima, K. a. O., Nääs, I.A., Salgado, D.D., Pilecco, M., Belloni, M., 2014. Feeding behavior and crop damage caused by capybaras (*Hydrochoerus hydrochaeris*) in an agricultural landscape. Braz. J. Biol. 74, 779–786. https://doi.org/10.1590/1519-6984.02113

Ferraz, S.F.B., Ferraz, K.M.P.M.B., Cassiano, C.C., Brancalion, P.H.S., da Luz, D.T.A., Azevedo, T.N., Tambosi, L.R., Metzger, J.P., 2014. How good are tropical forest patches for ecosystem services provisioning? Landscape Ecol 29, 187–200. https://doi.org/10.1007/s10980-014-9988-z

Funk, C.C., Peterson, P.J., Landsfeld, M.F., Pedreros, D.H., Verdin, J.P., Rowland, J.D., Romero, B.E., Husak, G.J., Michaelsen, J.C., Verdin, A.P., 2014. A quasi-global precipitation time series for drought monitoring (USGS Numbered Series No. 832), A quasi-global precipitation time series for drought monitoring, Data Series. U.S. Geological Survey, Reston, VA. https://doi.org/10.3133/ds832

Gibb, R., Redding, D.W., Chin, K.Q., Donnelly, C.A., Blackburn, T.M., Newbold, T., Jones, K.E., 2020. Zoonotic host diversity increases in human-dominated ecosystems. Nature 584, 398–402. https://doi.org/10.1038/s41586-020-2562-8

Gillespie, J.J., Williams, K., Shukla, M., Snyder, E.E., Nordberg, E.K., Ceraul, S.M., Dharmanolla, C., Rainey, D., Soneja, J., Shallom, J.M., Vishnubhat, N.D., Wattam, R., Purkayastha, A., Czar, M., Crasta, O., Setubal, J.C., Azad, A.F., Sobral, B.S., 2008. Rickettsia phylogenomics: unwinding the intricacies of obligate intracellular life. PLoS One 3, e2018. https://doi.org/10.1371/journal.pone.0002018

Harris, E.K., Verhoeve, V.I., Banajee, K.H., Macaluso, J.A., Azad, A.F., Macaluso, K.R., 2017. Comparative vertical transmission of Rickettsia by Dermacentor variabilis and Amblyomma maculatum. Ticks and Tick-borne Diseases 8, 598–604. https://doi.org/10.1016/j.ttbdis.2017.04.003

Herrador, Z., Fernandez-Martinez, A., Gomez-Barroso, D., León, I., Vieira, C., Muro, A., Benito, A., 2017. Mediterranean spotted fever in Spain, 1997-2014: Epidemiological situation based on hospitalization records. PLoS One 12, e0174745. https://doi.org/10.1371/journal.pone.0174745

IDPH, I.D. of P.H., 2023. Rocky Mountain Spotted Fever [WWW Document]. URL https://dph.illinois.gov/topics-services/diseases-and-conditions/tickborne-illnesses/rocky-mountain-spotted-fever.html (accessed 1.15.24).

Instituto Brasileiro de Geografia e Estatística - IBGE, 2022. Malha Municipal | IBGE [WWW Document]. URL https://www.ibge.gov.br/geociencias/organizacao-do-territorio/malhas-territoriais/15774-malhas.html?edicao=36516&t=sobre (accessed 6.13.23).

IRI, 2023. NOAA NCEP CPC GHCN_CAMS gridded deg0p5: CPC Monthly Global Surface Air Temperature Data Set at 0.5 degree from 1948-present. https://doi.org/10.1029/2003JD004345

IRI, 2020. CHIRPS v2p0 dekad from UCSB: UC Santa Barbara.

Kassambara, A., Mundt, F., 2020. factoextra: Extract and Visualize the Results of Multivariate Data Analyses.

Keesing, F., Ostfeld, R.S., 2021. Impacts of biodiversity and biodiversity loss on zoonotic diseases. Proceedings of the National Academy of Sciences 118, e2023540118. https://doi.org/10.1073/pnas.2023540118

Kristensen, K., McGillycuddy, M., 2023. Covariance structure with glmmTMB.

Labruna, M.B., 2013. Brazilian Spotted Fever: The Role of Capybaras, in: Moreira, J.R., Ferraz, K.M.P.M.B., Herrera, E.A., Macdonald, D.W. (Eds.), Capybara: Biology, Use and Conservation of an Exceptional Neotropical Species. Springer, New York, NY, pp. 371–383. https://doi.org/10.1007/978-1-4614-4000-0_23

Labruna, M.B., 2009. Ecology of Rickettsia in South America. Annals of the New York Academy of Sciences 1166, 156–166. https://doi.org/10.1111/j.1749-6632.2009.04516.x

Labruna, M.B., Kerber, C.E., Ferreira, F., Faccini, J.L.H., De Waal, D.T., Gennari, S.M., 2001. Risk factors to tick infestations and their occurrence on horses in the state of São Paulo, Brazil. Veterinary Parasitology 97, 1–14. https://doi.org/10.1016/S0304-4017(01)00387-9

Labruna, M.B., Santos, F.C.P., Ogrzewalska, M., Nascimento, E.M.M., Colombo, S., Marcili, A., Angerami, R.N., 2014. Genetic Identification of Rickettsial Isolates from Fatal Cases of Brazilian Spotted Fever and Comparison with Rickettsia rickettsii Isolates from the American Continents. J Clin Microbiol. 52, 3788. https://doi.org/10.1128/JCM.01914-14

Labruna, M.B., V, S.M., 2011. Rickettsioses in Latin America, Caribbean, Spain and Portugal. Revista MVZ Córdoba 16, 2435–2457. https://doi.org/10.21897/rmvz.282

Lê, S., Josse, J., Husson, F., 2008. FactoMineR: An R Package for Multivariate Analysis. Journal of Statistical Software 25, 1–18. https://doi.org/10.18637/jss.v025.i01

Lira, P.K., Portela, R. de C.Q., Tambosi, L.R., 2021. Land-Cover Changes and an Uncertain Future: Will the Brazilian Atlantic Forest Lose the Chance to Become a Hopespot?, in: Marques, M.C.M., Grelle, C.E.V. (Eds.), The Atlantic Forest: History, Biodiversity, Threats and Opportunities of the Mega-Diverse Forest. Springer International Publishing, Cham, pp. 233–251. https://doi.org/10.1007/978-3-030-55322-7_11

Loh, E.H., Zambrana-Torrelio, C., Olival, K.J., Bogich, T.L., Johnson, C.K., Mazet, J.A.K., Karesh, W., Daszak, P., 2015. Targeting Transmission Pathways for Emerging Zoonotic Disease Surveillance and Control. Vector Borne Zoonotic Dis 15, 432–437. https://doi.org/10.1089/vbz.2013.1563

Lopes, M.G., Muñoz-Leal, S., de Lima, J.T.R., Fournier, G.F. da S.R., Acosta, I. da C.L., Martins, T.F., Ramirez, D.G., Gennari, S.M., Labruna, M.B., 2018. Ticks, rickettsial and erlichial infection in small mammals from Atlantic forest remnants in northeastern Brazil. International Journal for Parasitology: Parasites and Wildlife 7, 380–385. https://doi.org/10.1016/j.ijppaw.2018.10.001

Lüdecke, D., Ben-Shachar, M., Patil, I., Waggoner, P., Makowski, D., 2021. performance: An R Package for Assessment, Comparison and Testing of Statistical Models. JOSS 6, 3139. https://doi.org/10.21105/joss.03139

Lytras, S., Xia, W., Hughes, J., Jiang, X., Robertson, D.L., 2021. The animal origin of SARS-CoV-2. Science 373, 968–970. https://doi.org/10.1126/science.abh0117

MacDonald, A.J., Mordecai, E.A., 2019. Amazon deforestation drives malaria transmission, and malaria burden reduces forest clearing. Proceedings of the National Academy of Sciences 116, 22212–22218. https://doi.org/10.1073/pnas.1905315116

Magalhães-Matos, P.C., Araújo, I.M. de, Valim, J.R. de A., Ogrzewalska, M., Guterres, A., Cordeiro, M.D., Cepeda, M.B., Fonseca, A.H. da, 2022. Detection of Rickettsia spp. in ring-tailed coatis (Nasua nasua) and ticks of the Iguaçu National Park, Brazilian Atlantic Rainforest. Ticks and Tick-borne Diseases 13, 101891. https://doi.org/10.1016/j.ttbdis.2021.101891

Mansueto, P., Vitale, G., Cascio, A., Seidita, A., Pepe, I., Carroccio, A., di Rosa, S., Rini, G.B., Cillari, E., Walker, D.H., 2011. New insight into immunity and immunopathology of Rickettsial diseases. Clin Dev Immunol 2012, 967852. https://doi.org/10.1155/2012/967852

MapBiomas Brasil, 2021. Mapbiomas Brasil | Infográficos [WWW Document]. MapBiomas [Barsil]. URL https://mapbiomas.org/infograficos-1?cama_set_language=pt-BR (accessed 4.29.23).

MapBiomas Project, 2022a. Collection 7 of the Annual Series of Coverage and Land Use Maps of Brazil [WWW Document]. MapBiomas [Barsil]. URL https://mapbiomas.org/ (accessed 5.19.23).

MapBiomas Project, 2022b. Method for Deforestation Analisys [WWW Document]. MapBiomas [Barsil]. URL https://mapbiomas.org/en/metodo-desmatamento?cama_set_language=en (accessed 7.10.23).

MapBiomas Project, 2022c. Códigos de Legenda [WWW Document]. Mapbiomas [Brasil]. URL https://mapbiomas.org/codigos-de-legenda (accessed 5.31.23).

MapBiomas Project, 2015. Visão geral da metodologia [WWW Document]. URL https://mapbiomas.org/visao-geral-da-metodologia (accessed 5.23.23).

Martins, T.F., Barbieri, A.R.M., Costa, F.B., Terassini, F.A., Camargo, L.M.A., Peterka, C.R.L., de C. Pacheco, R., Dias, R.A., Nunes, P.H., Marcili, A., Scofield, A., Campos, A.K., Horta, M.C., Guilloux, A.G.A., Benatti, H.R., Ramirez, D.G., Barros-Battesti, D.M., Labruna, M.B., 2016. Geographical distribution of Amblyomma cajennense (sensu lato) ticks (Parasitiformes: Ixodidae) in Brazil, with description of the nymph of A. cajennense (sensu stricto). Parasites Vectors 9, 186. https://doi.org/10.1186/s13071-016-1460-2

McGarigal, K., Marks, B.J., 1995. FRAGSTATS: spatial pattern analysis program for quantifying landscape structure. Gen. Tech. Rep. PNW-GTR-351. Portland, OR: U.S. Department of Agriculture, Forest Service, Pacific Northwest Research Station. 122 p 351. https://doi.org/10.2737/PNW-GTR-351

Ministério da Saúde, 2021. Guia de Vigilância em Saúde - 5ª edição — Ministério da Saúde [WWW Document]. Gov.br - Ministério da Saúde. URL https://www.gov.br/saude/pt-br/centrais-de-conteudo/publicacoes/publicacoes-svs/vigilancia/guia-de-vigilancia-em-saude_5ed_21nov21_isbn5.pdf/view (accessed 3.16.23).

Ministério da Saúde do Brazil, 1991. DATASUS – Ministério da Saúde [WWW Document]. Ministério da Saúde DATASUS. URL https://datasus.saude.gov.br/ (accessed 3.18.23).

Moerbeck, L., Vizzoni, V.F., Machado-Ferreira, E., Cavalcante, R.C., Oliveira, S.V., Soares, C.A.G., Amorim, M., Gazêta, G.S., 2016. Rickettsia (Rickettsiales: Rickettsiaceae) Vector Biodiversity in High Altitude Atlantic Forest Fragments Within a Semiarid Climate: A New Endemic Area of Spotted-Fever in Brazil. J. Med. Entomol. 53, 1458–1466. https://doi.org/10.1093/jme/tjw121

Molin, P.G., Chazdon, R., Frosini de Barros Ferraz, S., Brancalion, P.H.S., 2018. A landscape approach for cost-effective large-scale forest restoration. Journal of Applied Ecology 55, 2767–2778. https://doi.org/10.1111/1365-2664.13263

Morand, A., Angelakis, E., Ben Chaabane, M., Parola, P., Raoult, D., Gautret, P., 2018. Seek and Find! PCR analyses of skin infections in West-European travelers returning from abroad with an eschar. Travel Medicine and Infectious Disease 26, 32–36. https://doi.org/10.1016/j.tmaid.2018.02.009

Morand, S., Lajaunie, C., 2021a. Outbreaks of Vector-Borne and Zoonotic Diseases Are Associated With Changes in Forest Cover and Oil Palm Expansion at Global Scale. Front Vet Sci 8, 661063. https://doi.org/10.3389/fvets.2021.661063

Morand, S., Lajaunie, C., 2021b. Outbreaks of Vector-Borne and Zoonotic Diseases Are Associated With Changes in Forest Cover and Oil Palm Expansion at Global Scale. Front Vet Sci 8, 661063. https://doi.org/10.3389/fvets.2021.661063

NASA JPL, 2013. NASA Shuttle Radar Topography Mission Global 1 arc second. https://doi.org/10.5067/MEASURES/SRTM/SRTMGL1.003

NIH, 2018. NIAID Emerging Infectious Diseases/ Pathogens [WWW Document]. NIH: National Institute of Allergy and Infectious Diseases. URL https://www.niaid.nih.gov/research/emerging-infectious-diseases-pathogens (accessed 5.17.23).

Ogrzewalska, M., Pinter, A., 2016. Ticks (Acari: Ixodidae) as ectoparasites of Brazilian wild birds and their association with rickettsial diseases. Brazilian Journal of Veterinary Research and Animal Science 53, 1–31. https://doi.org/10.11606/issn.1678-4456.v53i1p1-31

Ogrzewalska, M., Saraiva, D.G., Moraes-Filho, J., Martins, T.F., Costa, F.B., Pinter, A., Labruna, M.B., 2012. Epidemiology of Brazilian spotted fever in the Atlantic Forest, state of São Paulo, Brazil. Parasitology 139, 1283–1300. https://doi.org/10.1017/S0031182012000546

Oliveira, S.V. de, Guimarães, J.N., Reckziegel, G.C., Neves, B.M. da C., Araújo-Vilges, K.M. de, Fonseca, L.X., Pinna, F.V., Pereira, S.V.C., Caldas, E.P. de, Gazeta, G.S., Gurgel-Gonçalves, R., 2016. An update on the epidemiological situation of spotted fever in Brazil. J. Venom. Anim. Toxins incl. Trop. Dis 22, 22. https://doi.org/10.1186/s40409-016-0077-4

Oliveira, S.V. de, Romero-Alvarez, D., Martins, T.F., Santos, J.P. dos, Labruna, M.B., Gazeta, G.S., Escobar, L.E., Gurgel-Gonçalves, R., 2017. Amblyomma ticks and future climate: Range contraction due to climate warming. Acta Tropica 176, 340–348. https://doi.org/10.1016/j.actatropica.2017.07.033

Oliveira, M.A., Grillo, A.S., Tabarelli, M., 2004. Forest edge in the Brazilian Atlantic forest: drastic changes in tree species assemblages. Oryx 38, 389–394. https://doi.org/10.1017/S0030605304000754

Olivero, J., Fa, J.E., Real, R., Márquez, A.L., Farfán, M.A., Vargas, J.M., Gaveau, D., Salim, M.A., Park, D., Suter, J., King, S., Leendertz, S.A., Sheil, D., Nasi, R., 2017. Recent loss of closed forests is associated with Ebola virus disease outbreaks. Sci Rep 7, 14291. https://doi.org/10.1038/s41598-017-14727-9

Openshaw, J.J., Swerdlow, D.L., Krebs, J.W., Holman, R.C., Mandel, E., Harvey, A., Haberling, D., Massung, R.F., McQuiston, J.H., 2010. Rocky Mountain Spotted Fever in the United States, 2000–2007: Interpreting Contemporary Increases in Incidence. Am J Trop Med Hyg 83, 174–182. https://doi.org/10.4269/ajtmh.2010.09-0752

Osava, C.F., Ramos, V. do N., Rodrigues, A.C., dos Reis Neto, H.V., Martins, M.M., Pascoal, J.O., Yokosawa, J., Szabó, M.P.J., 2016. Amblyomma sculptum (Amblyomma cajennense complex) tick population maintained solely by domestic pigs. Veterinary Parasitology: Regional Studies and Reports 6, 9–13. https://doi.org/10.1016/j.vprsr.2016.11.002

Paris, D.H., Dumler, J.S., 2016. State of the art of diagnosis of rickettsial diseases: the use of blood specimens for diagnosis of scrub typhus, spotted fever group rickettsiosis, and murine typhus. Curr Opin Infect Dis 29, 433–439. https://doi.org/10.1097/QCO.0000000000000298

Parola, P., Paddock, C.D., Socolovschi, C., Labruna, M.B., Mediannikov, O., Kernif, T., Abdad, M.Y., Stenos, J., Bitam, I., Fournier, P.-E., Raoult, D., 2013. Update on tick-borne rickettsioses around the world: a geographic approach. Clin Microbiol Rev 26, 657–702. https://doi.org/10.1128/CMR.00032-13

Patz, J.A., Campbell-Lendrum, D., Holloway, T., Foley, J.A., 2005. Impact of regional climate change on human health. Nature 438, 310–317. https://doi.org/10.1038/nature04188

Patz, J.A., Daszak, P., Tabor, G.M., Aguirre, A.A., Pearl, M., Epstein, J., Wolfe, N.D., Kilpatrick, A.M., Foufopoulos, J., Molyneux, D., Bradley, D.J., 2004. Unhealthy Landscapes: Policy Recommendations on Land Use Change and Infectious Disease Emergence. Environ Health Perspect 112, 1092–1098. https://doi.org/10.1289/ehp.6877

Pekkanen, J., Pearce, N., 2001. Environmental epidemiology: challenges and opportunities. ehp 109, 1–5. https://doi.org/10.1289/ehp.011091

Pereira, D.P., Fiedler, N.C., Lima, J.S. de S., Bauer, M. de O., Rezende, A.V., Missiaggia, A.A., Simão, J.B.P., 2011. Lateral stability limits of farm tractors for forest plantations in steep areas. Limites da estabilidade lateral de tratores agrícolas para plantações forestais em áreas inclinadas 39, 433–439.

Pfeifer, M., Lefebvre, V., Peres, C.A., Banks-Leite, C., Wearn, O.R., Marsh, C.J., Butchart, S.H.M., Arroyo-Rodríguez, V., Barlow, J., Cerezo, A., Cisneros, L., D’Cruze, N., Faria, D., Hadley, A., Harris, S.M., Klingbeil, B.T., Kormann, U., Lens, L., Medina-Rangel, G.F., Morante-Filho, J.C., Olivier, P., Peters, S.L., Pidgeon, A., Ribeiro, D.B., Scherber, C., Schneider-Maunoury, L., Struebig, M., Urbina-Cardona, N., Watling, J.I., Willig, M.R., Wood, E.M., Ewers, R.M., 2017. Creation of forest edges has a global impact on forest vertebrates. Nature 551, 187–191. https://doi.org/10.1038/nature24457

Piffer, P.R., Rosa, M.R., Tambosi, L.R., Metzger, J.P., Uriarte, M., 2022. Turnover rates of regenerated forests challenge restoration efforts in the Brazilian Atlantic forest. Environ. Res. Lett. 17, 045009. https://doi.org/10.1088/1748-9326/ac5ae1

Pinter, A., França, A., Souza, C., Sabbo, C., Nascimento, E.M. do, Santos, F., Katz, G., Labruna, M., Holcman, M., Alves, M., Horta, M., Mascheretti, M., Mayo, R., Angerami, R., Brasil, R., Leite, R., Souza, S., Colombo, S., Oliveira, V., 2011. Febre Maculosa Brasileira. Boletim Epidemiológico Paulista 8, 35.

Piranda, E.M., Faccini, J.L.H., Pinter, A., Pacheco, R.C., Cançado, P.H.D., Labruna, M.B., 2011. Experimental infection of Rhipicephalus sanguineus ticks with the bacterium Rickettsia rickettsii, using experimentally infected dogs. Vector Borne Zoonotic Dis 11, 29–36. https://doi.org/10.1089/vbz.2009.0250

QGIS Development Team, 2022. QGIS Geographic Information System.

R Core Team, 2021. R: A language and environment for statistical computing.

Regan, J.J., Traeger, M.S., Humpherys, D., Mahoney, D.L., Martinez, M., Emerson, G.L., Tack, D.M., Geissler, A., Yasmin, S., Lawson, R., Williams, V., Hamilton, C., Levy, C., Komatsu, K., Yost, D.A., McQuiston, J.H., 2015. Risk Factors for Fatal Outcome From Rocky Mountain Spotted Fever in a Highly Endemic Area—Arizona, 2002–2011. Clin Infect Dis 60, 1659–1666. https://doi.org/10.1093/cid/civ116

Reiczigel, J., Rozsa, L., 2010. A brief guide to Quantitative Parasitology 3.0.

Reynolds, M.G., Doty, J.B., McCollum, A.M., Olson, V.A., Nakazawa, Y., 2019. Monkeypox re-emergence in Africa: a call to expand the concept and practice of One Health. Expert Review of Anti-infective Therapy 17, 129–139. https://doi.org/10.1080/14787210.2019.1567330

Rezende, C.L., Scarano, F.R., Assad, E.D., Joly, C.A., Metzger, J.P., Strassburg, B.B.N., Tabarelli, M., Fonseca, G.A., Mittermeier, R.A., 2018. From hotspot to hopespot: An opportunity for the Brazilian Atlantic Forest. Perspectives in Ecology and Conservation 16, 208–214. https://doi.org/10.1016/j.pecon.2018.10.002

Ribeiro, M.C., Martensen, A.C., Metzger, J.P., Tabarelli, M., Scarano, F., Fortin, M.-J., 2011. The Brazilian Atlantic Forest: A Shrinking Biodiversity Hotspot, in: Zachos, F.E., Habel, J.C. (Eds.), Biodiversity Hotspots: Distribution and Protection of Conservation Priority Areas. Springer, Berlin, Heidelberg, pp. 405–434. https://doi.org/10.1007/978-3-642-20992-5_21

Rulli, M.C., Santini, M., Hayman, D.T.S., D'Odorico, P., 2017. The nexus between forest fragmentation in Africa and Ebola virus disease outbreaks. Sci Rep 7, 41613. https://doi.org/10.1038/srep41613

Sakai, R.K., Costa, F.B., Ueno, T.E.H., Ramirez, D.G., Soares, J.F., Fonseca, A.H., Labruna, M.B., Barros-Battesti, D.M., 2014. Experimental infection with Rickettsia rickettsii in an Amblyomma dubitatum tick colony, naturally infected by Rickettsia bellii. Ticks and Tick-borne Diseases 5, 917–923. https://doi.org/10.1016/j.ttbdis.2014.07.003

Silva, N., Eremeeva, M.E., Rozental, T., Ribeiro, G.S., Paddock, C.D., Ramos, E.A.G., Favacho, A.R.M., Reis, M.G., Dasch, G.A., de Lemos, E.R.S., Ko, A.I., 2011. Eschar-associated Spotted Fever Rickettsiosis, Bahia, Brazil. Emerg Infect Dis 17, 275–278. https://doi.org/10.3201/eid1702.100859

Silveira, I., Pacheco, R.C., Szabó, M.P.J., Ramos, H.G.C., Labruna, M.B., 2007. Rickettsia parkeri in Brazil. Emerg Infect Dis 13, 1111–1113. https://doi.org/10.3201/eid1307.061397

Soares, J.F., Soares, H.S., Barbieri, A.M., Labruna, M.B., 2011. Experimental infection of the tick Amblyomma cajennense, Cayenne tick, with Rickettsia rickettsii, the agent of Rocky Mountain spotted fever. Medical and Veterinary Entomology 26, 139–151. https://doi.org/10.1111/j.1365-2915.2011.00982.x

Souza, C.E., Camargo, L.B., Pinter, A., Donalisio, M.R., 2016. High Seroprevalence for Rickettsia rickettsii in Equines Suggests Risk of Human Infection in Silent Areas for the Brazilian Spotted Fever. PLoS One 11, e0153303. https://doi.org/10.1371/journal.pone.0153303

Souza, C.E., Moraes-Filho, J., Ogrzewalska, M., Uchoa, F.C., Horta, M.C., Souza, S.S.L., Borba, R.C.M., Labruna, M.B., 2009. Experimental infection of capybaras Hydrochoerus hydrochaeris by Rickettsia rickettsii and evaluation of the transmission of the infection to ticks Amblyomma cajennense. Veterinary Parasitology 161, 116–121. https://doi.org/10.1016/j.vetpar.2008.12.010

Spolidorio, M.G., Labruna, M.B., Mantovani, E., Brandão, P.E., Richtzenhain, L.J., Yoshinari, N.H., 2010. Novel Spotted Fever Group Rickettsiosis, Brazil. Emerg Infect Dis 16, 521–523. https://doi.org/10.3201/eid1603.091338

Suryowati, K., Bekti, R.D., Faradila, A., 2018. A Comparison of Weights Matrices on Computation of Dengue Spatial Autocorrelation. IOP Conf. Ser.: Mater. Sci. Eng. 335, 012052. https://doi.org/10.1088/1757-899X/335/1/012052

Sutherland, C., Hare, D., Johnson, P.J., Linden, D.W., Montgomery, R.A., Droge, E., 2023. Practical advice on variable selection and reporting using Akaike information criterion. Proceedings of the Royal Society B: Biological Sciences 290, 20231261. https://doi.org/10.1098/rspb.2023.1261

Symonds, M.R.E., Moussalli, A., 2011. A brief guide to model selection, multimodel inference and model averaging in behavioural ecology using Akaike's information criterion. Behav Ecol Sociobiol 65, 13–21. https://doi.org/10.1007/s00265-010-1037-6

Szabó, M., Pinter, A., Labruna, M., 2013. Ecology, biology and distribution of spotted-fever tick vectors in Brazil. Front. Cell. Infect. Microbiol. 3. https://doi.org/doi.org/10.3389/fcimb.2013.00027

Szabó, Matias P. J., Castro, M.B., Ramos, H.G.C., Garcia, M.V., Castagnolli, K.C., Pinter, A., Veronez, V.A., Magalhães, G.M., Duarte, J.M.B., Labruna, M.B., 2007. Species diversity and seasonality of free-living ticks (Acari: Ixodidae) in the natural habitat of wild Marsh deer (Blastocerus dichotomus) in Southeastern Brazil. Veterinary Parasitology 143, 147–154. https://doi.org/10.1016/j.vetpar.2006.08.009

Szabó, M.P.J., Labruna, M.B., Garcia, M.V., Pinter, A., Castagnolli, K.C., Pacheco, R.C., Castro, M.B., Veronez, V.A., Magalhães, G.M., Vogliotti, A., Duarte, J.M.B., 2009. Ecological aspects of the free-living ticks (Acari: Ixodidae) on animal trails within Atlantic rainforest in south–eastern Brazil. Annals of Tropical Medicine & Parasitology 103, 57–72. https://doi.org/10.1179/136485909X384956

Szabó, M.P.J., Nieri-Bastos, F.A., Spolidorio, M.G., Martins, T.F., Barbieri, A.M., Labruna, M.B., 2013. In vitro isolation from Amblyomma ovale (Acari: Ixodidae) and ecological aspects of the Atlantic rainforest Rickettsia, the causative agent of a novel spotted fever rickettsiosis in Brazil. Parasitology 140, 719–728. https://doi.org/10.1017/S0031182012002065

Szabó, Matias Pablo Juan, Olegário, M.M.M., Santos, A.L.Q., 2007. Tick fauna from two locations in the Brazilian savannah. Exp Appl Acarol 43, 73–84. https://doi.org/10.1007/s10493-007-9096-8

Teixeira, A.M.G., Soares-Filho, B.S., Freitas, S.R., Metzger, J.P., 2009. Modeling landscape dynamics in an Atlantic Rainforest region: Implications for conservation. Forest Ecology and Management 257, 1219–1230. https://doi.org/10.1016/j.foreco.2008.10.011

Todd, S.R., Dahlgren, F.S., Traeger, M.S., Beltrán-Aguilar, E.D., Marianos, D.W., Hamilton, C., McQuiston, J.H., Regan, J.J., 2015. No Visible Dental Staining in Children Treated with Doxycycline for

Suspected Rocky Mountain Spotted Fever. The Journal of Pediatrics 166, 1246–1251. https://doi.org/10.1016/j.jpeds.2015.02.015

Vassari-Pereira, D., Valverde, M.C., Asmus, G.F., 2022. Impacto das mudanças climáticas e da qualidade do ar em hospitalizações por doenças respiratórias em municípios da Região Metropolitana de São Paulo (RMSP), Brasil. Ciênc. saúde coletiva 27, 2023–2034. https://doi.org/10.1590/1413-81232022275.08632021

Verdade, L.M., Ferraz, K.M.P.M.B., 2006. Capybaras in an anthropogenic habitat in Southeastern Brazil. Braz. J. Biol. 66, 371–378. https://doi.org/10.1590/S1519-69842006000200019

Veronez, V.A., Freitas, B.Z., Olegário, M.M.M., Carvalho, W.M., Pascoli, G.V.T., Thorga, K., Garcia, M.V., Szabó, M.P.J., 2010. Ticks (Acari: Ixodidae) within various phytophysiognomies of a Cerrado reserve in Uberlândia, Minas Gerais, Brazil. Exp Appl Acarol 50, 169–179. https://doi.org/10.1007/s10493-009-9294-7

Vezzulli, L., Colwell, R.R., Pruzzo, C., 2013. Ocean Warming and Spread of Pathogenic Vibrios in the Aquatic Environment. Microb Ecol 65, 817–825. https://doi.org/10.1007/s00248-012-0163-2

Walker, D.H., Paddock, C.D., Dumler, J.S., 2008. Emerging and Re-emerging Tick-Transmitted Rickettsial and Ehrlichial Infections. Med Clin North Am., New and Emerging Infectious Diseases 92, 1345–1361. https://doi.org/10.1016/j.mcna.2008.06.002

WHO team, 2023a. Weekly epidemiological update on COVID-19 (No. Edition 131), Emergency Situational Updates. World Health Organization.

WHO team, 2023b. WHO Coronavirus (COVID-19) Dashboard [WWW Document]. World Health Organization. URL https://covid19.who.int (accessed 2.26.23).

WHO team, 2022. Mpox (monkeypox) outbreak 2022 [WWW Document]. World Health Organization. URL https://www.who.int/emergencies/situations/monkeypox-oubreak-2022 (accessed 5.17.23).

WHO team, 2020. Vector-borne diseases [WWW Document]. World Health Organization. URL https://www.who.int/news-room/fact-sheets/detail/vector-borne-diseases (accessed 2.26.23).

Wu, Y.-C., Chen, C.-S., Chan, Y.-J., 2020. The outbreak of COVID-19: An overview. Journal of the Chinese Medical Association 83, 217. https://doi.org/10.1097/JCMA.0000000000000270

7 Appendices

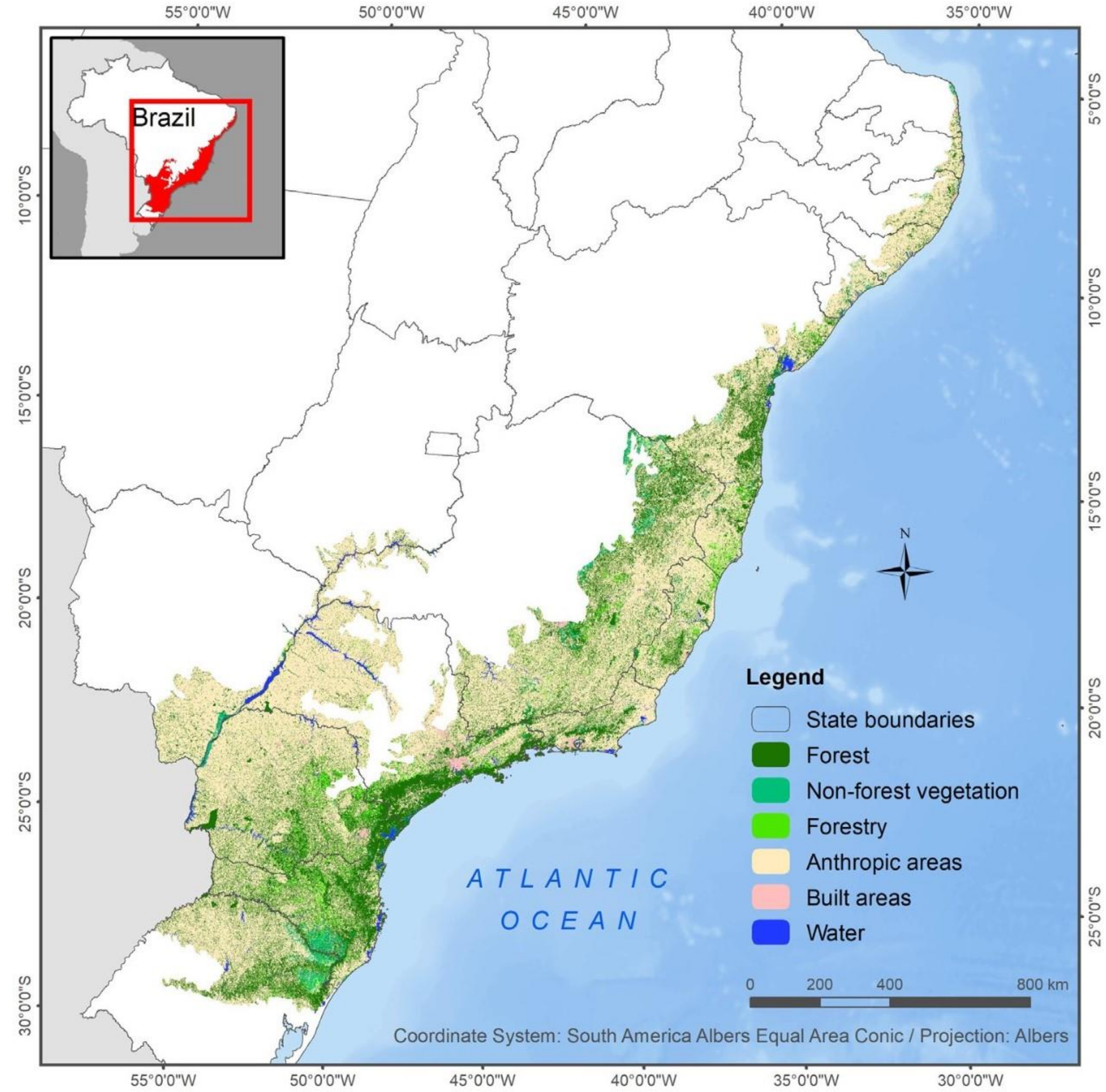

Figure A1 : Atlantic Forest biome land use and land cover, Brazil, 2013. Forest (26%), native vegetation in intermediate or late successional stages, and non-forest vegetation (2%), shrubs and grassland, are both considered as the native vegetation cover (28% of the biome). Built areas (2%), water surfaces (2%), forestry (3%)(tree monocultures, mostly Eucalyptus spp. and Pinus spp.), anthropic areas (65%) which include non-built areas such as agriculture, pasture, mining and degraded areas (Rezende et al., 2018).

Table A1 : Classes of the MapBiomas LULC collection 7 with their respective ID and colour (MapBiomas Project, 2022c).

MAPBIOMAS

Codes of the legend classes and color palette used in MapBiomas Collection 7

COLEÇÃO 7 - CLASSES	COLLECTION 7 CLASSES	NEW ID	Color number	
1. Floresta	**1. Forest**	1	#129912	
1.1 Formação Florestal	1.1. Forest Formation	3	#006400	
1.2. Formação Savânica	1.2. Savanna Formation	4	#00ff00	
1.3. Mangue	1.3. Mangrove	5	#687537	
1.4. Restinga Arborizada	1.4. Wooded Sandbank Vegetation	49	#6b9932	
2. Formação Natural não Florestal	**2. Non Forest Natural Formation**	10	#bbfcac	
2.1. Campo Alagado e Área Pantanosa	2.1. Wetland	11	#45c2a5	
2.2. Formação Campestre	2.2. Grassland	12	#b8af4f	
2.3. Apicum	2.3. Salt Flat	32	#968c46	
2.4. Afloramento Rochoso	2.4. Rocky Outcrop	29	#ff8C00	
2.5 Restinga Herbácea	2.5. Herbaceous Sandbank Vegetation	50	#66ffcc	
2.6. Outras Formações não Florestais	2.5. Other non Forest Formations	13	#bdb76b	
3. Agropecuária	**3. Farming**	14	#ffffb2	
3.1. Pastagem	3.1. Pasture	15	#ffd966	
3.2. Agricultura	3.2. Agriculture	18	#e974ed	
3.2.1. Lavoura Temporária	3.2.1. Temporary Crop	19	#d5a6bd	
3.2.1.1. Soja	3.2.1.1. Soybean	39	#c59ff4	
3.2.1.2. Cana	3.2.1.2. Sugar cane	20	#c27ba0	
3.2.1.3. Arroz (beta)	3.2.1.3. Rice	40	#982c9e	
3.2.1.4. Algodão (beta)	3.2.1.4. Cotton (beta)	62	#660066	
3.2.1.5. Outras Lavouras Temporárias	3.2.1.5. Other Temporary Crops	41	#e787f8	
3.2.2. Lavoura Perene	3.2.2. Perennial Crop	36	#f3b4f1	
3.2.2.1. Café	3.2.1.1. Coffee	46	#cca0d4	
3.2.2.2. Citrus	3.2.1.2. Citrus	47	#d082de	
3.2.1.3. Outras Lavouras Perenes	3.2.1.3. Other Perennial Crops	48	#cd49e4	
3.3. Silvicultura	3.3. Forest Plantation	9	#935132	
3.4. Mosaico de Usos	3.4. Mosaic of Uses	21	#fff3bf	
4. Área não Vegetada	**4. Non vegetated area**	22	#ea9999	
4.1. Praia, Duna e Areal	4.1. Beach, Dune and Sand Spot	23	#dd7e6b	
4.2. Área Urbanizada	4.2. Urban Area	24	#af2a2a	
4.3. Mineração	4.3. Mining	30	#8a2be2	
4.4. Outras Áreas não Vegetadas	4.4. Other non Vegetated Areas	25	#ff99ff	
5. Corpo D'água	**5. Water**	26	#0000ff	
5.1. Rio, Lago e Oceano	5.1. River, Lake and Ocean	33	#0000ff	
5.2 Aquicultura	5.2. Aquaculture	31	#29eee4	
6. Não observado	6. Non Observed	27	#D5D5E5	

Table A2 : Reclassification summary of the MapBiomas LULC classes from the collection 7, with their new ID and colour attributed. Savanna formation is an exception within the non-forest class.

LULC classes reclassified	New ID	Colour number	colour
1. Native Forest	1	#129912	
1.1. Forest Formation		#129912	
1.2. Mangrove		#129912	
1.3. Wooded Sandbank Vegetation		#129912	
2. Native Non-Forest Natural Formation	10	#D1F6B2	
2.1. Wetland		#D1F6B2	
2.2. Grassland		#D1F6B2	
2.3. Salt Flat		#D1F6B2	
2.4. Rocky Outcrop		#D1F6B2	
2.5. Herbaceous Sandbank Vegetation		#D1F6B2	
2.5. Other non-Forest Formations		#D1F6B2	
2.6. Savanna Formation		#D1F6B2	
3. Pasture	15	#bdb76b	
4. Agriculture	18	#ffd966	
4.1 Temporary Crop		#ffd966	
4.2 Soybean		#ffd966	
4.3 Sugar cane		#ffd966	
4.4 Rice		#ffd966	
4.5 Cotton (beta)		#ffd966	
4.6 Other Temporary Crops		#ffd966	
4.7 Perennial Crop		#ffd966	
4.8 Coffee		#ffd966	
4.9 Citrus		#ffd966	
4.10 Other Perennial Crops		#ffd966	
5. Mosaic of Uses (agriculture and pasture)	21	#ffffb2	
6. Silviculture (Forest Plantation)	9	#6F7D3B	
7. Non vegetated area	22	#85596B	
7.1 Beach, Dune, and Sand Spot		#85596B	
7.2 Mining		#85596B	
7.3 Other non-vegetated Areas		#85596B	
8. Urban area	24	#af2a2a	
9. Water	26	#2B7AED	
9.1 River, Lake, and Ocean		#2B7AED	
9.2 Aquaculture		#2B7AED	
10. Non observed	27	#D5D5E5	

Table A3 : Detailed description of the 7th collection of LULC from MapBiomas (MapBiomas Project, 2022c).

MAPBIOMAS [BRASIL]

DESCRIÇÃO DA LEGENDA
COLEÇÃO 7.0

Nivel 1	Nivel 2	Nivel 3	Nivel 4	Biomas	Descrição breve	Clasificação IBGE (1999; 2012)	Clasificação FAO (2012)	Clasificação Inventário Nacional de Emissões de GEE (2015)
Floresta	Formação Florestal			Amazônia	Floresta Ombrófila Densa, Floresta Estacional Sempre-Verde, Floresta Ombrófila Aberta, Floresta Estacional Semidecidual, Floresta Estacional Decidual, Savana Arborizada, Áreas que sofreram ação do fogo ou exploração madeireira, Floresta resultante de processos naturais de sucessão, após supressão total ou parcial de vegetação primária por ações antrópicas ou causas naturais, podendo ocorrer árvores remanescentes de vegetação primária. Floresta Ombrófila Aberta Aluvial estabelecida ao longo dos cursos de água, ocupa as planícies e terraços periodicamente ou permanentemente inundados, que na Amazônia constituem fisionomias de matas-de-várzea ou matas-de-igapó, respectivamente, Floresta de bambu (Acre).	Da, Db, Ds, Dm, Ha, Hb, Hs, Ld, La, Aa, Ab, As, Am, Fa, Fb, Fs, Fm, Ca, Cb, Cs, Cm, Vsp	FDP, FEP, FSP, FEM, FDM, FSM	FMN, FM, FSec
				Caatinga	Tipos de vegetação com predomínio de dossel contínuo - Savana-Estépica Florestada, Floresta Estacional Semi-Decidual e Decidual.	Td, Cs, Cm, Fm, Fs, Pa, As, Fb, Pf, Pm, Fa, Cb, Ds, Am, Ab, Sd	FEP, FSP	FMN, FM
				Cerrado	Tipos de vegetação com predomínio de espécies arbóreas, com formação de dossel contínuo (Mata Ciliar, Mata de Galeria, Mata Seca e Cerradão) (Ribeiro & Walter, 2008), além de florestas estacionais semideciduais.	Aa, Ab, As, Cb, Cm, Cs, Da, Dm, Ds, F, Ml, Mm, P, Sd, Td	FEP, FDP, FSP	FMN, FM
				Mata Atlântica	Floresta Ombrófila Densa, Aberta e Mista e Floresta Estacional Semi-Decidual, Floresta Estacional Decidual e Formação Pioneira Arbórea.	D, A, M, F, C, Pma	FEP, FSP	FMN, FM
				Pampa	Vegetação lenhosa com espécies arbóreas ou arbóreo-arbustivas, com predomínio de dossel contínuo. Inclui as tipologias florestais: ombrófila, decidual e semidecidual e parte das formações pioneiras.	Da, Db, Ds, Dm, Ma, Ms, Mm, Ml, Fa, Fb, Fs, Fm, Ca, Cb, Cs, Cm, P,	FEP, FDP, FSP	FMN, FM, FSec, CS
				Pantanal	Árvores altas e arbustos no estrato inferior: Floresta Estacional Decidual e Semidecidual, Savana Florestada, Savana-Estépica Florestada e Formações Pioneiras com influência fluvial e/ou lacustre.	Ca, Cb, Cs, Fa, Fb, Fs, SN, Sd, Td, Pa	FEP, FSP	FMN, FM
	Formação Savânica			Amazônia	Formação vegetal aberta com um estrato arbustivo e/ou arbóreo mais ou menos desenvolvido, estrato herbáceo sempre presente.	Sa, Ta	WS	FMN, FM
				Caatinga	Tipos de vegetação com predomínio de espécies de dossel semi-contínuo - Savana-Estépica Arborizada, Savana Arborizada.	Ta, Sa	FDP	FMN, FM
				Cerrado	Formações savânicas com estratos arbóreo e arbustivo-herbáceos definidos (Cerrado Sentido Restrito: Cerrado denso, Cerrado típico, Cerrado ralo e Cerrado rupestre).	Sa, Ta	WS	FMN, FM
				Mata Atlântica	Savanas, Savanas-Estépicas Florestadas e Arborizadas.	Sd, Td, Sa, Ta	FDP, FSP, WS	FMN, FM
				Pantanal	Espécies arbóreas de pequeno porte, distribuídas de forma esparsa e dispostas em meio à vegetação contínua de porte arbustivo e herbáceo. A vegetação herbácea se mistura com arbustos eretos e decumbentes.	Sa, Sp, Sg, Td, Ta, Tp	FDP, FSP, WS	FMN, FM
	Mangue				Formações florestais, densas, sempre-verdes, frequentemente inundadas pela maré e associadas ao ecossistema costeiro de Manguezal.	Pf	FEP, FEM	FMN, FM
	Restinga Arborizada			Mata Atlântica	Formações florestais que se estabelecem sobre solos arenosos ou sobre dunas na zona costeira.	Pma	FEP, FEM	FMN, FM
Formação Natural não Florestal	Campo Alagado e Área Pantanosa			Amazônia	Vegetação de várzea ou campestre que sofre influência fluvial e/ou lacustre.	Pa	OM	GNM, GM, GSec
				Cerrado	Vegetação com predomínio de estrato herbáceo sujeita ao alagamento sazonal (ex. Campo Úmido) ou sobre influência fluvial/lacustre (ex. Brejo). Em algumas regiões a matriz herbácea ocorre associada às espécies arbóreas de formação savânica (ex. Parque de Cerrado) ou de palmeiras (Vereda, Palmeiral).	Pa, Sp	OM	GNM, GM, GSec
				Mata Atlântica	Vegetação com influência fluvial e/ou lacustre.	Pa	OM	GNM, GM, GSec
				Pampa	Áreas pantanosas, denominadas regionalmente de banhados ou marismas (influência salina). Vegetação tipicamente higrófila, com plantas aquáticas emergentes, submersas ou flutuantes. Ocupam planícies e depressões do terreno com solo encharcado e também as margens rasas de lagoas ou reservatórios de água.	P, Pa, Pm	OM	A, Res
				Pantanal	Vegetação herbácea com predomínio de gramíneas sujeitas ao alagamento permanente ou temporário (pelo menos uma vez ao ano) de acordo com os pulsos naturais de inundação. O elemento lenhoso pode estar presente sobre a matriz campestre formando um mosaico com plantas arbustivas ou arbóreas (ex: cambarazal, paratudal e carandazal). As áreas pantanosas ocorrem geralmente nas margens das lagoas temporárias ou permanentes ocupadas por plantas aquáticas emergentes, submersas ou flutuantes (ex: brejos e baceiros). Áreas com superfície de água, mas de difícil classificação devido a quantidade de macrófitas, eutrofização ou sedimentos, também foram incluídas nesta categoria.	Tg, Sp, Pa, Tp	OM	GNM, GM, GSec
	Formação Campestre			Amazônia	Savana, Savana Parque (Marajó), Savana-Estépica (Roraima), Savana Gramíneo-Lenhosa, Campinarana, para regiões fora do Ecótono Amazônia/Cerrado. E para regiões dentro do Ecótono Amazônia/Cerrado predominância de estrato herbáceo.	Sa, Sp, Sg, Ta, Tp, Tg	WG, OG, WS	GNM, GM, GSec
				Caatinga	Tipos de vegetação com predomínio de espécies herbáceas (Savana-Estépica Parque, Savana-Estépica Gramíneo-Lenhosa, Savana Parque, Savana Gramíneo-Lenhosa) + (Áreas inundáveis com uma rede de lagoas interligadas, localizadas ao longo dos cursos de água e em áreas de depressões que acumulam água, vegetação predominantemente herbácea a arbustiva).	Tp, Sg, Rm, Sp, Tg, Rl	WG, OG, WS	GNM, GM, GSec
				Cerrado	Formações campestres com predominância de estrato herbáceo (campo sujo, campo limpo e campo rupestre) e algumas áreas de formações savânicas como o Cerrado rupestre.	Sg, Tp, Tg	WG, OG	GNM, GM, GSec
				Mata Atlântica	Savanas e Savanas-Estépicas Parque e Gramíneo-Lenhosa, Estepe e Pioneiras Arbustivas e Herbáceas.	Sp, Sg, Tp, Tg, E, Pa	WS,OG	GNM, GM, GSec
				Pampa	Vegetação com predomínio de estrato herbáceo graminóide, com presença de dicotiledôneas herbáceas e subarbustivas. A composição botânica é influenciada pelos gradientes edáficos e topográficos e pelo manejo pastoril (pecuária). Ocorrem em solos profundos até solos rasos, incluindo terrenos rochosos (campos rupestres) e arenosos (campos arenosos ou psamófilos). Ocupam desde solos bem drenados (campos mésicos), até solos com maior teor de umidade (campos úmidos - com presença marcante de ciperáceas). Na maioria dos casos corresponde à vegetação nativa, mas podem estar presentes manchas de vegetação exótica invasora ou de uso forrageiro (pastagem plantada).	E, Ea, Ep, Eg, T, Ta, Tp, P, Pa, Pm	WG, OG	GNM, GM, GSec
				Pantanal	Vegetação com predomínio de estrato herbáceo graminóide, com presença de arbustivas isoladas e lenhosas raquíticas. A composição botânica é influenciada pelos gradientes edáficos e topográficos e pelo manejo pastoril (pecuária). Manchas de vegetação exótica invasora ou de uso forrageiro (pastagem plantada) podem estar presentes formando mosaicos com a vegetação nativa.	Sg, Sp, Ta, Tg	WG, OG	GNM, GM, GSec

	Apicum				Apicuns ou Salgados são formações quase sempre desprovidas de vegetação arbórea, associadas a uma zona mais alta, hipersalina e menos inundada do manguezal, em geral na transição entre este e a terra firme.	Pf, Pfh	OM, OX	
	Afloramento Rochoso			Caatinga	Rochas naturalmente expostas na superfície terrestre sem cobertura de solo, muitas vezes com presença parcial de vegetação rupícola e alta declividade.	Ar	OX	ArM, ArNM
				Cerrado	Rochas naturalmente expostas na superfície terrestre sem cobertura de solo, muitas vezes com presença parcial de vegetação rupestre e alta declividade.	Ar	OX	ARM, ArNM
				Mata Atlântica	Rochas naturalmente expostas na superfície terrestre sem cobertura de solo, muitas vezes com presença parcial de vegetação rupícola e alta declividade.	Ar	OX	ARM, ArNM
				Pampa	Rochas naturalmente expostas na superfície terrestre sem cobertura de solo, muitas vezes com presença parcial de vegetação rupícola.	Ar	OX	ArM, ArNM
	Restinga Herbácea			Caatinga	Vegetação herbácea com influência fluviomarinha.	Pmb, Pmh	WG, OG	GNM, GM
				Mata Atlântica	Vegetação herbácea com influência fluviomarinha.	Pmb, Pmh	WG, OG	GNM, GM
				Pampa	Vegetação herbácea que se estabelece sobre solos arenosos ou sobre dunas na zona costeira.	Pmb, Pmh	WG, OG	GNM, GM
	Outras Formações não Florestais			Mata Atlântica	Outras Formações Naturais não florestais que não puderam ser categorizadas.	Pfh, Pmb, Pmh	WG, OG	GNM, GM, GSec
Agropecuária	Pastagem				Área de pastagem, predominantemente plantadas, vinculadas a atividade agropecuária. As áreas de pastagem natural são predominantemente classificadas como formação campestre que podem ou não ser pastejadas.	AP, PE, PS	OP, OG	Ap
	Agricultura	Lavoura Temporária	Soja		Áreas cultivadas com a cultura da soja.	AMc (s)	OCA	AC
			Cana		Áreas cultivadas com a cultura da cana-de-açúcar	AMc (c)	OCA	AC
			Arroz		Áreas cultivadas com cultura de arroz, exclusivamente sob sistema de irrigação, nos estados do Rio Grande do Sul, Tocantins, Santa Catarina e Litoral do Paraná. Este mapa é o mesmo apresentado no módulo irrigação na classe "Arroz Irrigado".	AMc	OCA	AC
			Algodão (Versão BETA)		Áreas cultivadas com a cultura do algodão.	AMc (s)	OCA	AC
			Outras Lavouras Temporárias		Áreas ocupadas com cultivos agrícolas de curta ou média duração, geralmente com ciclo vegetativo inferior a um ano, que após a colheita necessitam de novo plantio para produzir.	AMc	OCA	AC
		Lavoura Perene	Café		Áreas cultivadas com a cultura do café.	AMp (c)	OCP	PER
			Citrus		Áreas cultivadas com a cultura do citrus.	AMp	OCP	PER
			Outras Lavouras Perenes		Áreas ocupadas com cultivos agrícolas de ciclo vegetativo longo (mais de um ano), que permitem colheitas sucessivas, sem necessidade de novo plantio. Nessa versão, o mapa abrange majoritariamente áreas de caju, no litoral do nordeste e dendê na região nordeste do Pará, porém sem distinção entre eles.	AMp	OCP	PER
	Silvicultura				Espécies arbóreas plantadas para fins comerciais (ex. pinus, eucalipto, araucária).	R	FPB, FPC, FPM	Ref
	Mosaico de Usos			Caatinga	Areas de uso agropecuário onde não foi possível distinguir entre pastagem e agricultura.	AP, PE, PS, ATp, ATc, ATpc	OCA, OCM, OP, OG	AC, PER, Ap, APD
				Cerrado	Areas de uso agropecuário onde não foi possível distinguir entre pastagem e agricultura.	AP, PE, PS, ATp, ATc, ATpc	OCA, OCM, OP, OG	AC, PER
				Mata Atlântica	Areas de uso agropecuário onde não foi possível distinguir entre pastagem e agricultura.	AP, PE, PS, ATp, ATc, ATpc	OCA, OCM, OP, OG	AC, PER
				Pampa	Áreas de uso agropecuário, onde não foi possível distinguir entre pastagem e agricultura. Pode incluir áreas de cultivos, pastagens de inverno ou de verão e de horticultura. Inclui as áreas de descanso entre safras agrícolas (pousio).	AP, AS, AT, AM, PE, PS, Ag, Ap, Ac, Acc, Acp, AA	OCA, OCM, OP, OG, OF	AC, PER, Ap, APD
				Áreas Urbanizadas	Áreas de vegetação urbana, incluindo vegetação cultivada e vegetação natural florestal e não-florestal.		OB	S
	Praia, Duna e Areal				Cordões arenosos, de coloração branco brilhante, onde não há o predomínio de vegetação de nenhum tipo.	Dn	OX	DnM,DnNM
Área Não Vegetada	Área Urbanizada				Áreas com significativa densidade de edificações e vias, incluindo áreas livres de construções e infraestrutura.		OB	S
	Mineração				Áreas referentes a extração mineral de porte industrial ou artesanal (garimpos), havendo clara exposição do solo por ação por ação antrópica. Somente são consideradas áreas proximas a referências espacias de recursos mineirais do CPRM (GeoSGB), da AhkBrasilien (AHK), do projeto DETER (INPE), do Instituto Socioambiental (ISA) e de FL Lobo et al. 2018.	MCA	OQ	Min
	Outras Áreas não Vegetadas			Amazônia	Áreas de superfícies não permeáveis (infra-estrutura, expansão urbana ou mineração) não mapeadas em suas classes.	AU, MCA	OB, OQ	S, Min
				Caatinga	Áreas de superfícies não permeáveis (infra-estrutura, expansão urbana ou mineração) não mapeadas em suas classes.	AU,MCA	OB, OQ	S, Min
				Cerrado	Áreas de superfícies não permeáveis (infra-estrutura, expansão urbana ou mineração) não mapeadas em suas classes e regiões de solo exposto em área natural ou em áreas de cultura em entresafra.	AU, MCA	OB, OQ	S, Min
				Mata Atlântica	Áreas de superfícies não permeáveis (infra-estrutura, expansão urbana ou mineração) não mapeadas em suas classes.	AU, MCA	OB, OQ	S, Min
				Pampa	Classe mista que contempla áreas naturais e áreas antropizadas. As áreas naturais incluem superfícies arenosas como as praias fluviais e os areais. As áreas antropizadas incluem áreas de solo exposto e superfícies não permeáveis (infra-estrutura, expansão urbana ou mineração).	AU, MCA, Dn, Iu	OB, OQ, OX	S, SE, DnM, DnNM, Min
				Pantanal	Áreas de solo exposto (principalmente solo arenoso) não classificadas na classe de Formação Campestre ou Pastagem.	PE, Sg	OX	Ap, GNM, GSec
Corpos D'água	Rio, Lago e Oceano				Rios, lagos, represas, reservatórios e outros corpos d'água.		IRP, IRS, IL, ID	A, Res
	Aquicultura				Área referente a lagos artificiais, onde predominam atividades aquícolas e/ou de salicultura.			
Não Observado					Áreas bloqueadas por nuvens ou ruído atmosférico, ou com ausência de observação.			NO

Referências: Instituto Brasileiro de Geografia e Estatística - IBGE. Manual técnico de uso da terra, IBGE: Rio de Janeiro, Brazil, 1999, 58p.; Instituto Brasileiro de Geografia e Estatistica - IBGE. Manual técnico da vegetação brasileira, 2nd ed., IBGE: Rio de Janeiro, Brazil, 2012. pp.157-160; Food and Agriculture Organization of the United Nations - FAO. Manual for integrated field data collection. FAO: Rome, Italy, 2012, 175p.; Ministério da Ciência, Tecnologia e Inovações. Secretaria de Pesquisa e Formação Científica. Quarta Comunicação Nacional do Brasil à Convenção-Quadro das Nações Unidas sobre Mudança do Clima, Brasília, 2020, 620p.

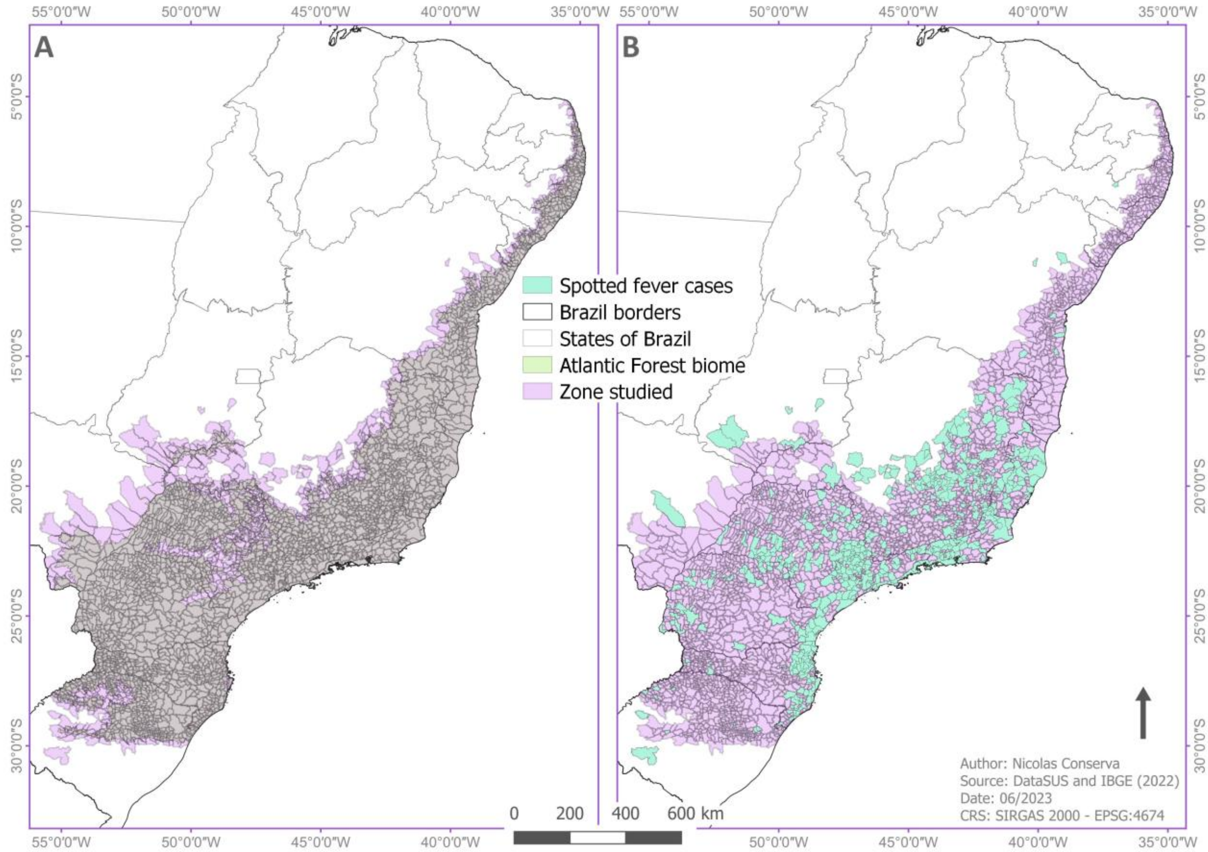

Figure A2 : **A.** Extended zone considered in the present study and comparison with the Atlantic Forest biome extent, municipalities were selected when intercepting the AF, or presenting BSF cases and intercepting a 100 km buffer around the AF biome. **B.** Studied zone in perspective with the municipalities positive to BSF within the 2001 – 2021 period (562/3121 municipalities).

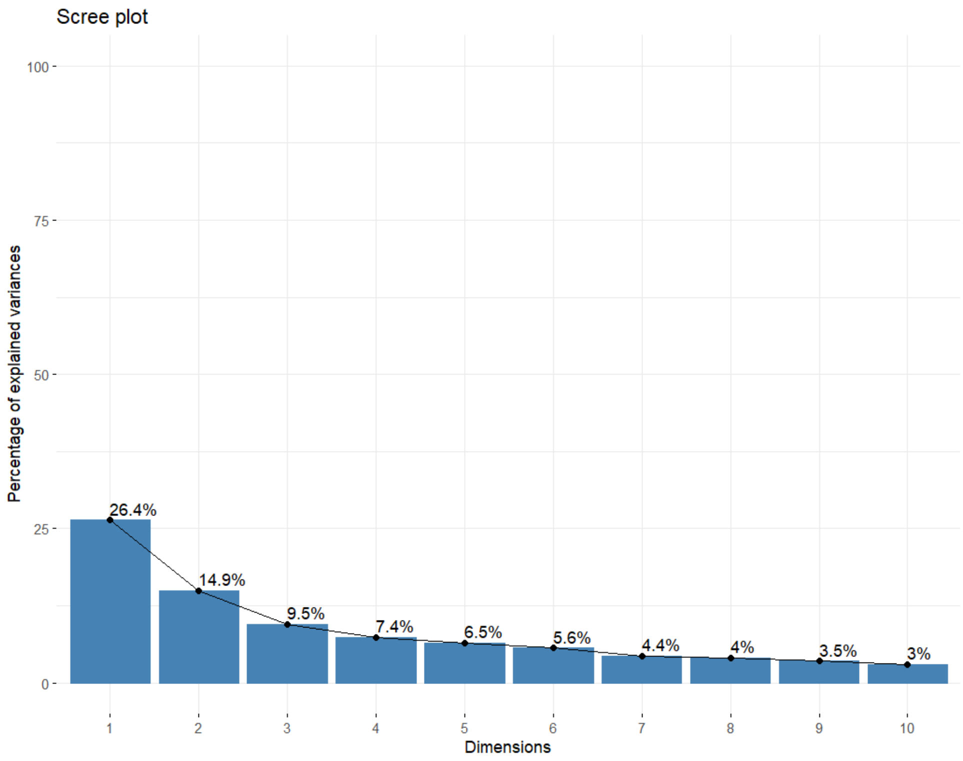

Figure A3 : Scree plot of the principal component analysis (PCA) showing the percentage of explained variances by PCA axes (Dimensions).

Table A4 : List of variables contained in the dataset and their abbreviations used in models formulation.

Variable header	Meaning	Variable type/calculation
CD_NUM	Municipality code	categorical nominal
NM_MUN	Municipality name	categorical nominal
SIGLA_UF	Federal Unit acronym	categorical nominal
AREA_KM2	Superficies of the municipality (km2)	numerical continue
NM_UF	Federal Unit name	categorical nominal
NM_REGIAO	Region of Brazil	categorical nominal
BSF	Spotted fever cases incidence (per 100.000 inhabitants)	numerical continue : (number of cases/estimated number of inhabitants)*100.000
Year	Year	categorical ordinal
Matrix	Dominant land use or land cover type	categorical nominal
CA	Total area of Forest cover (ha)	numerical continue
PLAND	Percentage of Forest cover (%)	numerical continue : CA/AREA_KM2
PD	Patch density (patches/100 ha)	numerical continue : number of patch/AREA_KM2
TE	Total Edge (m)	numerical continue
ED	Edge Density (m/ha)	numerical continue: ED/AREA_KM2
PROX_MN	Mean Proximity Index	numerical continue
ENN_MN	Mean Nearest Neighbour distance (m)	numerical continue, with NA value
ENN_SD	Nearest Neighbour standard deviation (m)	numerical continue, with NA value
ENN_CV	Nearest Neighbour Coefficient of Variation (%)	numerical continue, with NA value : ENN_SD/ENN_MN

Riparian_Forest	Percentage of riparian Forest (%)	numerical continue
Riparian_Non_Forest	Percentage of riparian Non Forest vegetation (%)	numerical continue
Riparian_Pasture	Percentage of riparian Pasture (%)	numerical continue
Riparian_Agriculture	Percentage of riparian Agriculture (%)	numerical continue
Riparian_Mosaic	Percentage of riparian Mosaic (%)	numerical continue
Main_str_Forest	Percentage of riparian Forest considering only the main streams (river width > 10 m) and waterbodies (%)	numerical continue
Main_str_Non_Forest	Percentage of riparian Non Forest vegetation considering only the main streams (river width > 10 m) and waterbodies (%)	numerical continue
Main_str_Pasture	Percentage of riparian Pasture considering only the main streams (river width > 10 m) and waterbodies (%)	numerical continue
Main_str_Agriculture	Percentage of riparian Agriculture considering only the main streams (river width > 10 m) and waterbodies (%)	numerical continue
Main_str_Mosaic	Percentage of riparian Mosaic considering only the main streams (river width > 10 m) and waterbodies (%)	numerical continue
CA_Agriculture	Total area of Agriculture (ha)	numerical continue
PLAND_Agriculture	Percentage of Agriculture cover (%)	numerical continue : CA_Agriculture/AREA_KM2
CA_Pasture	Total area of Pasture (ha)	numerical continue
PLAND_Pasture	Percentage of Pasture cover (%)	numerical continue : CA_Pasture/AREA_KM2
CA_Mosaic_of_Uses	Total area of Mosaic of Uses (ha)	numerical continue
PLAND_Mosaic_of_Uses	Percentage of Mosaic of Uses cover (%)	numerical continue : CA_Mosaic_of_Uses/AREA_KM2
CA_Urban_area	Total area of Urban area (ha)	numerical continue
PLAND_Urban_area	Percentage of Urban area cover (%)	numerical continue : CA_Urban_area/AREA_KM2
trans_ha	Transition areas from Pasture to Agriculture (ha)	numerical continue
trans_p	Percentage of transitions from Pasture to Agriculture (%)	numerical continue : trans_ha/AREA_KM2
PLAND_Savanna	Percentage of Savanna cover (%)	numerical continue : CA_Savanna/AREA_KM2
PLAND_Savanna_Forest	Percentage of Savanna and Forest cover (%)	numerical continue : ((CA_Savanna + CA)/AREA_KM2)*100
Primary_Forest	Percentage of Primary Forest (% per municipality)	numerical continue, with NA value
Secondary_Forest	Percentage of Secondary Forest (% per municipality)	numerical continue, with NA value
alt_1	Percentage of pixels within the category 1 of altitude classes (%)	numerical continue
alt_2	Percentage of pixels within the category 2 of altitude classes (%)	numerical continue
alt_3	Percentage of pixels within the category 3 of altitude classes (%)	numerical continue
alt_4	Percentage of pixels within the category 4 of altitude classes (%)	numerical continue

alt_5	Percentage of pixels within the category 5 of altitude classes (%)	numerical continue
Main_alt	Main altitude class present in the municipality	categorical nominal
steep_slope	Percentage of steep slope (%)	numerical continue
temp	Mean annual temperature (°C)	numerical continue
cold_temp	Mean temperature of the coldest month of the year (°C)	numerical continue
hot_temp	Mean temperature of the hottest month of the year (°C)	numerical continue
prec	Mean annual total monthly precipitation (mm)	numerical continue
Population	Estimated population per municipality	numerical discrete
BSF_cases	number of confirmed cases of spotted fever	numerical discrete

Table A5 : Description of the fitted models by hypothesis/Use. For each models, the response variable was the BSF cases, Population (estimation of inhabitants per municipality) was set as an offset variable with a log function, Municipality (CD_NUM) and Year were set as random intercept variables. Each model of the 5 tested hypotheses were fitted with and without the temperature (temp). See Table A4 for the abbreviations.

Model name	Predictor variables
Full model with the PCA axes	
mod_full	Dim.1 + Dim.3 + Dim.4 + Dim.5 + Dim.6 + Dim.7 + Matrix + Main_alt
Null model	
mod_null	(Intercept only model)
Climatic models	
modclima_1	temp
modclima_2	prec
modclima_3	temp + prec
modclima_4	cold_temp
modclima_5	hot_temp
modclima_6	cold_temp + prec
modclima_7	hot_temp + prec
Hypothesis 1 : Forest cover and secondary forest	
H1mod_1 (H1mod_16)	CA (+ temp)
H1mod_2 (H1mod_17)	PLAND (+ temp)
H1mod_3 (H1mod_18)	Matrix (+ temp)
H1mod_4 (H1mod_19)	PLAND_Savanna (+ temp)
H1mod_5 (H1mod_20)	PLAND_Savanna_Forest (+ temp)
H1mod_6 (H1mod_21)	Primary_Forest (+ temp)
H1mod_7 (H1mod_22)	Secondary_Forest (+ temp)
H1mod_8 (H1mod_23)	CA + PLAND (+ temp)
H1mod_9 (H1mod_24)	PLAND + PLAND_Savanna (+ temp)
H1mod_10 (H1mod_25)	Primary_Forest + Secondary_Forest (+ temp)
H1mod_11 (H1mod_26)	PLAND_Savanna_Forest + Secondary_Forest
H1mod_12 (H1mod_27)	CA + PLAND_Savanna + PLAND_Savanna_Forest (+ temp)
H1mod_13 (H1mod_28)	CA + PLAND_Savanna + PLAND_Savanna_Forest + Secondary_Forest (+ temp)
H1mod_14 (H1mod_29)	PLAND + PLAND_Savanna + Secondary_Forest (+ temp)
H1mod_15 (H1mod_30)	Primary_Forest + Secondary_Forest + PLAND_Savanna (+ temp)
Hypothesis 2 : Land configuration	

H2mod_1 (H2mod_45)	CA (+ temp)
H2mod_2 (H2mod_46)	PLAND (+ temp)
H2mod_3 (H2mod_47)	PD (+ temp)
H2mod_4 (H2mod_48)	TE (+ temp)
H2mod_5 (H2mod_49)	ED (+ temp)
H2mod_6 (H2mod_50)	PROX_MN (+ temp)
H2mod_7 (H2mod_51)	ENN_MN (+ temp)
H2mod_8 (H2mod_52)	ENN_SD (+ temp)
H2mod_9 (H2mod_53)	ENN_CV (+ temp)
H2mod_10 (H2mod_54)	CA_Agriculture (+ temp)
H2mod_11 (H2mod_55)	PLAND_Agriculture (+ temp)
H2mod_12 (H2mod_56)	CA_Pasture (+ temp)
H2mod_13 (H2mod_57)	PLAND_Pasture (+ temp)
H2mod_14 (H2mod_58)	CA_Mosaic_of_Uses (+ temp)
H2mod_15 (H2mod_59)	PLAND_Mosaic_of_Uses (+ temp)
H2mod_16 (H2mod_60)	CA_Urban_area (+ temp)
H2mod_17 (H2mod_61)	PLAND_Urban_area (+ temp)
H2mod_18 (H2mod_62)	Matrix (+ temp)
H2mod_19 (H2mod_63)	CA + PD + ED + Matrix (+ temp)
H2mod_20 (H2mod_64)	CA + PD + ED + CA_Agriculture + CA_Pasture + CA_Mosaic_of_Uses + CA_Urban_area (+ temp)
H2mod_21 (H2mod_65)	CA + PD + ED + Matrix + CA_Agriculture + CA_Pasture + CA_Mosaic_of_Uses + CA_Urban_area (+ temp)
H2mod_22 (H2mod_66)	CA + PD + ED + Matrix + CA_Agriculture + CA_Pasture + CA_Mosaic_of_Uses (+ temp)
H2mod_23 (H2mod_67)	CA + PD + ED + CA_Agriculture + CA_Pasture + CA_Mosaic_of_Uses (+ temp)
H2mod_24 (H2mod_68)	CA + PD + ED + PLAND_Agriculture + PLAND_Pasture + PLAND_Mosaic_of_Uses (+ temp)
H2mod_25 (H2mod_69)	PLAND + PD + TE + PLAND_Agriculture + PLAND_Pasture + PLAND_Mosaic_of_Uses (+ temp)
H2mod_26 (H2mod_70)	PLAND + PD + PLAND_Agriculture + PLAND_Pasture + PLAND_Mosaic_of_Uses (+ temp)
H2mod_27 (H2mod_71)	CA + PD + ED + Matrix + PLAND_Agriculture + PLAND_Pasture + PLAND_Mosaic_of_Uses + PLAND_Urban_area (+ temp)
H2mod_28 (H2mod_72)	CA + PD + ED + PLAND_Agriculture + PLAND_Pasture + PLAND_Mosaic_of_Uses + PLAND_Urban_area (+ temp)
H2mod_30 (H2mod_74)	Matrix + PD + ENN_MN (+ temp)
H2mod_31 (H2mod_75)	Matrix + PD + ENN_SD (+ temp)
H2mod_32 (H2mod_76)	Matrix + PD + ENN_CV (+ temp)
H2mod_33 (H2mod_77)	Matrix + ENN_MN (+ temp)
H2mod_34 (H2mod_78)	Matrix + ENN_SD (+ temp)
H2mod_35 (H2mod_79)	Matrix + ENN_CV (+ temp)
H2mod_36 (H2mod_80)	Matrix + PROX_MN + ENN_CV (+ temp)
H2mod_38 (H2mod_82)	Matrix + PD + ENN_MN (+ temp)
H2mod_39 (H2mod_83)	Matrix + PD + ENN_SD (+ temp)
H2mod_40 (H2mod_84)	Matrix + PD + ENN_CV (+ temp)
H2mod_41 (H2mod_85)	Matrix + ENN_MN + PLAND_Agriculture + PLAND_Pasture + PLAND_Mosaic_of_Uses (+ temp)
H2mod_42 (H2mod_86)	Matrix + ENN_SD + PLAND_Agriculture + PLAND_Pasture + PLAND_Mosaic_of_Uses (+ temp)
H2mod_43 (H2mod_87)	Matrix + ENN_CV + PLAND_Agriculture + PLAND_Pasture + PLAND_Mosaic_of_Uses (+ temp)
H2mod_44 (H2mod_88)	Matrix + PROX_MN + ENN_CV + PLAND_Agriculture + PLAND_Pasture + PLAND_Mosaic_of_Uses (+ temp)

H2mod_45 (H2mod_89)	ENN_MN + PLAND_Agriculture + PLAND_Pasture + PLAND_Mosaic_of_Uses (+ temp)
H2mod_46 (H2mod_90)	ENN_SD + PLAND_Agriculture + PLAND_Pasture + PLAND_Mosaic_of_Uses (+ temp)
H2mod_91	ENN_CV + PLAND_Agriculture + PLAND_Pasture + PLAND_Mosaic_of_Uses + temp
H2mod_92	PROX_MN + ENN_CV + PLAND_Agriculture + PLAND_Pasture + PLAND_Mosaic_of_Uses + temp
H2mod_93	PD + ED + PLAND_Agriculture + PLAND_Pasture + PLAND_Mosaic_of_Uses + temp
H2mod_94	CA + PD + ED + PLAND_Agriculture + PLAND_Pasture + PLAND_Mosaic_of_Uses + temp
H2mod_97	ENN_MN + PLAND_Agriculture + PLAND_Pasture + PLAND_Mosaic_of_Uses
H2mod_98	ENN_SD + PLAND_Agriculture + PLAND_Pasture + PLAND_Mosaic_of_Uses
H2mod_99	ENN_CV + PLAND_Agriculture + PLAND_Pasture + PLAND_Mosaic_of_Uses
H2mod_100	PROX_MN + ENN_CV + PLAND_Agriculture + PLAND_Pasture + PLAND_Mosaic_of_Uses
Hypothesis 3 : Riparian forests	
H3mod_1 (H3mod_42)	CA (+ temp)
H3mod_2 (H3mod_43)	PLAND (+ temp)
H3mod_3 (H3mod_44)	TE (+ temp)
H3mod_4 (H3mod_45)	ED (+ temp)
H3mod_5 (H3mod_46)	Riparian_Forest (+ temp)
H3mod_6 (H3mod_47)	Riparian_Non_Forest (+ temp)
H3mod_7 (H3mod_48)	Riparian_Agriculture (+ temp)
H3mod_8 (H3mod_49)	Riparian_Pasture (+ temp)
H3mod_9 (H3mod_50)	Riparian_Mosaic (+ temp)
H3mod_10 (H3mod_51)	Main_str_Forest (+ temp)
H3mod_11 (H3mod_52)	Main_str_Non_Forest (+ temp)
H3mod_12 (H3mod_53)	Main_str_Agriculture (+ temp)
H3mod_13 (H3mod_54)	Main_str_Pasture (+ temp)
H3mod_14 (H3mod_55)	Main_str_Mosaic (+ temp)
H3mod_15 (H3mod_56)	Matrix (+ temp)
H3mod_16 (H3mod_57)	PLAND_Agriculture (+ temp)
H3mod_17 (H3mod_58)	PLAND_Pasture (+ temp)
H3mod_18 (H3mod_59)	PLAND_Mosaic_of_Uses (+ temp)
H3mod_19 (H3mod_60)	CA + ED + PLAND_Agriculture (+ temp)
H3mod_20 (H3mod_61)	PLAND + TE + PLAND_Agriculture (+ temp)
H3mod_21 (H3mod_62)	CA + ED + PLAND_Agriculture + PLAND_Pasture (+ temp)
H3mod_22 (H3mod_63)	CA + ED + PLAND_Agriculture + PLAND_Pasture + PLAND_Mosaic_of_Uses (+ temp)
H3mod_23 (H3mod_64)	CA + ED + PLAND_Agriculture + PLAND_Pasture + PLAND_Mosaic_of_Uses + Matrix (+ temp)
H3mod_24 (H3mod_65)	Riparian_Agriculture + PLAND + TE (+ temp)
H3mod_25 (H3mod_66)	Riparian_Forest + TE + PLAND_Agriculture + PLAND_Pasture + PLAND_Mosaic_of_Uses (+ temp)
H3mod_26 (H3mod_67)	Riparian_Forest + TE + PLAND_Agriculture + PLAND_Pasture + PLAND_Mosaic_of_Uses + Matrix (+ temp)
H3mod_27 (H3mod_68)	Riparian_Forest + TE + Matrix (+ temp)
H3mod_28 (H3mod_69)	Riparian_Pasture + PLAND + TE (+ temp)
H3mod_29 (H3mod_70)	Riparian_Mosaic + PLAND + TE (+ temp)
H3mod_30 (H3mod_71)	Riparian_Non_Forest + PLAND + TE (+ temp)

H3mod_31 (H3mod_72)	Main_str_Forest + TE + PLAND_Agriculture + PLAND_Pasture + PLAND_Mosaic_of_Uses (+ temp)
H3mod_32 (H3mod_73)	Main_str_Non_Forest + TE + PLAND_Agriculture + PLAND_Pasture + PLAND_Mosaic_of_Uses (+ temp)
H3mod_33 (H3mod_74)	Main_str_Agriculture + TE + PLAND_Pasture + PLAND + PLAND_Mosaic_of_Uses (+ temp)
H3mod_34 (H3mod_75)	Main_str_Pasture + TE + PLAND_Agriculture + PLAND + PLAND_Mosaic_of_Uses (+ temp)
H3mod_35 (H3mod_76)	Main_str_Mosaic + TE + PLAND_Agriculture + PLAND + PLAND_Pasture (+ temp)
H3mod_36 (H3mod_77)	Main_str_Forest + TE + PLAND_Agriculture (+ temp)
H3mod_37 (H3mod_78)	Main_str_Forest + ED + PLAND_Agriculture (+ temp)
H3mod_38 (H3mod_79)	Main_str_Forest + ED + Matrix (+ temp)
H3mod_39 (H3mod_80)	Riparian_Forest + TE + PLAND_Agriculture (+ temp)
H3mod_40 (H3mod_81)	Riparian_Forest + ED + PLAND_Agriculture (+ temp)
H3mod_41 (H3mod_82)	Riparian_Forest + ED + Matrix (+ temp)
H3mod_83	PLAND + ED + Matrix + temp
Hypothesis 4 : Land conversion	
H4mod_1 (H4mod_18)	trans_ha (+ temp)
H4mod_2 (H4mod_19)	trans_p (+ temp)
H4mod_3 (H4mod_20)	PLAND_Agriculture (+ temp)
H4mod_4 (H4mod_21)	PLAND_Pasture (+ temp)
H4mod_5 (H4mod_22)	PLAND_Mosaic_of_Uses (+ temp)
H4mod_6 (H4mod_23)	trans_p + PLAND_Agriculture (+ temp)
H4mod_7 (H4mod_24)	trans_p + PLAND_Pasture (+ temp)
H4mod_8 (H4mod_25)	trans_p + PLAND_Mosaic_of_Uses (+ temp)
H4mod_9 (H4mod_26)	trans_p + PLAND_Agriculture + PLAND_Pasture (+ temp)
H4mod_10 (H4mod_27)	trans_p + PLAND_Agriculture + PLAND_Pasture + PLAND_Mosaic_of_Uses (+ temp)
H4mod_11 (H4mod_28)	trans_p + PLAND_Agriculture + PLAND_Mosaic_of_Uses (+ temp)
H4mod_12 (H4mod_29)	trans_ha + PLAND_Agriculture (+ temp)
H4mod_13 (H4mod_30)	trans_ha + PLAND_Pasture (+ temp)
H4mod_14 (H4mod_31)	trans_ha + PLAND_Mosaic_of_Uses (+ temp)
H4mod_15 (H4mod_32)	trans_ha + PLAND_Agriculture + PLAND_Pasture (+ temp)
H4mod_16 (H4mod_33)	trans_ha + PLAND_Agriculture + PLAND_Pasture + PLAND_Mosaic_of_Uses (+ temp)
H4mod_17 (H4mod_34)	trans_ha + PLAND_Agriculture + PLAND_Mosaic_of_Uses (+ temp)
Hypothesis 5 : Topography	
H5mod_1 (H5mod_26)	alt_1 (+ temp)
H5mod_2 (H5mod_27)	alt_2 (+ temp)
H5mod_3 (H5mod_28)	alt_3 (+ temp)
H5mod_4 (H5mod_29)	alt_4 (+ temp)
H5mod_5 (H5mod_30)	alt_5 (+ temp)
H5mod_6 (H5mod_31)	Main_alt (+ temp)
H5mod_7 (H5mod_32)	steep_slope (+ temp)
H5mod_8 (H5mod_33)	alt_1 + alt_2 + alt_3 + alt_4 + alt_5 + steep_slope + Main_alt (+ temp)
H5mod_9 (H5mod_34)	alt_1 + alt_2 + alt_3 + alt_4 + alt_5 + steep_slope (+ temp)
H5mod_10 (H5mod_35)	alt_1 + alt_2 + alt_3 + alt_4 + alt_5 (+ temp)
H5mod_11 (H5mod_36)	steep_slope + Main_alt (+ temp)
H5mod_12 (H5mod_37)	alt_1 + alt_2 + alt_3 (+ temp)
H5mod_13 (H5mod_38)	alt_2 + alt_3 (+ temp)
H5mod_14 (H5mod_39)	alt_1 + alt_2 + alt_3 + steep_slope (+ temp)
H5mod_15 (H5mod_40)	alt_2 + alt_3 + steep_slope + Main_alt (+ temp)
H5mod_16 (H5mod_41)	alt_2 + alt_3 + Main_alt (+ temp)
H5mod_17 (H5mod_42)	alt_4 + alt_5 + steep_slope (+ temp)

H5mod_18 (H5mod_43)	alt_4 + alt_5 + steep_slope + Main_alt (+ temp)
H5mod_19 (H5mod_44)	alt_4 + alt_5 + Main_alt (+ temp)
H5mod_20 (H5mod_45)	alt_3 + Main_alt (+ temp)
H5mod_21 (H5mod_46)	alt_3 + steep_slope (+ temp)
H5mod_22 (H5mod_47)	alt_3 + steep_slope + Main_alt (+ temp)
H5mod_23 (H5mod_48)	alt_2 + Main_alt (+ temp)
H5mod_24 (H5mod_49)	alt_2 + steep_slope (+ temp)
H5mod_25 (H5mod_50)	alt_2 + steep_slope + Main_alt (+ temp)
Spatial models	
H3mod_82_spa (no convergence)	Riparian_Forest + ED + Matrix + temp + mat(pos + 0 | group)
H3mod_82_spa_2	Riparian_Forest + ED + Matrix + temp + exp(pos + 0 | group)
H3mod_82_spa_3	Riparian_Forest + ED + Matrix + temp + ar1(pos + 0 | group)
H3mod_82_spa_4	Riparian_Forest + ED + Matrix + temp + X + Y
H3mod_82_spa_5	Riparian_Forest + ED + Matrix + temp + acd
H3mod_82_spa_6	Riparian_Forest + ED + Matrix + temp + acd2
H3mod_82_spa_7	Riparian_Forest + ED + Matrix + temp + acd3

Note: The 3 first models use different covariate terms from the glmmTMB package (Brooks et al., 2023; Kristensen and McGillycuddy, 2023), X and Y are the UTM latitude and longitude (scaled), acd are distance-weighted autocovariate structure using different weighting schemes: one (acd), inverse (acd2), inverse.squared (acd3) (Bivand, 2022).

Table A6 : Presence frequencies and weights of variables in the dredged models set from the PCA axes models. Weights represent the relative importance of variables, it is calculated as the sum of the models AICc weights that contain the variable, the interpretation is the probability of the variable to be in the best model if the data were resampled.

Variables	Frequency	Weight
Intercept	1.0	1.000
offset(log(Population))	1.0	1.000
Random intercept variables	1.0	1.000
Dim.1	0.5	1.000
Main alt	0.5	0.984
Dim.7	0.5	0.976
Dim.5	0.5	0.969
Dim.3	0.5	0.906
Matrix	0.5	0.891
Dim.6	0.5	0.732
Dim.4	0.5	0.637
Dim.2	0.5	0.354

Table A7 : AICc models selections by Hypothesis/Use. The table shows only the best models of each model selections (ΔAICc < 2). See Table A4 for the abbreviations. Df: degree of freedom, LogLik: log likelihood.

Model name	Predictors variables	AICc	ΔAICc	AICc weight	Df	LogLik	Deviance
Dredged models of the PCA axes full model							
510	Dim.1 + Dim.3 + Dim.4 + Dim.5 + Dim.6 + Dim.7 + Main_alt + Matrix	11870.68	0.000	0.290	21	-5914.3	3602.7
512	Dim.1 + Dim.2 + Dim.3 + Dim.4 + Dim.5 + Dim.6 + Dim.7 + Main_alt + Matrix	11872.15	1.477	0.138	22	-5914.0	3602.4
502	Dim.1 + Dim.3 + Dim.5 + Dim.6 + Dim.7 + Main_alt + Matrix	11872.41	1.733	0.122	20	-5916.1	3599.5
Climatic models							
modclima_1	temp	11943.46	0.000	0.403	5	-5966.7	11933.5
modclima_4	cold_temp	11944.53	1.077	0.235	5	-5967.3	11934.5
modclima_3	Temp + prec	11944.62	1.168	0.225	6	-5966.3	11932.6
Hypothesis 1 : Forest cover and secondary forest							
H1mod_21	Primary_Forest + temp	11919.29	0.000	0.272	6	-5953.6	11907.3
H1mod_17	PLAND + temp	11919.83	0.541	0.207	6	-5953.9	11907.8
H1mod_25	Primary_Forest + Secondary_Forest + temp	11920.74	1.445	0.132	7	-5953.4	11906.7
H1mod_23	CA + PLAND + temp	11921.23	1.938	0.103	7	-5953.6	11907.2
Hypothesis 2 : Land configuration							
H2mod_69	PLAND + PD + TE + PLAND_Agriculture + PLAND_Pasture + PLAND_Mosaic_of_Uses + temp	11901.63	0.000	0.983	11	-5939.8	11879.6
Hypothesis 3 : Riparian forests							
H3mod_82	Riparian_Forest + ED + Matrix + temp	11886.0	0.0	0.978	14	-5929.0	11858.0
Hypothesis 4 : Land conversion							
H4mod_27	trans_p + PLAND_Agriculture + PLAND_Pasture + PLAND_Mosaic_of_Uses + temp	11933.17	0.000	0.162	9	-5957.6	11915.2
H4mod_33	trans_ha + PLAND_Agriculture + PLAND_Pasture + PLAND_Mosaic_of_Uses + temp	11933.21	0.038	0.159	9	-5957.6	11915.2
H4mod_26	trans_p + PLAND_Agriculture + PLAND_Pasture + temp	11933.71	0.536	0.124	8	-5958.9	11917.7
H4mod_32	trans_ha + PLAND_Agriculture + PLAND_Pasture + temp	11933.72	0.542	0.124	8	-5958.9	11917.7
H4mod_28	trans_p + PLAND_Agriculture + PLAND_Mosaic_of_Uses + temp	11933.77	0.594	0.121	8	-5958.9	11917.8
H4mod_34	trans_ha + PLAND_Agriculture + PLAND_Mosaic_of_Uses + temp	11933.94	0.764	0.111	8	-5959.0	11917.9
H4mod_20	PLAND_Agriculture + temp	11933.96	0.785	0.110	6	-5961.0	11922.0
Hypothesis 5 : Topography							
H5mod_46	alt_3 + steep_slope + temp	11848.5	0.0	0.7	7	-5917.3	11834.5
H5mod_39	alt_1 + alt_2 + alt_3 + steep_slope + temp	11850.2	1.7	0.3	9	-5916.1	11832.2
Spatial models							
H3mod_82_spa_2	Riparian_Forest + ED + Matrix + temp + exp(pos + 0 | group)	11138.11	0.0	1	16	-5553.0	11106.1

Table A8 : Moran's I test for spatial autocorrelation. Moran's I statistics are provided and their respective p-value by year, based on distances between the centroids of municipalities, and based on a contiguity matrix using the Queen neighbourhood relation.

	Distance based		Queen contiguity matrix	
Year	**Moran I statistic**	**p-value**	**Moran I statistic**	**p-value**
2001	0.00015924	0.4886	0.032662305	0.0001665***
2002	0.00408747	8.223e-09***	0.0485083604	7.475e-07***
2003	0.00890779	2.2e-16***	0.1772017569	2.2e-16***
2004	0.00669378	2.2e-16***	0.01920351	0.02452*
2005	0.00018649	0.4813	-0.01895160	0.9745
2006	0.00078274	0.1284	0.04281812	3.612e-06***
2007	0.00667601	2.2e-16***	0.0835435287	1.867e-15***
2008	0.00250973	0.0004605***	0.0197807868	0.03023*
2009	0.00098170	0.09843	-0.0088464078	0.7928
2010	0.00219064	0.001485**	0.0610183148	2.346e-09***
2011	-0.00299631	0.000447**	-0.0199545104	0.9741
2012	0.00303726	2.528e-05***	0.0358413825	0.0003104***
2013	-0.00260637	0.004057**	-0.0334044709	0.9991
2014	0.00478377	2.624e-10***	0.1034723632	2.2e-16***
2015	0.00748062	2.2e-16***	0.0988669984	2.2e-16***
2016	0.00038556	0.375	0.0536910853	1.584e-07***
2017	0.00358004	1.122e-06***	0.0355094889	0.0003719***
2018	0.00081090	0.1598	-0.0085213562	0.7789
2019	0.01691277	2.2e-16***	0.1813108077	2.2e-16***

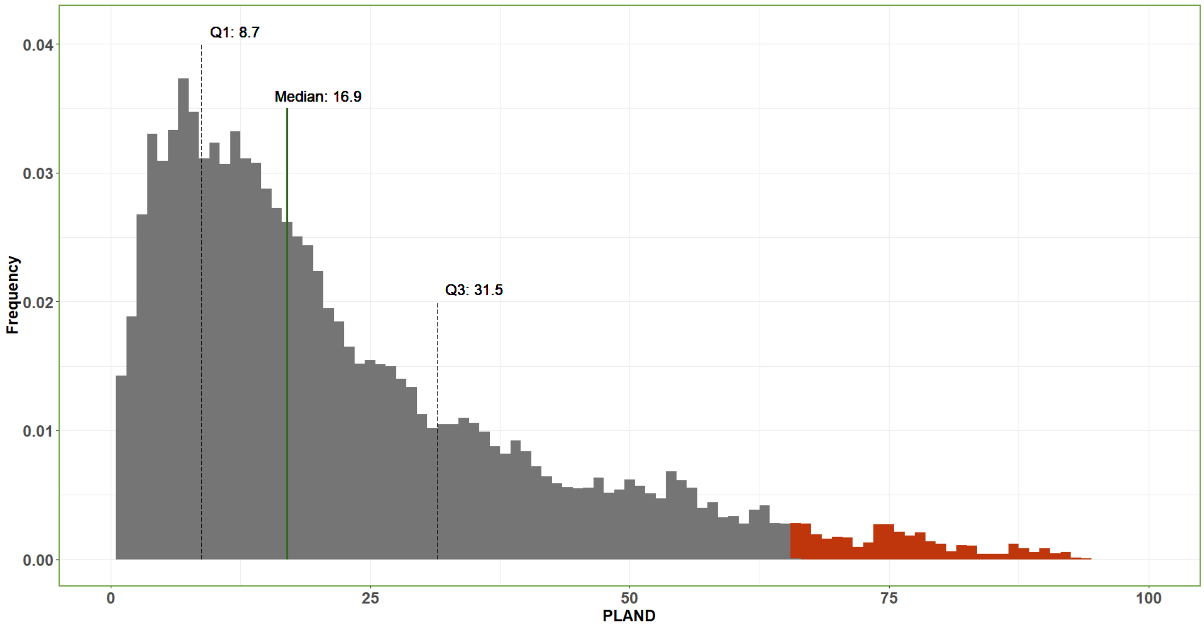

Figure A4: Frequency of observations by PLAND value (percentage of forest cover in a municipality). First, second and third quantile values are shown. The red histogram part are the potential outliers.

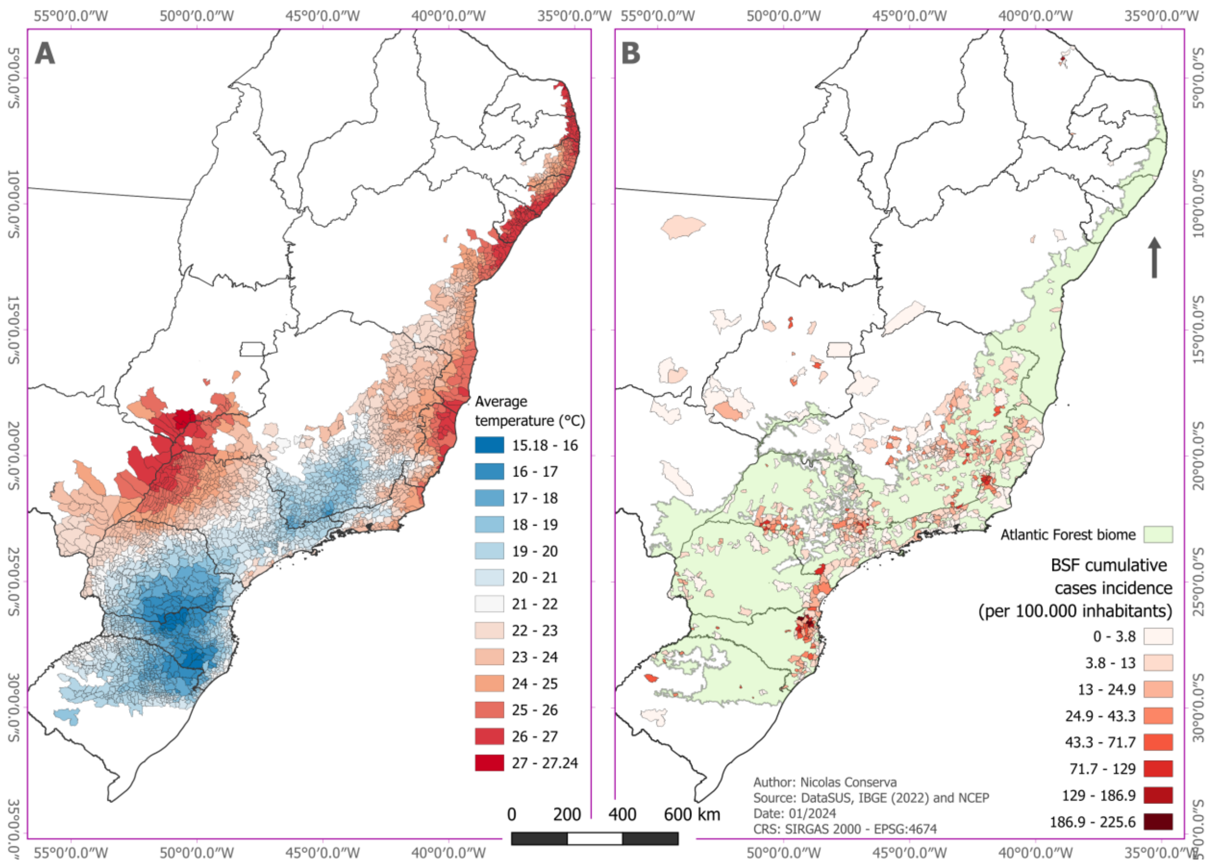

Figure A5 : **A.** Average for the 2001-2021 period of the mean annual temperature by municipality in the Atlantic Forest. **B.** BSF cumulative cases incidence per 100.000 inhabitants by municipality of Brazil for the 2001-2021 period. Only municipalities with confirmed BSF cases are reported.

Figure A6 : Santo André, São Paulo. Regular exchange student enjoying riparian environments associated with high spotted fever risk for leisure instead of writing his master thesis. You have been appendices easter egged.